Title
Multi-Temporal Variability Within Antarctic Coastal Polynyas and Their Relationships To Large-Scale Atmospheric Phenomena

Author
Ward, Jason Michael

Publication Date
2018

Peer reviewed|Thesis/dissertation

UNIVERSITY OF CALIFORNIA

Los Angeles

Multi-Temporal Variability Within Antarctic Coastal Polynyas and Their Relationships To Large-Scale Atmospheric Phenomena

A dissertation submitted in partial satisfaction of the

requirements for the degree Doctor of Philosophy

in Geography

by

Jason Michael Ward

2018

ABSTRACT OF THE DISSERTATION

Multi-Temporal Variability Within Antarctic Coastal Polynyas and Their Relationships To Large-Scale Atmospheric Phenomena

by

Jason Michael Ward

Doctor of Philosophy in Geography

University of California, Los Angeles, 2018

Professor Marilyn N Raphael, Chair

Open water and thin ice areas, known as coastal polynyas, form along the Antarctic coastline and allow continued interaction between the ocean and atmosphere throughout the sea ice advance season. Coastal polynyas are the most productive locations of sea ice formation, Antarctic bottom water formation, and biological activity in the Southern Ocean. Changes in these elements are greatly controlled by polynya area variability. To carry out an in-depth study of polynya area variability, a 26-year 25-polynya daily area dataset was created and analyzed. The long term trend and the daily, monthly, seasonal, and annual variations are separated to analyze the multi-temporal variability of the polynyas and investigate their individual and regional responses to prominent large-scale atmospheric circulation patterns. Results indicate that most polynya variability occurs at the daily scale, followed by monthly and seasonal variations. Very little variability occurs interannually. Thus, studies done at the annual scale mask most of the polynya

activity. Only five of the polynyas have long term trends, which are all non-linear and arise from abrupt changes in the icescape. Three of the significant trends occur within the top four most significant regions of sea ice and bottom water formation. Long term changes in polynya area cause long term changes in the overall productivity of the Southern Ocean. The Southern Annular Mode (SAM), El Nino-Southern Oscillation (ENSO), and the Amundsen Sea Low (ASL) significantly contribute to individual and regional coastal polynya variability. Influence from the SAM and the ASL is primarily driven at the monthly and seasonal scales. Influence from ENSO is driven at the annual scale. Using Pearson correlations, principal component analysis, gaussian mixture models, and hierarchical agglomerative clustering, six regional polynya groups are delineated based on the strength and direction of inter-polynya co-variability. The mean polynya variability within each region is significantly correlated, which is driven at the seasonal scale. While the SAM, ENSO, and ASL are not the primary drivers of regional polynya group delineations, they are significantly influential in the mean variability of each group.

The dissertation of Jason Michael Ward is approved.

Alexander Dean Hall

Yongwei Sheng

Yongkang Xue

Marilyn N Raphael, Committee Chair

University of California, Los Angeles

2018

Dedication

The completion of this dissertation is dedicated to my three children – Monique, Jamari, and Jana. I am continually amazed and inspired by each of them. It is my hope that this accomplishment inspires them to find their passion and strive for excellence. Hard work, dedication, and family are key components of success.

Table of contents

List of Figures

Acknowledgments

I would like to acknowledge the following people who have supported me, not only during the completion of this project, but also throughout my graduate career. They all contributed to my growth as a student, teacher, researcher, and father.

First, I want to acknowledge Kasi McMurray and the Geography Department staff. They worked very hard and contributed to my smooth progression through the program.

I thank my Ph.D. committee – Alex Hall, Yongwei Sheng, Yongkang Xue, and Marilyn Raphael. I could not accomplish many of my educational goals and fulfill my potential without their advice on research and publication. I thank them for all the time and energy they put into my work and my growth as a researcher.

I especially thank my faculty advisor and mentor, Marilyn Raphael, for her continued belief, encouragement, and wisdom. Her availability and generosity are greatly appreciated.

I am also very grateful to my friends. Anthony Howell, Tom Narins, Anna Dvorak, and Diane Ward were extremely supportive, gave great advice, and created an enjoyable experience for me. Ashlea McLaughlin, Eric Ferrer-Vaughn, Melody Davis, Ty-Juana Taylor, and Siyu Cai were great sources of inspiration, encouragement, and friendship. They are amazing people. I love and admire each of them dearly.

Lastly, I thank my children, parents, grandparents, godmother, siblings, and close family friends. They taught me the importance of hard work, dedication, and service. They have immense belief in me, which provides encouragement and confidence. I love them all for who they are and thank them for the love they show me.

Vita

Education — University of California, Los Angeles

- C.Phil. (2017), M.A. (2014), B.A. (2011)
- Major: Geography
- Concentrations: Climate Science; GIS and Technologies

Experience — University of California, Los Angeles

Teaching Fellow (10/01/2012 – 12/31/2018)

Duties: Design and promote student learning outcomes, deliver lectures, lead discussions, design and lead labs, hold regular office hours, and advise in project design and execution.

- Geographic Information Systems
  - Terms: Fall 2012; Fall 2013; Winter, Spring, Fall 2015; Spring 2016; Winter, Spring, Summer 2017; Winter 2018
- People and earth's ecosystems
  - Terms: Spring 2013; Fall 2014; Fall 2017; Fall 2018
- Cultural geography
  - Terms: Summer, Fall 2016; Summer 2017
- World Regions
  - Terms: Spring 2018
- Population geography
  - Terms: Winter 2016
- Ethnicity in American cities
  - Terms: Winter 2016

Graduate Student Researcher (10/01/2011 – 09/30/2014)

Duties: Collection, quality assessment, processing, management, and analysis of geographic data sets. Research design and execution, production of research papers, and conference presentations.

Funding Awarded: Graduate Research Mentorship Program, Graduate Summer Research Mentorship Program, Rose and Sam Gilbert Fellowship

Teaching Interests

- Physical geography
- GIS and remote sensing
- Climate and weather
- World regions
- Humans and the environment
- Cultural geography
- Geography of CA
- Water resources

Skills

- Sensitivity to diverse groups and learning
- Commitment to student success
- Mentorship
- Community service and outreach
- Organizing and conducting field trips
- Teach online and hybrid courses
- Interdisciplinary teaching
- Teach science and technology
- Teach evenings and weekends
- Quantitative analysis

Software & Programming

GIS/RS:	ArcGIS, QGIS, SQL, IDL, ENVI, Tableau, Google Web Designer, Panoply
Statistics:	R, R-Studio, GeoDa
Teaching:	Moodle, Zoom, Skype, Blackboard Collaborate
Other:	Microsoft Office, Libre Office, Stella, UNIX (experience)

Professional Affiliations

- American Association of Geographers
- American Geophysical Union
- Association of Pacific Coast Geographers
- California Geographical Society
- Diversity Climate Network

Research Interests

- Polynya variability
- High latitude coastal dynamics
- Antarctic climate
- Daily to interannual climate variability
- Human-environment interaction

Conference Presentations

Ward, J. (2014, May) Relationships in areal variability: The Ross Sea Polynya and Ice. Talk presented at the annual meeting of the California Geographical Society, Los Angeles, CA.

Ward, J. (2014, December) Formative processes governing Ross Sea Polynya areal variability. Poster presented at the annual meeting of the American Geophysical Union, San Francisco, CA.

Ward, J. (2015, April) A comparison of methods that update the Ross Ice Shelf land mask through the use of SSM/I satellite imagery. Poster presented at the annual meeting of the American Association of Geographers, Chicago, IL.

Ward, J., and Raphael, M. (2016, March) Monthly variability and inter-annual trend analysis for SSM/I-derived Ross Ice Shelf Polynya area. Poster presented at the annual meeting of the American Association of Geographers, San Francisco, CA.
Raphael, M., and Ward, J. (2016, April) Ross Ice Shelf Polynya – Contribution to Antarctic sea ice variability. Talk presented at the annual meeting of the American Association of Geographers, San Francisco, CA.

Ward, J. (2018, October) The circumpolar influence of large-scale atmospheric circulations on Antarctic coastal polynyas. Talk presented at the annual meeting of the Association of Pacific Coast Geographers, Reno, NV.

Ward, J., and Raphael, M. (2018, December) The circumpolar influence of large-scale atmospheric circulations on Antarctic coastal polynyas. Poster presented at the annual meeting of the American Geophysical Union, Washington, DC.

Chapter 1

Introduction

Every year, during the austral ice advance season, the sea ice field expands to cover approximately 19 million km^2 of the Southern Ocean [Maksym et al., 2012]. The ice creates a barrier between the ocean and atmosphere, significantly reducing gas, heat, and mass transfers [Fiedler et al., 2010; Arrigo and van Dijken, 2003]. However, situated around the Antarctic continent, in the pack ice and along the coastal regions, are *polynyas*. Polynyas are areas of open water or minimal sea ice concentration and thickness (< 15% and 20cm, respectively) surrounded by ice [Nihashi et al., 2017; Nihashi and Ohshima, 2015; Comiso et al., 2011; Drucker et al., 2011; Tamura et al., 2008; Martin et al., 2007; Kwok et al., 2007; Arrigo and van Dijken, 2003]. Their formation, decay, and function are products of sea ice production, melt, and transport processes. Polynyas are found within the polar regions because the temperatures are constantly cool enough for formative processes to occur. Within the polar regions, the ocean surface reaches temperatures of approximately -1.8^oC, at which point the sea surface freezes [Nicholls, 2001; Smith et al., 1990].

Due to their recurrent nature, coastal polynyas are also important biological habitats [Anderson, 1993; Kottmeier and Engelbart, 1992; Smith et al., 1990]. They are sites of the earliest and greatest amounts of insolation penetrating the sea surface each spring. This provides suitable conditions for the earliest and greatest amounts of primary productivity (phytoplankton blooms) in the Southern Ocean. Thus, polynyas provide food sources for microscopic and subsequently macroscopic fauna. The largest and most common of which are penguin colonies that also use polynyas as access points to aquatic environments for hunting [Arrigo and van Dijken, 2003]. Human populations also used polynyas in hunting 3,000 years ago [Smith et al., 1990].

There are two mechanisms responsible for polynya development – sensible heat convection and latent heat transfer [Arrigo and van Dijken, 2003]. Offshore polynya formation is driven by entrainment of sensible heat through convection of relatively warm and buoyant water to the surface. This process may result from the sinking of denser water that forms through the brine rejection process [Fiedler et al., 2010; Smith et al., 1990], from mechanical mixing of the mixed ocean layer from storms, or from spin up of ocean gyres that cause upwelling [Cheon et al., 2018]. All forms of vertical heat transport aid in basal ice melt.

Polynya formation requires reduction of the local ice cover to expose the relatively warm, dark ocean. Open water areas efficiently absorb insolation, while pack ice efficiently reflects it. During the ice retreat season, the ice-free sea surface may absorb up to approximately 90% of insolation and snow-covered surfaces may absorb as little as approximately 20% [Hall and Rothrock, 1987]. The contrast in surface albedo creates disparities in surface temperature and long wave radiation emission [Andreas et al., 2002]. During winter, ice-free oceanic heat flux is estimated to be up to two orders of magnitude greater than fluxes from pack ice. When thick ice dominates the surface cover, even small areas of open water or snow-free thin ice can dominate the regional heat budget [Worby and Allison, 1991], allowing polynyas to influence local and regional temperature, pressure, wind speed, and wind direction [Adolphs and Wendler, 1995].

Heterogeneity in sea ice thickness and concentration and the underlying ocean temperatures control the development of the boundary layer. The internal boundary layer over the Antarctic continent and ice shelves is relatively cool, shallow, and stable with low moisture content and very high relative humidity [Raddatz et al., 2012; Andreas et al., 2002, 1979]. As air parcels travel

across the continental margins and ice shelves they are katabatically driven seaward. Contact with the rough open water regions, such as polynyas and leads that contain various size floes, reduces surface winds and causes friction-induced overturning [Andreas et al., 1979]. However, the greatest source of turbulence within the boundary layer is convective heating from the exposed ocean surface [Raddatz et al., 2012]. Large heat and moisture fluxes from the ice-free sea surface increase the heat and moisture content, inducing significant vertical mixing and deepening the boundary layer [Fiedler et al., 2010]. Once air parcels migrate downwind of open water regions, the ocean-atmosphere heat and moisture gradients increase again but cause large downward heat and moisture fluxes onto the ice surface. Surface momentum also increases due to the transition onto a smoother, ice covered surface [Fiedler et al., 2010; Renfrew et al., 2002; Andreas et al., 2002]. Boundary layer mixing decreases and the vertical profile is realigned.

Coastal polynyas develop from wind-driven ice divergence away from a static feature such as a coastline, ice tongue, or iceberg. While offshore polynyas are able to balance heat lost to the atmosphere with heat added to the surface from below [Goosse and Fichefet, 2001], most coastal polynya heat loss is not replaced from below because the entire water column in shallow shelf regions is near freezing [Nicholls, 2001; Zwally et al., 1985]. The net negative energy imbalance results in a change of state through freezing [Adolphs and Wendler, 1995]. This process is so pronounced that coastal polynyas bordering Antarctica's winter coastlines are known as "ice factories" [Barber and Massom, 2007]. Coastal polynyas are maintained through continuous rates of sea ice export that equal or exceed rates of sea ice production. The coastline, or other virtually static features, form the windward coastal polynya boundaries. The transported pack ice provides the leeward boundaries [Adolphs and Wendler, 1995; Smith et al., 1990]. While both polynya types – offshore and coastal – are associated with local sea ice reduction, only coastal polynyas are

sites of continued rapid ice production throughout the ice advance season [Ackley et al., 2001; Massom et al., 1998]. Because of their contributions through the ice production process, coastal polynyas are the primary focus of this study.

Even though ice producing coastal polynyas are formed in both polar regions, the Antarctic offers a particularly interesting and useful lens through which coastal polynyas may be studied. Latent heat transfer within polynyas is the result of temperature and moisture gradients between atmospheric and oceanic environments. Unlike the Arctic, the Antarctic has a relatively warm sea surface and a below freezing atmosphere. Thus, heat and moisture are transferred from the ocean to the atmosphere. Also, the Antarctic has experienced net positive trends in sea ice extent, concentration, and seasonal duration since the mid-20th century [Stammerjohn et al., 2012; Maksym et al., 2012; Comiso et al., 2011; Liu et al., 2004]. This observation is contrasted by the decreasing Arctic sea ice trends during the same period. Mean annual sea ice coverage has decreased at a rate of approximately 3% per decade in the Arctic, while it has increased at approximately 1.1% per decade in the Antarctic [NSIDC, 2018]. The decline in Arctic sea ice agrees with the intuitive and predicted effects of global warming. The observed Antarctic sea ice trend is a counter-intuitive phenomenon that was not predicted. Thus, only in the Antarctic can coastal polynyas be investigated within a sea ice increasing context.

Total Antarctic coastal polynya extent covers approximately 1% of the sea ice surface area, but the ice generated within them constitutes approximately 10% of the Southern Ocean sea ice. Thus, Antarctic coastal polynyas are the most productive areas of Southern Ocean sea ice formation [Tamura et al., 2008]. However, the proportional contribution of polynya-generated sea ice varies regionally. The polynyas generate 5-10% of total sea ice in the Weddell Sea and 20-50% of sea ice

in the Ross Sea. With much of the sea ice content originating at the coast [Kwok et al., 2007], variability in coastal polynya productivity may influence changes in the sea ice field.

Coastal polynyas contribute to the spatial variability of sea ice downwind of their zones of sea ice production Kimura and Wakatsuchi [2011]. Currently, most studies of polynya-sea ice relationships do not account for temporal dynamics. While Kimura and Wakatsuchi [2011] do present monthly variations of the negative coastal and positive downstream sea ice production pattern, their study does not analyze the temporal relationship between the two regions of the pattern, which would establish the association between the two surface features and potential influence of coastal polynya variability on the spatiotemporal dynamics of the regional sea ice field.

While polynyas are of great interest for their roles in macro- and micro- biological activity, local and regional heat budgets, small scale human activity, and more, their greatest geographical influence occurs through deep water formation. Most brine is rejected during the freezing process. Thus, as the surface layer becomes cooler, it also becomes more saline and denser. Due to the continued, rapid ice formation in coastal polynyas, surface waters become dense enough to sink to the continental shelf, contribute to high salinity shelf water, and eventually spill into Antarctic Bottom Water [Fiedler et al., 2010; Ushio et al. 1999; Smith et al., 1990]. Antarctic Bottom Water feeds into the Thermohaline Circulation, also known as the Meridional Overturning Circulation. This process gives coastal polynyas global influence. Deep ocean processes like the Thermohaline Circulation occur on the order of centuries and provide important long-term storage for greenhouse gases, such as carbon dioxide, which is another crucial function of coastal polynyas [Ohshima et al., 2016; Kitade et al., 2014; Beckmann et al., 1999].

Coastal polynyas have very significant roles in the earth-atmosphere system as they are sites of continued atmosphere-sea ice-ocean interaction throughout winter. These small features have important roles in sea ice production [Smith et al., 1990], regional sea ice spatial distribution [Kimura and Wakatsuchi, 2011], and large scale atmospheric influence on oceanic processes such as bottom water formation [Jacobs, 2004; Cai and Baines, 1996]. Currently, ocean-sea ice-atmosphere interactions are not fully understood. Similarly, our knowledge of polynya interaction with these mediums must continue to grow. Having a better understanding of these polynya relationships will give insight to their susceptibility to and influence on climatic changes.

The current study produces a 26-year circumpolar Antarctic coastal polynya area dataset using the method described by Tamura et al. [2016, 2007] and Nihashi and Ohshima [2015]. The methods for polynya detection and analysis are described in Chapter 2. The resulting dataset is used to determine scales of variability – daily, monthly, interannual, seasonality, and long-term trends – for each polynya, and the relative contribution from the various scales of variability. This allows more direct investigation of polynya variability and its relationship to other features, such as other polynyas, atmospheric drivers, and changes in the sea ice field. Along with introduction of the dataset, polynya variability at all scales is discussed in Chapter 2. Chapter 3 addresses the areal response of individual polynya systems to large-scale atmospheric circulation patterns. Chapter 4 addresses inter-polynya relationships to analyze regional dynamics.

Chapter 2

A new look at variability and trends

1. Introduction

Polynyas are variable in size and each polynya's size varies over time. To fully understand polynyas, researchers must understand their temporally dynamic nature at various scales. Previous studies have focused on daily and sub-daily coastal polynya variability [Fiedler et al., 2010; Kwok et al., 2007; and more]. Bromwich and Kurtz [1983, 1984] determined that approximately 60% of daily polynya events (days when the polynya is not completely closed by ice) are caused by katabatic winds. Nihashi and Ohshima [2015] suggests that this relationship is not directly detectable over long periods, such as their 13-year study period, due to changes in relatively static icescape features – ice bergs, landfast ice, ice tongues, and ice shelves. The Cape Darnley, Barrier, and Dalton polynyas (located along the coasts of western and eastern Prydz Bay and eastern Wilkes Land, respectively) have relatively weak relationships with the near surface meteorological forces, such as wind speed and direction and temperature, that normally drive polynya development. The presence and changing nature of various icescape features cause polynyas to have variable mean size, which complicates analysis of small scale polynya variability.

Monthly coastal polynya variability is greatly influenced by meso-scale atmospheric activity. Much of the variation in surface winds, and associated polynya variability, is attributed to storms [Bromwich et al., 1993, 1998]. With their speed of migration, individual storms may have effects on a region at sub-monthly timescales. Katabatic surge events driven by synoptic cyclones have an average duration of 5 days but may last up to 13 days [Bromwich et al., 1993]. Thus, synoptic scale storms may affect monthly variability, but are masked at the interannual level. Synoptic scale

processes alter wind direction, intensify offshore flow, and enhance coastal polynya development [Parish and Bromwich, 1998]. Coastal circumpolar migration of low-pressure cells increases meridional pressure gradients that enhance katabatic flow [Carrasco and Bromwich, 1993]. The associated geostrophic wind is also associated with enhanced near surface southerly flow and influences wind direction [Nihashi and Ohshima, 2015; Bromwich et al., 1993].

Interannual polynya variability is well represented in polynya studies [Tamura et al., 2016, 2008; Cheng et al., 2017; Martin et al., 2007; and more]. Comiso et al. [2011], Martin et al. [2007], and Arrigo et al. [2003, 2004] analyze the effects of calved icebergs on polynya size, ice production, and primary productivity, respectively. When relatively slow migrating Antarctic icebergs travel northward they cause ice build-up and close coastal polynyas to the immediate south. In these situations, the coastline-adjacent polynyas are replaced downwind by iceberg-adjacent polynyas. Due to the rate of motion and melt, migrating iceberg effects are generally limited to a single ice advance season. The iceberg events of years 2000 and 2002 drive important anomalous increases in polynya extent along the Ross Ice Shelf during those immediate years.

Massom et al. [1998] and Nihashi and Ohshima [2015] study the effects of ice tongue dynamics on interannual polynya activity. Many polynyas form adjacent jetting ice tongues. Drastic changes, such as a calving event, on jetting ice features produce substantial changes in polynya size, variability, location, and orientation. Removal of an ice tongue may even lead to a permanent regime change that last decades or longer [Campagne et al., 2015]. The changing icescape is able to produce large interannual variations in individual coastal polynyas. The Mertz Glacier Tongue calving event of 2010 drives interannual variability in the Mertz Glacier Polynya (MGP) found along the Adelie Land coast. The dynamic coastal icescape may have influences on polynya size

at smaller temporal scales as well. Temporal changes in more minor landfast ice and its magnitude of influence on polynya size remains to be explored.

Very few studies have directly analyzed the polynyas' seasonal variability. In fact, recent studies largely report on interannual variability [Tamura et al., 2016, 2008], which masks seasonality, and monthly variability, and does not consider the consistent yearly pattern of polynya variability and its drivers. Cheng et al. [2017] presents the seasonal variation in total Ross Ice Shelf Polynya sea ice production from April to October, 2003 to 2015. Monthly median ice production shows very weak seasonality and no consistent changes throughout the year. However, Tamura et al. [2016] reports consistent decrease in mean RIS sea ice production during the same months. Both studies do report a local maximum in September.

Much work has gone into identifying general trends in polynya in size, ice production, and biological activity [Tamura et al., 2016, 2008; Comiso et al., 2011; Kern, 2009]. However, very little work has identified causes of the polynya trends. Park et al. [2018] found that trends in RIS area and the RIS season timing (the annual time period within which polynyas form) are influenced by trends in ENSO and the SAM, respectively. Current polynya literature also lacks studies on the seasonality of the long-term trends. Understanding the seasonal pattern of polynya trends will give insight to the larger annual trends most commonly reported in the literature. In this chapter, monthly seasonality within the polynya trends is investigated.

Common practice in previous polynya studies uses simple averaging to produce aggregates for various temporal scales without accounting for cross influences from other scales of variability and trends [Tamura et al., 2016; Nihashi and Ohshima, 2015; Bromwich et al., 1998]. This may result

in potential under- or overestimation of polynya relationships such as correlations with large-scale atmospheric circulations at the annual level [Tamura et al., 2016; Arrigo and van Dijken, 2004; Bromwich et al., 1998]. It may also result in confusion as to which scale of influence is important for large-scale atmospheric influences on polynya activity, particularly from correlations calculated at the monthly level [Montes-Hugo and Yuan, 2012]. None of these studies mention accounting for long-term trends or seasonality, which would most often lead to overestimation of monthly correlations. Thus, analyses using more robust methods to analyze the various temporal components, as is done in this chapter, will provide better understanding of polynya dynamics at different scales, their interactions with other climate drivers, and forecasting.

Most of the previous Antarctic coastal polynya studies were limited by the lack of long-term polynya data that would allow observation of long-term norms and variability. Most of the multi-year studies use sub-decade long data sets to analyze polynya development and interactions [Bromwich et al., 1998; Arrigo and van Dijken, 2003a, 2003b; Nakata et al., 2015; Nihashi and Ohshima, 2015]. Thus far, only very few studies investigate polynya dynamics on a multi-decadal timescale using spatial resolutions fine enough to capture temporal changes in polynya size [Cheon et al., 2018; Nihashi et al., 2017; Tamura et al., 2016; Nihashi and Ohshima, 2015]. However, the data sets used in those studies lack the spatial density in their circumpolar polynya distributions required for proper regional analyses. Thus, a more up-to-date and inclusive multidecadal circumpolar Antarctic coastal polynya dataset is created and analyzed in this study.

2. Data and Methods

2.1 Input satellite data

This section describes the input data and algorithms used to derive daily circumpolar Antarctic coastal polynya areal extents, as well as the methods employed to analyze the output. The polynya dataset in this study is created using input from the Defense Meteorological Satellite Program's Special Sensor Microwave Imager (SSM/I) series brightness temperature data. SSM/I series data is provided by the National Snow and Ice Data Center (NSIDC) in the 'DMSP SSM/I-SSMIS Pathfinder Daily EASE-Grid Brightness Temperatures, Version 2' dataset [Armstrong et al., 1994]. This dataset provides brightness temperature information on a 12.5 x 12.5 km^2 equal-area scalable earth (EASE) grid at twice daily (ascending and descending) time steps. 3 of the 5 available spectral levels are utilized. 85 and 91GHz channels are used for their enhanced spatial resolution at 12.5 km, compared to the 19, 22, and 37GHz channels at 25 km [Markus and Burns 1995; Tamura et al., 2007]. The higher resolution channels' sensitivity to weather effects necessitates use of the 37GHz information, which is less sensitive to water vapor and may improve accuracy in detection of thin ice areas [Armstrong et al., 1994]. Vertical and horizontal polarizations are provided with each frequency level. A 12.5 km resolution land mask is also used to update the Antarctic coastline and is referenced to search for other relatively static ice features near the land mask's original coastline. The original land mask was acquired from NSIDC in the 'EASE-Grid Land-Ocean-Coastline-Ice Masks Derived from Boston University MODIS/Terra Land Cover Data, Version 1' dataset.

Complete SSM/I series temporal coverage ranges from July 9, 1987, to November 15, 2017. However, due to sensor degradation on the DMSP F08 platform between February 1989 and December 1991, January 1, 1992, marks the starting point for possible polynya studies at the 12.5

km spatial resolution. Thus, the current study spans 1992 to 2017. Since polynyas are exclusively winter features [Arrigo and van Dijken, 2003; Tamura et al., 2008], this study focuses on polynya area from April to October. DMSP platforms F11 and F13 collected data from December 3, 1991 to April 29, 2009. Platform F17 is the first to provide data at the 91 GHz spectral level. It began sampling December 14, 2006 and continues today. Missing or erroneous data are sparsely distributed throughout the dataset.

2.2 Circumpolar Antarctic coastal polynya area dataset

Microwave imagery is unable to detect differences between open water/thin ice and relatively static ice features due to the similarity in their microwave radiative properties. This results in systematic overestimation of polynya area in the presence of relatively static ice features [Tamura et al., 2007; Kern et al., 2007]. Tamura et al. [2007] developed a method to differentiate between these surface types. To initially identify potential thin ice (0-20 cm), their method takes advantage of the negative relationship between polarization ratios (PR), which is the normalized difference between vertical and horizontal brightness temperature, and thin sea ice thickness. The basis of this relationship depends on the increase in brightness temperatures with salinity and decrease in salinity with thin ice thickness. The thin ice detection is applied per pixel so it is not affected by changes in the extent of the region of interest, which also allows it to be applied to the circumpolar Antarctic at once. Then, a supervised classification is used to identify and mask relatively static ice features such as landfast ice, icebergs, ice tongues, continental ice, and ice shelves.

To measure polynya area, the current study makes use of the thin ice location capabilities of the method from Tamura et al. [2007] without need for actual thickness estimation. The following explanation of the polynya detection algorithm focuses on the 85GHz frequency data. 91GHz data are interchangeable in all 85GHz applications. Before the algorithm is enacted, the 37GHz data

are first resampled onto a 12.5 km grid to match the higher frequency data's spatial resolution (using method from Figure 2 of Tamura et al., 2007). Then, the PR is calculated for the 85GHz (and 37GHz) data. Pixels with PR_{85} values greater than 0.0495 are designated as open water or ice thinner than 10 cm. The remaining pixels with PR_{37} values greater than 0.0571 are designated as ice ranging 10–20 cm in thickness.

Some limitations of the thin ice thickness algorithm are not directly applicable to the current study but are important for further adaptations of the algorithm into future studies. First, their algorithm has discontinuities at the threshold between the PR_{85} and PR_{37} outputs, at a thickness of 10 cm. Second, there are discrepancies in thickness output from data at the two frequency levels. Third, susceptibility to atmospheric moisture causes erroneous thickness values.

To account for overestimation of polynya area, the static icescape features are located. Since onshore cover types are dominated by virtually static ice, changes in their polarization distribution should match that of similar coastal pixel types. The V85 and H85 polarization distribution of onshore pixels (50-250 km inland) are plotted. An ellipse is then drawn, centered at the means with amplitudes of 2.5 times the V&H standard deviations fitted along the major and minor axes, respectively. Then, coastal and offshore pixels (50 km inland to 250 km offshore) are plotted on the same axes. Offshore pixels within the ellipse are flagged as potential static ice features. This process is repeated twice daily. Tamura et al. [2007] determined that coastal and offshore pixels that fall within the ellipse at least 70% of the time are regarded as a static ice feature. In the current study, thresholds of 70%, 85%, and 92% are used to determine icebergs, the coastline, and other landfast ice features, respectively, because in our application of the algorithm, the output achieved using those values matched the fast ice distribution presented by Tamura et al. [2007].

Different icescape features are detected over various lengths of time depending on their general speed of change. The coastline is the most static and is detected at monthly time steps. However, to increase accuracy, the process is conducted using three consecutive months of data to determine the coastline extent during the middle month. For the faster moving landfast ice features, the process is conducted monthly using one month of data. The coastline and landfast ice may be applied to the entire Antarctic continent at once. Since icebergs are able to move out of a coastal region within a few months, detection is carried out over a five-day period and confined to the ice berg active regions of the Ross Sea, Adelie Land, Prydz Bay, and Weddell Sea.

A coastal polynya is identified as any thin ice area within the search regions that is completely detached from the open ocean by an ice bridge. Figure 1a shows percent frequency of occurrence for Antarctic coastal polynyas from April to October, 1992 to 2017. The search regions are displayed as white boxes. They are small enough to focus on coastal dynamics, and large enough to include changes in polynya area due to migrating icebergs. Of the 70 Antarctic coastal polynyas identified, this study focuses on the 25 polynyas at least 1562.5 km^2 in size, which is the area of 10 SSM/I 85 and 91 GHz pixels. Focusing on 25 circumpolar polynyas allows better analysis of co-variability. Smaller polynyas occur much less frequently and have relatively low variability. Some are even closed most of the winter. Virtually all polynya ice production occurs in the largest 25 polynyas. Tamura et al. [2007] identifies 13 Antarctic coastal polynyas as the largest contributors to Antarctic polynya sea ice production. All 13 are included in the 25-polynya system analyzed in the current study. The general size, geometry, frequency of occurrence, and location of the 25 polynyas are shown in Figure 1b. The color-coded regions correspond to areas with at least 30% polynya occurrence throughout the study period. Each polynya is numbered. The table in Figure

1 displays corresponding polynya numbers, names, and abbreviations. The names represent the geographic features near which each polynya develops. Figure 1c displays relevant place names.

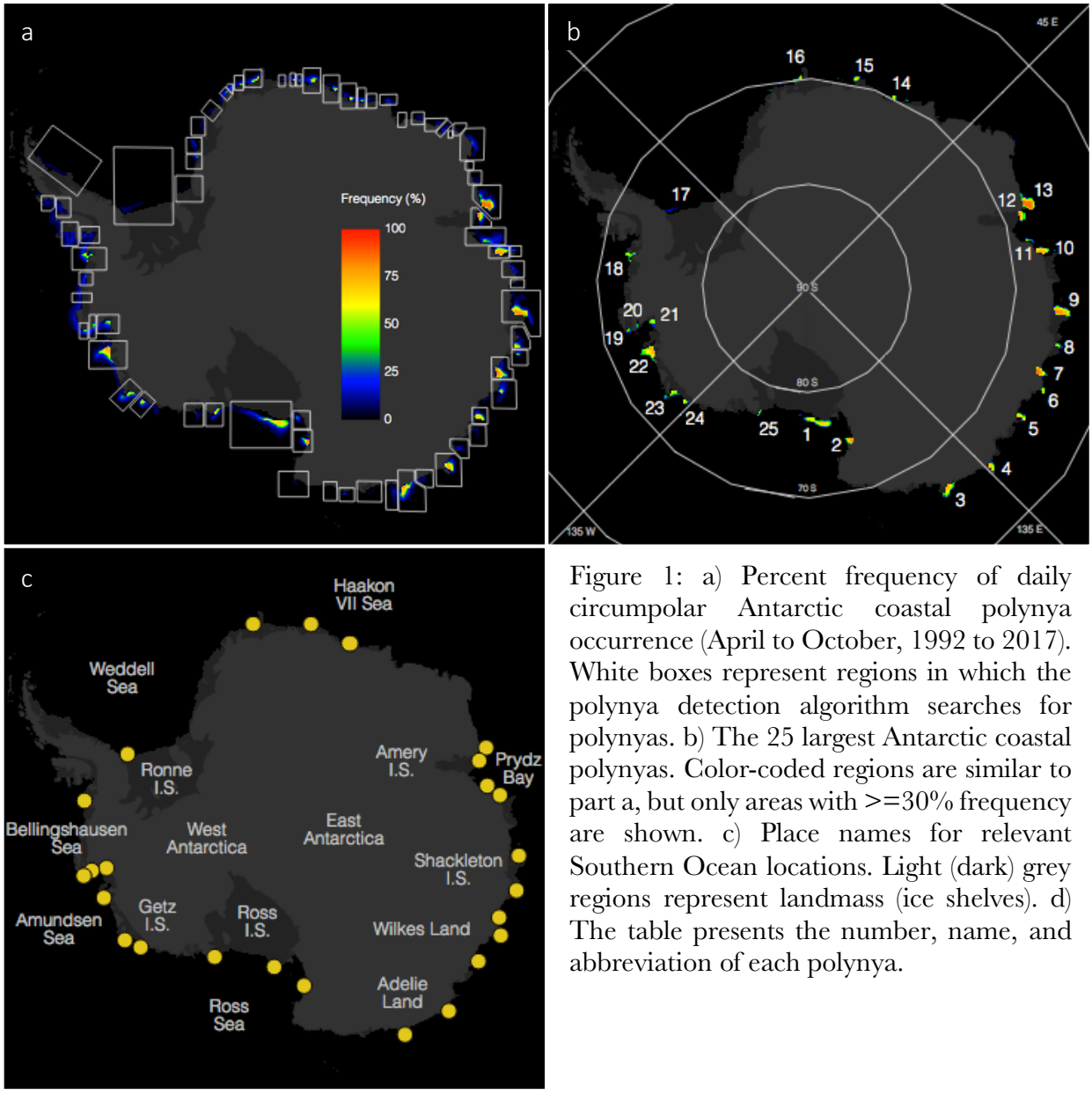

Figure 1: a) Percent frequency of daily circumpolar Antarctic coastal polynya occurrence (April to October, 1992 to 2017). White boxes represent regions in which the polynya detection algorithm searches for polynyas. b) The 25 largest Antarctic coastal polynyas. Color-coded regions are similar to part a, but only areas with >=30% frequency are shown. c) Place names for relevant Southern Ocean locations. Light (dark) grey regions represent landmass (ice shelves). d) The table presents the number, name, and abbreviation of each polynya.

1.	Ross Ice Shelf	(RIS)	14.	Breid Bay	(BrB)
2.	Terra Nova Bay	(TNB)	15.	East Lazarev Ice Shelf	(ELIS)
3.	Mertz Glacier	(MG)	16.	Jelbart Ice Shelf	(JIS)
4.	Dibble Glacier	(DG)	17.	Ronne Ice shelf	(RON)
5.	Dalton	(Da)	18.	Bellingshausen Sea	(BS)
6.	Cape Poinsett	(CP)	19.	Ferrero Bay	(FB)
7.	Vincennes Bay	(VB)	20.	Cranton Bay	(CB)
8.	Shackleton Ice Shelf	(SIS)	21.	Pine Island Bay	(PIB)
9.	Davis Sea	(DS)	22.	Amundsen Sea	(AS)
10.	Barrier Bay	(BaB)	23.	Wrigley Gulf	(WG)
11.	Prydz Bay	(PB)	24.	Getz Ice Shelf	(GIS)
12.	Mackenzie Bay	(MB)	25.	Okuma Bay	(OB)
13.	Cape Darnley	(CD)			

2.3 Method of trend analysis

To analyze the size variability of the polynyas in the circumpolar system, as well as the interaction between polynyas and large-scale systems, the general trend and annual, seasonal, monthly, and daily variability are separated into distinct components. This allows direct testing of polynya variability at various temporal scales. Each component is removed from each individual polynya data series successively using multiplicative linear regression models. This type of model accounts for changes in polynya variability which are functions of mean polynya size. The long-term trend, interannual variability, seasonality, and monthly means are calculated and extracted from the original daily data. The stepwise application results in uncorrelated temporal components, which is important for identifying influential scales of variability and interactions with other phenomena.

3. Statistical profiles

3.1 Total circumpolar polynya system

The circumpolar polynya system has a total mean area of $119 \times 10^3 \pm 70 \times 10^3$ km^2 with a statistically significant positive trend, discussed below. Its daily, monthly, seasonal, and interannual variability account for approximately 48%, 17%, 26.5%, and 4% of the total variability, respectively (Figure

2a). The unrepresented 4.5% of circumpolar variability is attributed to differences created by standardization. The disproportionately large amount of variability at the daily and seasonal levels underscore the need for studies of drivers at those two particular time scales. While many past polynya studies focus on interannual variability, Figure 2 shows that only a very small amount of polynya variability occurs at the annual scale. Figure 2 shows the relative contribution from each temporal component (daily, monthly, seasonal, and interannual) to the total circumpolar variability. Figure 2b also displays the relative contributions of each temporal component to the scaled circumpolar variability, which is calculated as the daily mean of the 25 individually standardized polynyas. This reduces the unequal influence of larger polynyas, such as the RIS, DB, BD, and AS (#1, 9, 13, 22, respectively; Figure 3a). The mean scaled circumpolar variability has a smaller (larger) contribution from daily (seasonal) scale variations.

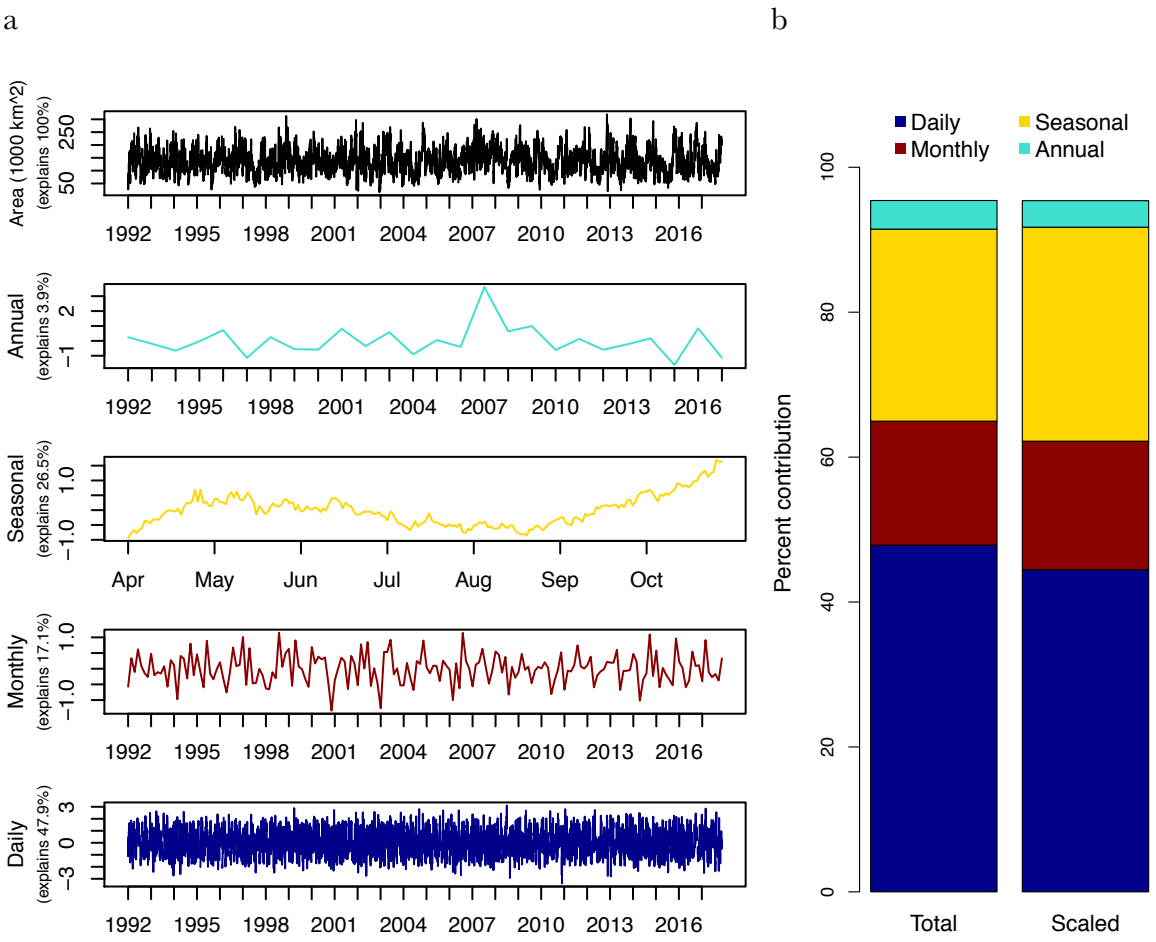

Figure 2: a) Time series decomposition of total area from the largest 25 Antarctic coastal polynyas. The top panel displays the original daily total polynya area. b) Percentage of total variability contributed by variability at various temporal scales. The height of each segment corresponds to the correlation (r^2) between the corresponding component and the original daily area variability. The right stacked bar displays the percent contribution using scaled polynya area, which accounts for mean sizes between each polynya. Thus, each polynya is weighted equally. In parts a and b, blue, red, gold, and turquoise represent variability at the daily, monthly, seasonal, and interannual scales.

There is a strong positive association between coastal polynya size and variance. The strength of this relationship varies between individual polynyas systems (Figure 3a). Accounting for the change in variance with mean size, by not allowing that relationship to propagate from the original polynya variance through the various temporal components, allows more straightforward comparisons to other features. This is done using standard deviations instead of raw deviations for each temporal component. While statistically significant, the generalized trend in total circumpolar polynya area accounts for less than 1% of the cumulative circumpolar system's total variability. Thus, the unrepresented portion (4.5%) is almost entirely attributed to the standardization method. The detailed trend analysis provided in later sections of this chapter describes the lack of contribution from generalized trends.

3.2 Individual polynya systems

The mean size and standard deviation of the 25 polynyas is 4,760 and 6,120 km^2, respectively. Here, it is noted that polynya variability is skewed to smaller sizes so the standard deviation does not capture the spread of a normal distribution. Figure 3b displays the percent contribution of each temporal component to each polynya. Calculations are similar to that of Figure 2b. On average, 53.5%, 16.2%, and 9.1% of polynya variability occurs at the daily, monthly, and seasonal scales, respectively. Interannual variability and the linear trend only account for 5.3% and 0.5% of polynya variance on average, respectively. Analyzing the statistical profiles of each polynya reveals an approximately 17% smaller contribution from seasonal scale variability. Thus, each polynya does not contribute to the seasonal variability discussed earlier in this chapter.

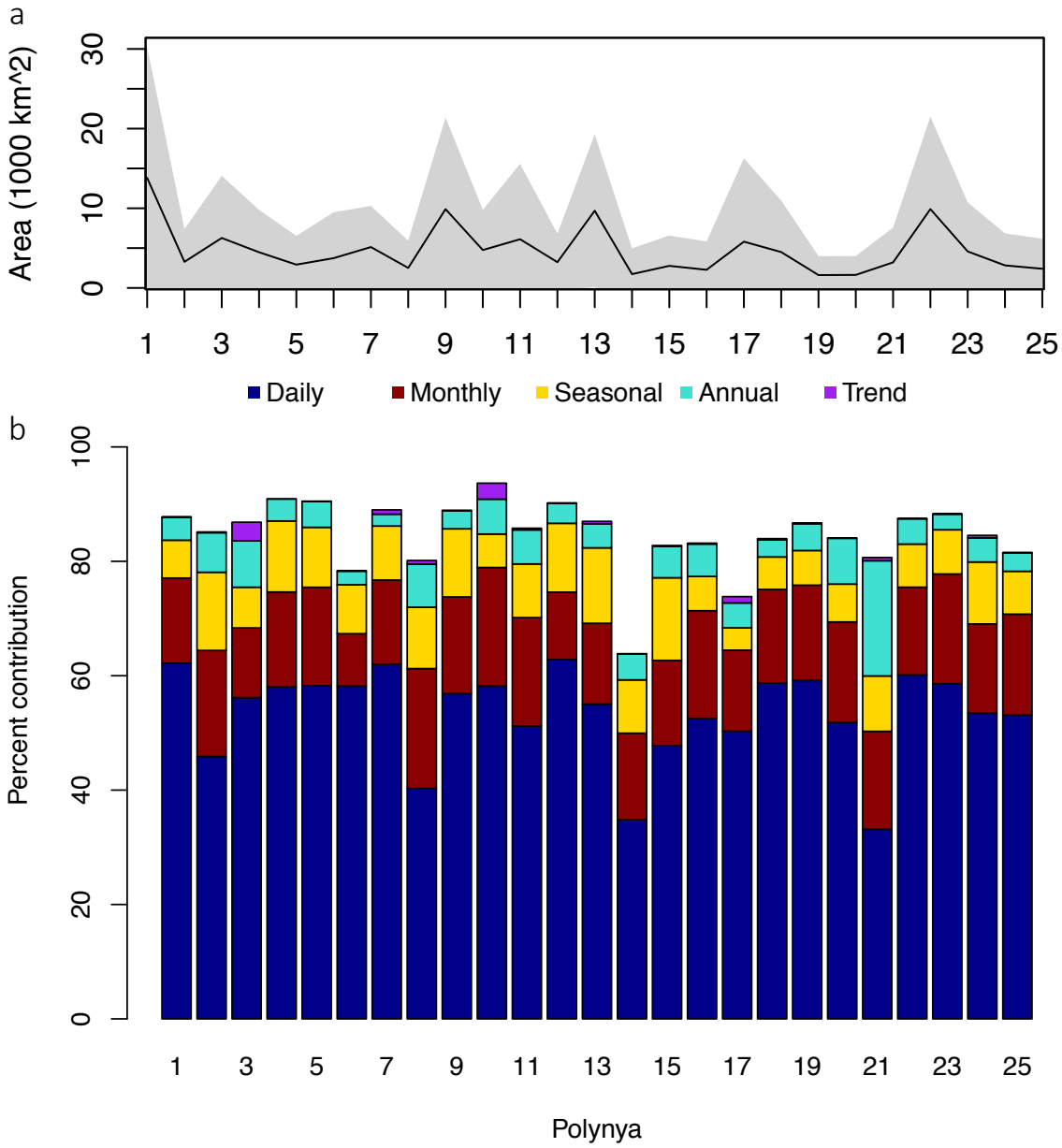

Figure 3: a) Mean area and standard deviation for each of the 25 largest Antarctic coastal polynyas. Black line indicates the mean. Grey region represents values within one standard deviation from the mean. Time series range April to October, 1992 to 2017. b) Scales of variability for the 25 largest Antarctic coastal polynyas. Different colors represent percent contributions from different temporal components.

3.3 Trend analysis

Even when generalized, the statistically significant trend in daily cumulative circumpolar area accounts for less than 1% of the overall system variability. However, there is much variation in polynya trend over space and time. Figure 4 shows spatial clustering in the direction of polynya trends. Polynyas between the Ross Ice Shelf and Adelie Land coasts (#25 and 1-3) constitute a group with predominantly negative trends. This group contains 2 weak positive trends and one statistically significant negative trend. Polynyas spanning Wilkes Land, the Shackleton Ice Shelf, and eastern Prydz Bay (#4-10) coasts have exclusively positive trends. 2 of them have statistical significance trends. Polynyas between Prydz Bay and the Weddell Sea are strongly negative. This span of coastline has 2 polynyas with positive trends and 2 polynyas with statistically significant negative trends. Bellingshausen and Amundsen Sea polynyas (#18-24) exclusively exhibit positive non-significant trends. The 2 positive trending groups are spatially compact, while the 2 generally negative trending groups range much larger distances.

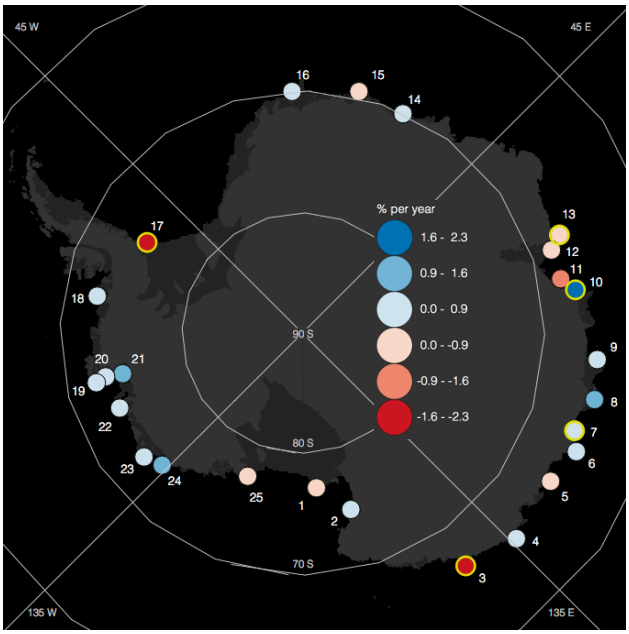

Figure 4: Linear trends (% change per year) for each of the 25 largest Antarctic coastal polynyas during April to October, 1992 to 2017. Red and blue points represent negative and positive trends, respectively. Color intensity corresponds to the strength of the trend. The five yellow point outlines indicate statistically significant trends in polynya size at the 90% significance level.

Antarctic coastal polynyas generally lack any significant long-term trends, but the MG, CD, and RON (#3, 13, 17, respectively) do have statistically significant negative trends, and the VB and BaB (#7 and 10, respectively) have statistically significant positive trends (Figure 4, indicated by yellow outline). However, considerations must be made when interpreting their trends. The MG (#3) has a strong negative trend due to the Mertz Glacier Tongue calving event of 2010 [Campagne et al., 2015; Nihashi and Ohshima, 2015; Shadwick et al., 2013], which removed the ice motion blocking feature partially responsible for its large size. The RON (#17) has a strong negative trend associated with a change in its general behavior starting in 2009 when its interannual mean and variance became greatly reduced. The CD (#13) has a strong negative trend due to its significantly low mean area in 2009, potentially due to an iceberg which limited ice motion in the western Prydz Bay. Thus, the trends in the MG, RON, and CD are most likely due to changes in the positioning of local icescape features whose influence on polynya size must be considered when analyzing areal dynamics.

The VB and BaB (#7 and 10, respectively) of eastern Wilkes Land and western Prydz Bay, respectively, have strong positive trends indicating their gradual increase in area throughout the study period. The increases are not associated with changes in iceberg or ice tongue locations. In both polynyas, the greatest increase occurs from 1992 to 2002, with no significant change after that. Thus, adjusting for linear trends in any polynya will lead to misrepresentation of other temporal components. Accounting for significant trends must be done for step increases (or decreases) as the significant trends are not linear or constant throughout the study period.

The MG (#3) that forms along the Adelie Land coast, will serve as a case to illustrate the statistical preparation of the dataset. The 2010 calving event of the Mertz Glacier Tongue caused a regime

shift in the MG [Campagne et al., 2015]. Particularly, the mean size and variability were greatly reduced. However, the linear decline is not representative of daily, monthly, or seasonal variability. Instead, the polynya has two periods of relatively stable size and variability – before and after the calving event. Thus, generalized linear trends, such as the ones reported in previous studies, are not included in the following chapters of this study. Instead, the inconsistent step declines in polynya area are accounted for at the interannual level. Performing polynya time series decomposition (the process of separating the data into temporal components) without accounting for linear trend reveals that the interannual component does sufficiently account for virtually 100% of the step declines and increases in area. The events and phenomena that cause these step changes usually last the entirety of a winter season such as with some ice bergs, or they may last decades to centuries such as ice tongue calving events. Thus, in later chapters of this study, the trend components (represented as purple in Figure 3a) are reattributed to the annual components (blue), while the daily, monthly, and seasonal components are unchanged.

The change in size variability associated with the MG (#3) regime shift is considered by use of the multiplicative model. After the 2010 event, polynya area fluctuated on a much smaller scale. This change has complicated correlations with long-term daily surface wind and temperature patterns in previous studies [Nihashi and Ohshima, 2015]. Using the multiplicative model to measure standard deviations instead of raw deviations allows proper co-variability analyses with other features, such as other polynyas, surface wind and temperature, and large scale atmospheric changes, because the local regime shift is not reflected in the other features.

The lack of general linear trends in the polynyas are largely due to the seasonality of the trends. Polynyas in the Bellingshausen and Amundsen Seas (#18-24) are getting smaller in April and larger

in October (Figure 5). This may suggest an earlier start and end to the polynya seasons (time of year when the polynya is disconnected from the open ocean). This region had the greatest rate of decrease in sea ice concentration [Liu et al., 2004]. This agrees with the earlier sea ice retreat presented by Stammerjohn et al. [2012] in that region. They found that near the Bellingshausen and Amundsen coasts sea ice concentration tends to decline below 15% earlier throughout their study period. That physical phenomenon corresponds to early polynya expansion and subsequent connection to the open ocean, which marks the end of the polynya season.

The later start to the sea ice advance season reported by Stammerjohn et al. [2012] in the same region disagrees with the earlier start to the polynya season found in the current study. This may result from significant differences in the metrics of interest. Stammerjohn et al. [2008] uses a 15% ice threshold to track the ice edge, which is near the coast on days of advance and far from the coast on days of retreat. The current study examines the rate of change in polynya area, which is exclusively coastal. Thus, days of advance are aligned with the start of the polynya season, while days of retreat are temporally misaligned with the end of the polynya season because they are spatially disconnected. With shifts toward an earlier start and end to the polynya season, the seasonal duration may be stable. The lack of significant trends in April and October in most of the other polynyas suggests no significant change in the start and end of their polynya seasons.

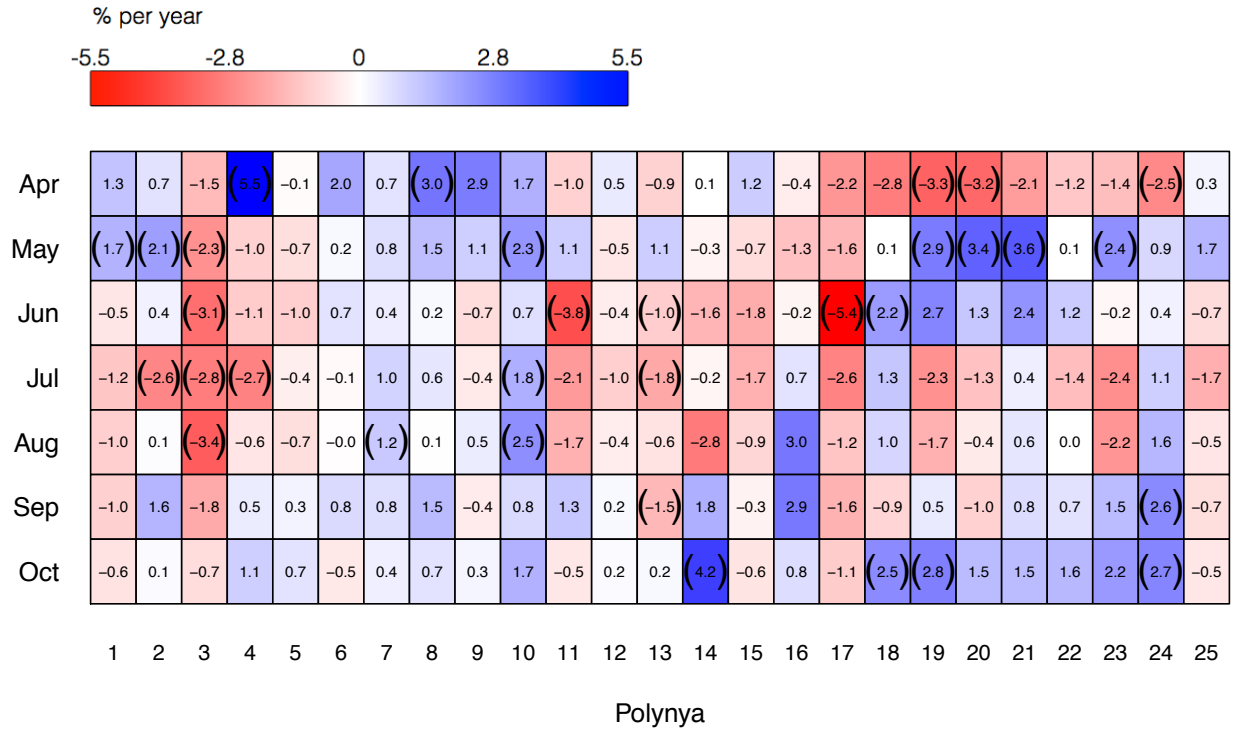

Figure 5: Monthly changes in each Antarctic coastal polynya trend. Red and blue represent negative and positive trends, respectively. Color intensity corresponds to strength of trends. The values in each cell indicate percent change per year. Curved brackets indicate months in which the corresponding polynya has statistically significant trends. Monthly trends are reported for winter months (Aril to October), 1992 to 2017.

The Ross Sea polynyas (polynyas 25, 1, 2) have relatively strong positive trends in April and May; polynyas 1 and 2 have statistically significant trends in May. Polynyas 25 and 1 have negative trends June-October, while polynya 2 stays at least slightly positive June-October, except during its statistically significant decline in July. This strong negative trend in July is consistent with polynyas 3 and 4's significant negative trends in July. The Ross Sea experienced the greatest rate of increased sea ice concentration in the Southern Ocean [Liu et al., 2004].

The MG (#3) has negative trends in all seven months with statistically significant trends from May to August. This reflects the long-term effects of the regime shift after the 2010 ice tongue calving event. Thus, similar patterns of persistent unidirectional trending in other polynyas are expected to possibly represent similar regime shifts. The RON polynya (#17) also has constant negative trends with a statistically significant trend in July, which is the strongest of all negative monthly trends.

Polynyas spanning between western Wilkes Land and the eastern Prydz Bay (#6-10) represent an entire region with predominantly positive trends throughout the season. 3 of the 5 polynyas in this region have at least one statistically significant positive trending month. The 2 polynyas with statistically significant positive trends at the broader annual scale, VB and BaB (#7 and 10, respectively), are located in this region (Figure 4). It is possible that the strong trends in the VB and BaB may be the result of larger scale phenomena that govern long-term regional changes. The strong positive trends in April may reflect a slightly earlier start to the polynya season in that region.

The PB, MB, and CD (#11-13, respectively) are all located in the Prydz Bay and have negative trends through most of the season. The PB and CD have statistically significant negative trends during at least 1 month. The Prydz Bay is an active icescape region that produces a great amount of polynya-generated sea ice. In comparison, the Haakon VII Sea polynyas (#14-16) have no inter-polynya consistency in their general and monthly trends.

The RIS, MG, CD, and RON (#1, 3, 13, 17, respectively) are the most significant sites of major sea ice production, brine rejection, and bottom water formation [Tamura et al., 2016]. 3 of the 4 have extreme negative trends in areal extent. The RIS does not have a strong negative trend

overall, but it has consistent non-significant negative trends from July to October that are offset by a statistically significant positive trend in May. With the significant relationship between polynya ice production and areal extent [Tamura et al., 2016], the consistent negative trends among the 4 polynyas suggest they have become less productive throughout the study period. If this tendency persists, it may have far-reaching implications such as a reduction in the deep-water formation that feeds into the Thermohaline Circulation. While not sources of major deep water formation, the VB, SIS, BaB, and AS (#7, 9, 10, 22, respectively) are the next largest sea ice producers [Tamura et al., 2016]. All 4 have positive trends in areal extent. While the SIS and AS are larger and more productive, the VB and BaB have much greater total growth. Thus, continued growth in these 4 polynyas may eventually allow them to become much more important contributors to total circumpolar polynya-generated sea ice in the future, especially with the declines in the current major ice producers.

4. Conclusion

A 26-year circumpolar Antarctic coastal polynya dataset was created to analyze multiscale polynya variability and long-term trends. In past studies, polynya variability at daily, monthly, and interannual scales are most frequently analyzed. However, analyses of seasonal scale variability and multiyear monthly trends are missing from the current literature. In addition, common practice in previous polynya studies uses simple calculations to determine system trends without accounting for various temporal components. Studies using more robust processes to account for the different temporal components may produce more accurate and interpretable results, better analyses of polynya dynamics at different scales, interactions with other climatic drivers, and predictions.

The large proportion of polynya variability at the monthly and seasonal levels promote the need for studies of drivers at those two particular scales. While many past polynya studies focused on interannual variability, a very small amount of polynya activity varies at the annual scale. Many past studies do focus on daily polynya variability so short-term, local scale interactions between surface atmospheric drivers for polynya variability are generally well understood compared to the larger-scale variations.

The cumulative circumpolar system of 25 coastal polynyas experiences total variability at the daily, seasonal, monthly, and annual scales, in descending order of percent contribution to total cumulative variability. The total Antarctic polynya system area has a statistically significant positive trend throughout the study period. However, only five individual polynya systems experience statistically significant long-term trends – 3 negative and 2 positive. This suggests that considerations must be made when interpreting the trends. Two of the significant negative trends are due to abrupt, long lasting regime shifts characterized by reductions in their mean and variability. The third significant negative trend is primarily driven by a single year of anomalously large extent caused by a calved iceberg migrating out of the region. The two significant positive trends occur as gradual increases in polynya size. The increases are not associated with changes in iceberg or ice tongue locations. In both polynyas, the greatest increase occurs from 1992 to 2002, with no significant change after that.

Each of the 5 statistically significant trends is more complex than simple linear models are able to capture. Studies of polynya trend, variability, and interaction with other features require less generalized representation of long-term increase or declines. The abrupt changes in polynya size

that drive the significant trends is better modeled as step changes, which are captured well by interannual variability.

The general linear trends exhibit spatial clustering, which delineate 4 major regions. Two of these have exclusively positive trends, and the others experience predominantly negative trends. The 5 polynyas that exhibit statistically significant trends exist within regions of corresponding dominant trend directions. This means the significant positive trends exist within a larger region of exclusively positive trends, and the significant negative trends exist within the regions of predominantly negative trends. While significant trends seldom occur at the annual scale, they are much more frequent at the monthly scale. Polynyas in the Bellingshausen and Amundsen Seas experience negative (positive) trends in April (October), which may suggest an earlier start (end) to the polynya season in the region.

The 4 historically most productive polynyas (the Ross Ice Shelf, Mertz Glacier, Cape Darnley, and Ronne Ice Shelf polynyas) decreased in areal extent, and thus ice production, throughout the study period. The Vincennes, Shackleton, Barrier, and Amundsen polynyas, the next largest producers of coastal sea ice, experienced increases in areal extent throughout the study period. Thus, the greatest contributors to polynya area and ice production may change as current tendencies continue.

Chapter 3

The multi-temporal influence of large-scale atmospheric patterns

1. Introduction

Strong, persistent surface winds rushing from the continental ice sheet are thought to be the primary drivers of coastal polynya development and variability [Nihashi and Ohshima, 2015; Kwok et al., 2007; Bromwich et al., 1998; Bromwich and Kurtz, 1984; many more]. However, this may not be the case for all Antarctic coastal polynyas. Studies on fast ice dynamics have given part of the credit to motion-blocking ice features such as the Drygalski Ice Tongue that forms the Terra Nova Bay and the Mertz Glacier Ice Tongue at the Adelie Land coast [Tamura et al., 2016; Nihashi and Ohshima, 2015; Lacarra et al., 2014; Kusahara et al., 2011; Tamura et al., 2007; Frezzotti and Mabin, 2004; Adolphs and Wendler, 1995; Kurtz and Bromwich, 1985]. Other studies have investigated the assistance that local offshore winds receive from larger systematic changes either on the coastal ice front, from the inland glacier passages, or meso-scale storm systems [Parish et al., 1993; Bromwich and Kurtz, 1984]. As continental air masses move through coastal glacier ridges they compress and increase wind velocity [Bromwich and Kurtz, 1984]. This wind enhancement is not continuous, but it is very frequent and reliable. As storm systems circle the continent, they increase surface wind speed and alter wind directions [Kwok et al. 2007; Parish et al., 1993]. To a lesser degree, studies have also investigated potential connections between coastal polynya variability and large-scale atmospheric patterns [Bromwich et al., 1998; Campagne et al., 2015]. Large-scale atmospheric phenomena influence general zonal and meridional air flow, and the frequency and strength of storm activity near the Antarctic coast [Gordon et al., 2007; Bromwich et al., 1998].

Changes in coastal polynya size are linked to wind-driven sea ice advection and thermodynamic processes that determine ice production rates [Holland and Kwok, 2012]. Surface winds may be enhanced or dampened by the Southern Ocean (SO) pressure field and its connections to large-scale upper atmospheric circulations [Turner et al., 2016]. With complex multiscale interactions, understanding the dynamics and relationships within the atmosphere-sea ice-ocean system will improve general understanding of current environments and help anticipate future climates. This chapter describes the role of polynyas in this integrated system, focusing on the influence that large-scale atmospheric circulations have on coastal polynya variability.

Currently, polynya literature lacks deep investigation and commentary on relationships between coastal polynyas and large-scale atmospheric circulations. Arrigo and van Dijken [2003b] pointed out that during their 6-year study, years of anomalously low Ross Sea Polynya area were concurrent with nearshore iceberg calving events and a strong positive El Niño-Southern Oscillation (ENSO) event, showing the importance of these 2 processes. During the same ENSO event, an unusually large summertime open water region, referred to as the Ronne Polynya, developed [Arrigo and van Dijken, 2003a; Ackley et al., 2001], showing the spatial asymmetry of polynya responses to ENSO.

Montes-Hugo and Yuan [2012] analyze the influence that the Southern Annular Mode (SAM), ENSO and other climate patterns have on the size of phytoplankton blooms in 4 Antarctic coastal *post-polynyas* – the full extent of open water areas that combine during the spring melt [Arrigo and van Dijken, 2003a]. The 4 regions include the Amundsen Sea (spans 4 polynyas in the current study), the western Ross Sea (spans 2 polynyas), Dumont d'Urville (1 polynya), and Prydz Bay (4 polynyas). The size of the bloom is correlated with the size of the post-polynya [Arrigo and van

Dijken, 2003a], thus, providing some insight into atmosphere-polynya relationships. They found a strong relationship between the SAM and concurrent bloom size in Dumont d'Urville. While their study covers 4 regions of major wintertime sea ice production and deep-water formation, phytoplankton bloom production is most active during spring-summer, which leads studies to focus on summertime open water conditions that mask or exclude winter polynyas. The current study focuses on interactions during the polynya season, April to October.

Bromwich et al. [1998] analyzes 4 years of automatic weather station data to link ENSO with polynya-producing katabatic surge events in coastal Ross Sea, Antarctica. Park et al. [2018] compares nonlinear trends within the annual area of the Ross Ice Shelf Polynya to the SAM and ENSO. They found that trends in RISP area and the RISP season timing are influenced by trends in ENSO and the SAM, respectively. Tamura et al. [2016] correlated the SAM and ENSO indices with circumpolar Antarctic coastal polynyas. They found generally weak correlations with both.

Very few studies analyze circumpolar relationships and none provide an in-depth regional analysis. Also, many studies are done at annual or 3-month seasonal time scales that are too broad to capture much of the co-variability. Broad timesteps also prevent potentially meaningful lagged co-variability analysis. The current study analyzes the concurrent and lagged monthly relationships between large-scale atmospheric circulation patterns and small scale coastal polynyas.

The link between large-scale atmospheric patterns and Antarctic coastal polynyas arise from the atmospheric patterns' influence on surface winds and the sea ice field. However, the connection is often complicated by coastal geometry, which influences direction of growth [Nihashi and Ohshima, 2015; Shadwick et al., 2013; Massom et al., 1998]. The most significant Antarctic sea

ice trends occur in the Ross, Amundsen, and Bellingshausen Seas. Thus, much of the recent popular literature on atmosphere-sea ice interactions has focused on mechanisms most influential around West Antarctica. The current study investigates the major large-scale atmospheric contributors to changes in the sea ice field, such as the SAM, ENSO, and the Amundsen Sea Low (ASL).

Southern Annular Mode

The SAM, alternatively known as the Antarctic Oscillation (AAO) and High Latitude Mode (HLM), is a mostly annular structure of opposing upper tropospheric pressure anomalies in the mid and high Southern Hemisphere latitudes. It is the primary mode of climate variability in the extratropical and high latitude Southern Hemisphere [Trenberth et al., 2007; Marshall, 2003; Thompson and Solomon, 2002; Thompson and Wallace, 2000a, 2000b]. Its significant influence is visible through temporal co-variations in the upper tropospheric pressure, wind, and sea ice fields [Simpkins et al., 2012; Hall and Visbeck, 2002; Arblaster and Meehl, 2006; Marshall, 2003]. Variability in mid-high latitude temperature and pressure gradients cause changes in the latitudinal position and magnitude of the polar front westerlies. Increased upper troposphere pressure gradients resulting from negative (positive) pressure anomalies in the high (mid) latitudes are identified as a positive SAM (+SAM) phase [Marshall, 2003]. In this case, the polar front jet (PFJ) stream is strengthened, the circumpolar trough shifts poleward, and mean westerly atmospheric flow is enhanced on the polar front. The reverse occurs during negative SAM (-SAM) phases where positive high (negative mid) latitude upper troposphere pressure anomalies cause a decrease in the pressure gradient, PFJ, latitude of the circumpolar trough, and westerly airflow [Turner et al., 2016].

An important process by which the SAM influences the SO ice field is through the meridional component of its circulation. Ekman transport deflects air perpendicular to its zonal flow to produce southerly winds to the north. Increased zonal winds associated with +SAM enhance southerly airflow and ice extent. The weakened zonal flow associated with -SAM leads to weaker southerly ice advection and smaller sea ice extent [Hobbs et al., 2016; Marshall, 2003; Hall and Visbeck, 2002; Kwok and Comiso, 2002b]. As +SAM enhances sea ice transport away from the coastline, it may reduce compaction in the coastal margins and allow polynyas to expand. This would be most prevalent in regions dominated by meridional ice motion, such as the Ross and Weddell Seas where 2 rapid ice producing polynyas form (Figure 1a-b). In regions of predominantly zonal ice flow, such as East Antarctica, variations in zonal ice transport may have a larger effect on polynya size variability than southerly flow. Thus, variability in the westerly winds associated with the SAM may provide the greatest SAM-induced responses in many of the Antarctic coastal polynyas.

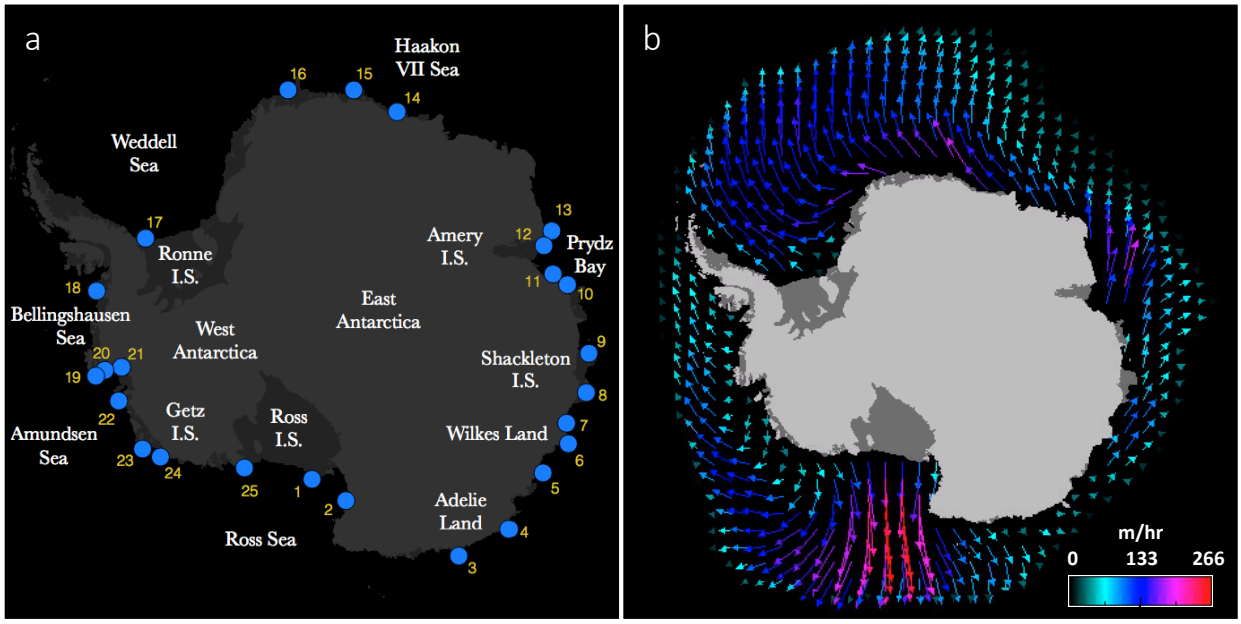

1. Ross Ice Shelf	(RIS)	14. Breid Bay	(BrB)
2. Terra Nova Bay	(TNB)	15. East Lazarev Ice Shelf	(ELIS)
3. Mertz Glacier	(MG)	16. Jelbart Ice Shelf	(JIS)
4. Dibble Glacier	(DG)	17. Ronne Ice shelf	(RON)
5. Dalton	(Da)	18. Bellingshausen Sea	(BS)
6. Cape Poinsett	(CP)	19. Ferrero Bay	(FB)
7. Vincennes Bay	(VB)	20. Cranton Bay	(CB)
8. Shackleton Ice Shelf	(SIS)	21. Pine Island Bay	(PIB)
9. Davis Sea	(DS)	22. Amundsen Sea	(AS)
10. Barrier Bay	(BaB)	23. Wrigley Gulf	(WG)
11. Prydz Bay	(PB)	24. Getz Ice Shelf	(GIS)
12. Mackenzie Bay	(MB)	25. Okuma Bay	(OB)
13. Cape Darnley	(CD)		

Figure 1: a) Locations of the largest 25 Antarctic coastal polynyas with place names for relevant Antarctic continent and oceanic locations. Light and dark grey areas represent landmass and ice shelves, respectively. b) Direction and magnitude of sea ice motion during the polynya season (May-October) of 1992-2016. c) The table presents the number, name, and abbreviation of each polynya.

El Niño-Southern Oscillation

ENSO is an ocean-atmosphere coupled phenomenon characterized by opposing anomalies of sea surface temperature (SST) and sea level pressure (SLP) between the eastern and western tropical Pacific. An ENSO warm phase (El Niño) is characterized by positive SST anomalies and negative SLP anomalies in the east, with reverse conditions in the west [Montes-Hugo and Yuan, 2012; Knuth and Cassano, 2011; Yuan, 2004; Yuan and Martinson, 2001]. During strong El Niño events, Tropical heating in the east tropical Pacific increases convection, strengthening the Hadley and Ferrel Cells and the subtropical jet (STJ) stream. The polar front jet (PFJ) stream weakens, decreasing the number of storms driven to the southern high latitudes and allows high pressure to develop in the Amundsen-Bellingshausen region in the south Pacific. At the same time in the west Atlantic Ocean, negative tropical SST anomalies decrease convection, meridional circulation, and

heat transfer to the Weddell Sea in the south Atlantic [Montes-Hugo and Yuan, 2012; Yuan, 2004; Yuan and Martinson, 2001].

An ENSO cold phase (La Niña) is characterized by negative SST anomalies with positive SLP anomalies in the east Pacific, and vice versa in the west. During strong La Niña events, negative SST anomalies in the tropical Pacific reduce convection, meridional flow, and northerly heat transport. The STJ weakens while the PFJ strengthens and directs more storms to the SO. This allows low pressure to develop in the Amundsen-Bellingshausen region. Corresponding positive SST anomalies in the west tropical Atlantic increase meridional transport of heat to the south Atlantic [Montes-Hugo and Yuan, 2012; Yuan, 2004; Yuan and Martinson, 2001].

The northerly transport of heat is guided by the Rossby wave train – an atmospheric channel that guides tropical climate variations to the high latitudes [Li et al., 2015a, 2015b, 2014; Yuan, 2004]. The Pacific-South American (PSA) pattern is the southern portion of the Rossby wave train that extends to West Antarctica. PSA influence is seen within the SO sea ice field as opposing concentration anomalies between the Bellingshausen and western Ross Seas, known as the 'Antarctic dipole' [ADP; Turner et al., 2016; Yuan and Li, 2008; Stammerjohn et al., 2008; Yuan, 2004; Yuan and Martinson, 2000, 2001]. The ADP response to ENSO is the strongest extra-tropical teleconnection to ENSO on earth [Liu et al., 2002]. Thus, polynya activity in that region is expected to be influenced by ENSO as well.

Amundsen Sea Low

While the SAM is the largest contributor to high latitude Southern Hemisphere climate variability [Trenberth et al., 2007; Marshall, 2003; Hall and Visbeck, 2002; Thompson and Solomon, 2002; Thompson and Wallace, 2000a, 2000b], its non-annular portion has gained attention as a distinct

feature known as the Amundsen Sea Low [ASL – Raphael et al., 2016; Turner et al., 2013] or the Amundsen-Bellingshausen Sea Low [ABSL – Hosking et al., 2013; Fogt et al., 2012]. In the current study, it is referred to as the 'ASL'. The ASL is a climatological low pressure region that develops from cumulative effects from a series of low pressure systems directed to the Bellingshausen, Amundsen, and Ross Seas by the PFJ. As a low pressure region, its cyclonic spin directs southerly (northerly) airflow on its western (eastern) side, promoting pack ice advection anomalies. Studies have analyzed its effects on sea ice distribution through the variability of its magnitude and location [Raphael et al., 2018; Turner et al., 2013; Fogt et al., 2012]. A relatively intense ASL enhances (suppresses) southerly sea ice expansion in the Ross Sea (Amundsen-Bellingshausen region). Thus, the influence of ASL on air and sea ice motion may promote expansion and shrinking of polynyas in the Ross and Amundsen-Bellingshausen Seas as well. Until now, ASL influence on Antarctic coastal polynya variability had not been studied.

Section 2 of this Chapter describes the datasets and methods used in the study. Section 3 presents the results. Section 4 provides a summary and concluding remarks.

2. Data and Methodology

2.1 Datasets

The dataset used in this chapter is the monthly polynya area data set discussed in Chapter 2. Figure 1a shows the circumpolar distribution of the 25 coastal polynyas analyzed in this study. The large-scale atmospheric circulation data were collected from multiple sources as monthly mean values. The SAM index used in the current study is described by Marshall [2003] and is housed at the British Antarctic Survey (BAS). The index is computed as the difference in zonal average mean SLP (MSLP) between the Southern Hemisphere's middle and high latitudes at 45° and 65°S,

respectively, from station data. Positive SAM anomalies represent an increase in zonal pressure gradient and results in intensification of circumpolar westerly winds. The SAM index has a very weak positive trend that accounts for only 0.6% of the total variability in the study period (Figure 2). Its annual, seasonal, and monthly variability account for approximately 24, 4.5, and 71% of the SAM index variability, respectively. SAM seasonality has its winter minimum (maximum) in June (August).

The Southern Oscillation Index (SOI) used to quantify the strength of ENSO and analyze its influence is described and archived by the National Oceanic and Atmospheric Administration. The SOI is computed as the difference in MSLP anomalies in Darwin, Australia and the island of Tahiti. Both are found in the tropical south Pacific. Since Tahiti is farther east, positive SOI anomalies (Tahiti minus Darwin) represent the positive and negative sea surface temperatures of the east and west Pacific, respectively, associated with El Niño. Negative SOI represents La Niña. While the SOI has a general decline over the last half century [Nicholls, 2008], it has a relatively strong positive trend during the study period that accounts for 5.4% of the total variability in the study period. It has virtually no seasonality with interannual and monthly variability accounting for approximately 55.4% and 39% of the total variability, respectively.

ASL data is also housed at the BAS and was created using the method described by Hosking et al. [2013]. 4 indices are provided – actual central pressure (ACP), relative central pressure (RCP), longitude (LON), and latitude (LAT). ACP indicates the minimum pressure within the ASL domain (approximately 60-75^{o}S, 170-290^{o}E). As a raw measure of minimum pressure, ACP is highly influenced by other large-scale processes in the Antarctic such as SAM, ENSO, and the Semi-Annual Oscillation [Coggins and McDonald, 2015]. RCP represents the regional effect of

the climatic low with the large-scale, background influence removed. RCP is computed as the difference between ACP and the actual sector pressure (ASP: the MSLP within the ASL domain). However, RCP is affected by a pressure ridge north of the ASL domain [Raphael et al., 2018], which means the RCP is not completely decoupled from large-scale systems beyond the ASL domain. During the study period, RCP variability is independent of ASP (r=0.00) and significantly linked to ACP (r=0.46). With ASP defined as a regional mean, it has smaller monthly variability (sd=5.45) than ACP (sd=6.15), a single grid point. ACP and ASP are highly correlated (r=0.88), as they are determined by the same large-scale circulation effects.

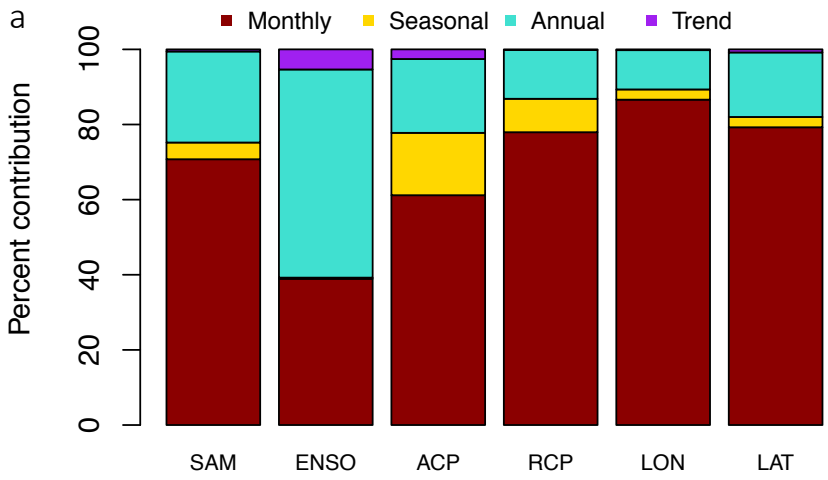

Figure 2: Relative contributions (a) and temporal variability (b-g) of each temporal component (linear trend and annual, seasonal, and monthly scales) to the total variability of large-scale atmospheric circulation patterns – b) the Southern Annular Mode, c) El Niño-Southern Oscillation, and the Amundsen Sea Low's d) actual central pressure, e) relative central pressure, f) longitude, and g) latitude. Units are displayed in standard deviations (b-c), hPa (d-e), and degrees (f-g).

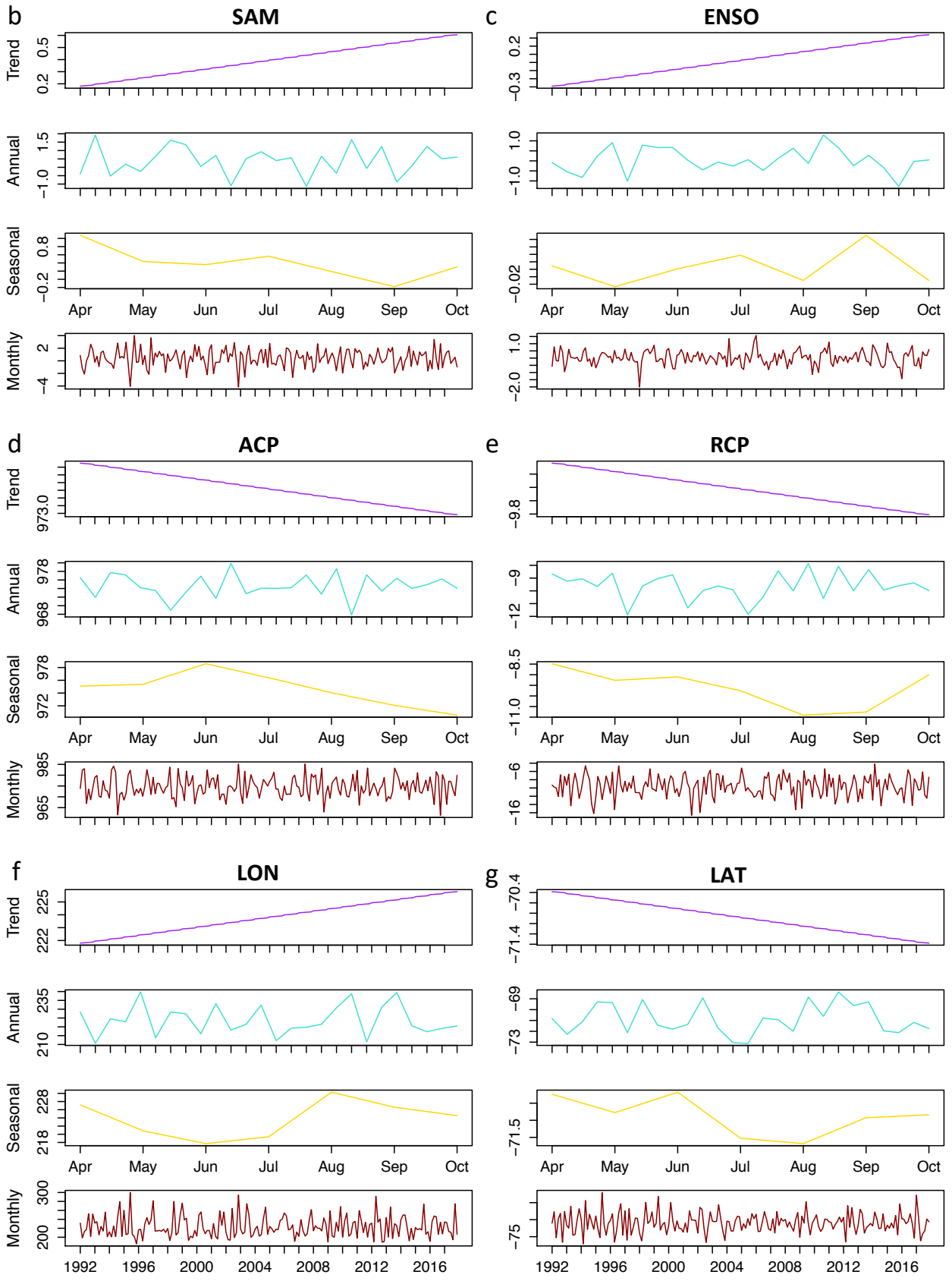
b
SAM
Trend
0.2 0.5
Annual
−1.0 1.5
Seasonal
−0.2 0.8
Apr May Jun Jul Aug Sep Oct
Monthly
−4 2
c
ENSO
−0.3 0.2
−1.0 1.0
−0.02
Apr May Jun Jul Aug Sep Oct
−2.0 1.0
d
ACP
973.0
968 978
972 978
Apr May Jun Jul Aug Sep Oct
965 985
e
RCP
−9.8
−12 −9
−11.0 −8.5
Apr May Jun Jul Aug Sep Oct
−16 −6
f
LON
222 225
210 235
218 228
Apr May Jun Jul Aug Sep Oct
200 300
1992 1996 2000 2004 2008 2012 2016
g
LAT
−71.4 −70.4
−73 −69
−71.5
Apr May Jun Jul Aug Sep Oct
−75
1992 1996 2000 2004 2008 2012 2016

Negative ACP and RCP anomalies represent periods of lower and higher pressure gradients, respectively, a deeper ASL structure, and relatively intense circulation. ACP and RCP have different effects on wind strength and sea ice concentration and extent [Raphael et al., 2018; Turner et al., 2013]. Thus, the two aspects of the ASL may have different influences on polynyas as well. Influence from ASL intensity (ACP and RCP) on surface conditions is complicated by its variable location. During winter, the location of ASL (LON and LAT) controls the spatial variability of its influence [Coggins and McDonald, 2015]. Thus, all 4 ASL metrics are used in the current study.

To analyze the partial contribution of each atmospheric pattern at various temporal scales, a time series decomposition method is applied to each index. For each atmospheric pattern, various temporal components are identified using additive time series decomposition with step-wise regression. Regression residuals from the linear trend are used to determine annual means. Then, the regression residuals from the annual means are used to determine the seasonal cycle. The process is repeated to determine monthly means. Figure 2b-g shows the variability of each temporal component and their percent contribution to the total pattern variability. To align with the temporal range of the polynya dataset and the seasonal definition of a polynya, the atmospheric data were retrieved for the polynya season (April to October) of 1992 to 2017 before the decomposition applied. Atmospheric data for February, March, and November are also utilized in lagged correlations. The decomposition process is reapplied with each lagged correlation.

Decomposition of the ACP and RCP indices reveal negative trends in both. The trend in ACP accounts for approximately 2.6% of its variability; the trend in RCP is negligible. Annual, seasonal, and monthly scale variability accounts for approximately 20, 16.6, and 61% of total ACP

variability, respectively, and 13%, 9%, and 78% of total RCP variability, respectively. Seasonally, ACP intensity has a general increase from April to June, then a consistent decline until October. Including ACP intensity beyond the April to October study period, ACP has a Semi-Annual Oscillation with local minima in April and October [Turner et al., 2016]. RCP intensity has a general decrease from April to August, then increases onto October. ASL location is variable as well with a southeastward trend over the study period. The zonal and meridional components of the trend are both small, accounting for less than 1% of the variability in both directions. Annual, seasonal, and monthly variability account for approximately 10.5, 3, and 86.6% of total LON variability, respectively, and 17, 3, and 79% of total LAT variability, respectively. Seasonally, LON and LAT have concurrent extremes with northern and western maxima in June and southern and eastern maxima in August, respectively. The seasonal variability of all ASL metrics presented are consistent with those found by Hosking et al. [2013] and Turner et al. [2013]. The only notable difference is the northern LAT maximum in May. The temporal range covered by Hosking et al. [2013] is much different than that covered by the current study, which may contribute to the discrepancy.

2.2 Method of analysis

Pearson correlations are used to establish linear relationships between the polynyas and the large-scale atmospheric patterns at the 90% significance level. For each polynya and atmospheric circulation, the full variability is correlated. The full polynya variability is also correlated with each temporal component of the atmospheric circulations. Results from the component correlations are presented as partial contributions to the total relationship. Cross correlation matrices (not shown) indicate no overlap between the temporal components. Thus, each temporal component uniquely contributes to the total correlation.

3. Results

Southern Annular Mode

Relationships between the coastal polynyas and SAM are particularly strong in East Antarctica from Adelie Land to Prydz Bay (Figure 3a). 8 of the eleven polynyas have statistically significant negative relationships suggesting that under +SAM conditions they shrink in size. The strong polynya relationships in that region are primarily driven by seasonal and monthly scale co-variability. The Haakon VII Sea and West Antarctica contain only 2 strong polynya-SAM relationships. Their co-variability is primarily driven at the monthly scale as well. In regions where coastal polynyas form along ice tongues and other meridionally oriented ice features, anomalous zonal ice flow may have a larger effect on polynya size than meridional anomalies. The increased westerly wind associated with +SAM contributes to westerly sea ice flow anomalies. Polynyas that grow with easterly winds, such as most East Antarctica polynyas [Nihashi and Ohshima, 2015], may generally decrease with the enhanced westerly winds of +SAM and increase with the weakened winds of -SAM.

East Antarctica polynyas, particularly between Adelie Land and Prydz Bay, generally form along the western edge of meridionally oriented features and, thus, grow westward toward more marginal ice areas. Two polynyas within this region are not strongly influenced by the SAM. The first of the two, the Shackleton Ice Shelf Polynya (#8), forms within a small bay of the Shackleton Ice Shelf and does not experience much zonal expansion. The second of the two, the MacKenzie Bay Polynya (#12), forms along the eastern edge of a fast ice feature, which prevents growth westward and allows growth eastward. However, its direction of growth is in competition with the direction of mean ice (Figure 1b) flow so it is greatly limited in its eastward expansion as well. This supports

the negative relationships found in the 9 significantly correlated polynyas of East Antarctica, and weak correlations within 2.

The strength and regionality of the significant relationships are much weaker when polynya variability is lagged (Figure 4a). A 1-month lagged response in polynya size is strongest along Wilkes Land, which contains the only statistically significant relationship around the continent. The relationships generally become weaker as the lags increase. Any strong correlations from lagged polynya responses may be due to factors such as hidden autocorrelation not related to linear trends or persistence of the large-scale atmospheric influence. Correlations are also relatively weak with a 1-month lag in the SAM. The region of high correlation shifts to the eastern Amundsen Sea. Any strong correlations from lagged atmospheric responses may be due to confounding relationships with sea ice coverage. For instance, sea ice coverage may produce immediate effects in polynya area but lagged large-scale effects in the atmosphere.

Tamura et al. [2016] reports no statistically significant relationships between SAM and the thirteen Antarctic coastal polynyas they studied. Their correlations use annual cumulative sea ice, instead of monthly polynya size like the current study. With very strong positive relationships between the 2 metrics, the two studies may be compared. Thus, annual polynya-SAM correlations (not displayed) were calculated but no statistically significant relationships were found. This highlights the importance of examining these relationships at different timescales of variability. The majority of the strong polynya-SAM relationships are driven by seasonal and monthly variability, which are both lost in the annual means and cumulative totals that are popularly presented in past studies. Tamura et al. [2016] generally found negative relationships, except in 1 polynya along each of the Ross, Weddell, and Adelie Land coasts.

Montes-Hugo and Yuan [2012] found a statistically significant relationship between mean summertime (December-February) SAM and concurrent phytoplankton bloom size in the Dumont d'Urville open water region, which corresponds to the summer extent of the polynya on the coast of Adelie Land. This strong relationship shows the influence of the SAM in that region, which generally agrees with the findings of this current study. However, they found only a weak relationship between the SAM and the Prydz Bay post-polynya bloom. That finding disagrees with the statistically significant correlation in 3 of the 4 polynyas found in the Prydz Bay in this current study. However, their results are presented for a different season than in the current study and therefore are not directly comparable. Park et al. [2018] found that the long-term nonlinear trend in RISP season timing is driven by the long-term nonlinear trend in the SAM. The current study only presents weak co-variability between the RISP and SAM, but a long-term trend comparison is not included in this study.

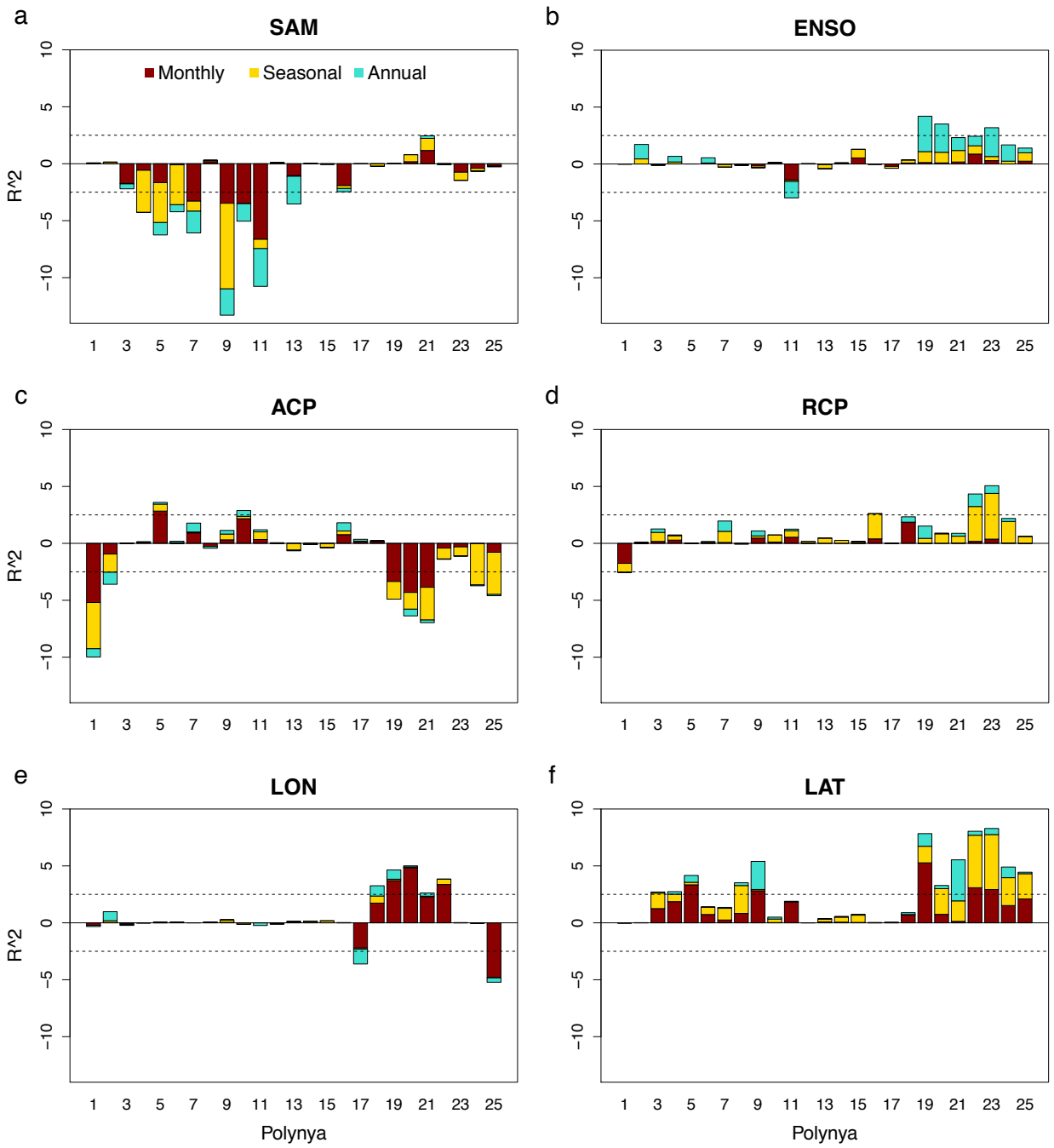

Figure 3: Coefficient of determination (R^2) for 25 Antarctic coastal polynyas correlated against large-scale atmospheric circulations – a) Southern Annular Mode, b) El Niño Southern Oscillation, and the Amundsen Sea Low's c) actual central pressure, d) relative central pressure, e) longitude, and f) latitude. Red, gold, and turquoise represent correlations at monthly, seasonal, and annual

scales of variability, respectively. Dashed lines indicate statistical significance at the 90% level. Data ranges April to October 1992 to 2017. Y-axis scales are consistent for ease of comparison.

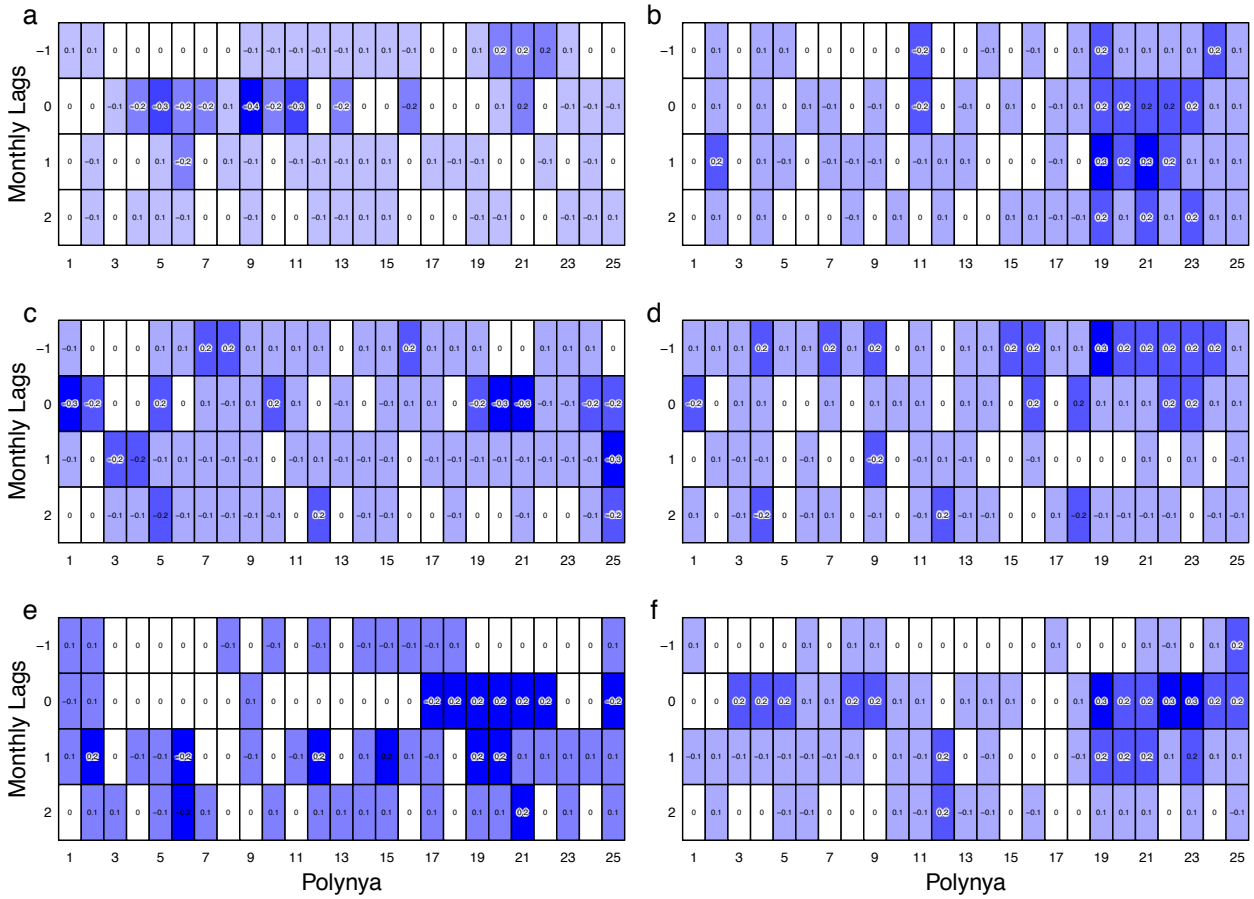

Figure 4: Coefficient of correlation (r) between monthly mean size for 25 Antarctic coastal polynyas and large-scale atmospheric circulations – a) Southern Annular Mode, b) El Niño Southern Oscillation, and the Amundsen Sea Low's c) actual central pressure, d) relative central pressure, e) longitude, and f) latitude. Rows represent monthly lags. Lags -1 through 2 represent polynya variability occurring in the previous, concurrent, and 1-2 months following variations the in atmospheric circulations, respectively. Color intensity corresponds to strength of correlation. Values in each cell display the coefficient of determination. White outlines indicate values with statistical significance at the 90% significance level. Polynya data ranges from April to October,

1992 to 2017. Atmospheric data ranges from February to November, depending on the lagged correlation.

El Niño-Southern Oscillation

Monthly relationships between coastal polynyas and ESNO are particularly strong throughout the Amundsen Sea, West Antarctica (Figure 3b). All 5 polynyas in the Amundsen Sea have very strong positive relationships with ENSO. Three of these are statistically significant. The rest of Antarctica contains only one statistically significant polynya-ENSO relationship, which is driven by interannual and monthly co-variability. During La Niña events, the STJ weakens and the PFJ strengthens, driving more storms to the SO, west of the Antarctic Peninsula. This allows a low pressure center to establish in the Bellingshausen Sea and promotes smaller polynya sizes in the Amundsen Sea. During El Niño events, the reverse conditions occur with more storm activity to the east of the peninsula. A high pressure center is established in the Bellingshausen Sea [Montes-Hugo and Yuan, 2012; Knuth and Cassano, 2011; Yuan, 2004; Yuan and Martinson, 2001] and polynya growth is promoted in the Amundsen Sea.

Much of the influence from ENSO is primarily exhibited in offshore regions of West Antarctica [Yuan, 2004; Kwok and Comiso, 2002a]. With large embayments and ice shelves in the Ross and Weddell Seas, the polynyas in those regions are spatially disconnected from the strongest ENSO effects on surface pressure, temperature, and ice concentrations. The relatively northern position of the Bellingshausen-Amundsen coast increases its connection to ENSO influence. El Niño (La Niña) events are associated with decreased (increased) sea ice concentrations in the Bellingshausen-Amundsen Seas, which may alleviate (exacerbate) polynya backfill pressure [Tamura et al., 2016] and promote (minimize) polynya growth.

The strong relationships are driven by interannual co-variability, thus the strength and regionality of the relationships are maintained through monthly lags (Figure 4b). Polynya size is strongly correlated with ENSO anomalies in the preceding, concurrent, and following months. In fact, the strength and regionality of the relationships are strongest with a 1-month lag in polynya size. During the study period, ENSO variability is strongest at the annual level, which accounts for 55.5% of its total variability (Figure 2c). This results in low monthly anomalies throughout each year and sustains the relationships with coastal polynyas even with increasing monthly lags.

Park et al. [2018] found that the long-term, nonlinear trend in total polynya area along the west Ross Ice Shelf is influenced by the long-term, nonlinear trend in ENSO. Arrigo and van Dijken [2004] report a statistically significant negative annual relationship between ENSO and the Ross Sea post-polynya. They correlate a multivariate ENSO index with all open water area within the Ross Sea embayment. While their open water area does not correspond to individual wintertime polynyas, their results give insight to ENSO influence on the timing of the polynya season's start, end, and duration. These relationships demonstrate the strong influence of ENSO in the Ross Sea region.

Montes-Hugo and Yuan [2012] found weak concurrent and lagged relationships between ENSO and the size of phytoplankton blooms in all 4 of their study areas. The weak relationships suggest a lack of influence in their study areas at the 3-month seasonal scale they use. However, the summer post-polynya focus is not consistent with winter polynya extents, which presents a distinct difference from the current study. Montes-Hugo and Yuan [2012] do attest that the weak relationships are not surprising as their relatively short study period, 1998-2006, would have trouble resolving ENSO variability.

Tamura et al. [2016] reports statistically significant negative (positive) relationships between ENSO and the largest polynya in the Prydz Bay (Amundsen Sea). Their reported positive polynya-ENSO relationship in the Bellingshausen Sea would be statistically significant at the 90% significance level used in the current study, but not at the 95% and 99% levels at which they report. Again, their correlations use annual cumulative sea ice production, which masks monthly and seasonal variations, while the current study uses monthly polynya area. Annual sea ice production and polynya area are significantly correlated in all polynyas [Tamura et al., 2016]. The current study also found statistically significant annual relationships (not shown) in three polynyas, one in each of the Prydz Bay, Haakon VII Sea, and Bellingshausen Sea.

Yuan and Martinson [2000] found the strongest correlation between ENSO and sea ice extent in the Amundsen Sea with a 6-month lag in ice extent. While there is a spatial, and thus potentially mechanical, disconnect between the sea ice edge and coastline, Yuan and Martinson's [2000] findings show a significant connection in that region of the SO, with a very strong lag effect. This agrees with the lagged polynya-ENSO relationships found in the Amundsen Sea in the current study.

Amundsen Sea Low: Actual Central Pressure

Relationships between coastal polynyas and ACP are particularly strong in the Amundsen and Ross Seas (Figure 3c). Seven of the nine polynyas in the region have statistically significant negative relationships with ACP. The strong relationships are primarily driven by variability at the monthly and seasonal levels. Only two polynyas in East Antarctica and the Bellingshausen and Weddell Seas have statistically significant relationships. Those relationships are primarily driven by monthly co-variability.

With ASL's exclusive West Antarctica domain, changes in ASL intensity are important for West Antarctic climate variability. Its average central location, which is located in the Amundsen Sea, promotes greater sea ice extent to the west and lower sea ice extent to the east [Turner et al., 2013; Fogt et al., 2012; Turner et al., 2009]. Thus, the strength of the ASL is expected to significantly influence polynyas differently on both sides of its mean central location as well. During the Ross Sea ice advance season (March-August), periods of relatively intense ACP are associated with negative (positive) southerly surface wind anomalies in the Bellingshausen Sea (Amundsen and Ross Seas) [Raphael et al., 2018]. The enhanced southerly airflow expands polynya area in the Amundsen and Ross Seas, supporting the negative polynya-ACP relationships in the region. The reduced southerly airflow in the Bellingshausen Sea is expected to reduce polynya area, supporting the positive polynya-ACP relationship found there, but that relationship is very weak.

Periods of an anomalously intense ACP are also associated with negative westerly surface wind anomalies along the west Bellingshausen/east Amundsen coast. With a northwest direction of maximum expansion for the largest polynyas in that region [Nihashi and Ohshima, 2015], the easterly sea ice flow from the Ross Gyre promotes polynya growth. This also supports the negative polynya-ACP relationship in that region where anomalously intense ACP is associated with enhanced easterly ice flow and polynya growth.

The strength and regionality of the polynya-ACP relationships are relatively weak when polynya variability either precedes or lags ACP (Figure 4c). With a 1 or 2-month lag in polynya response, there are only 2 statistically significant relationships each, one of which is maintained along the eastern edge of the Ross Ice Shelf through successive monthly lags in polynya response.

Amundsen Sea Low: Relative Central Pressure

Monthly relationships between coastal polynyas and RCP are particularly strong in West Antarctica (Figure 3d). Statistically significant polynya-RCP relationships are positive in the Amundsen Sea and negative in the Ross Sea. The strong relationships in the two regions are driven by seasonal and monthly co-variability, respectively. The rest of Antarctica contains two strong relationships, which have strong co-variability at the monthly and seasonal levels as well. Polynya-RCP relationships are generally weak compared to polynya responses to ACP. This difference may be related to the disproportionately large connection to the background pressure field. The regionality of the polynya-RCP connection changes with monthly lags in polynya response. One to two-month lags yield connections concentrated in various regions throughout East Antarctica. Since the ASL is located in the West Antarctica, these East Antarctica relationships may be due to confounding factors and are not supported by the direct physical connections between ASL and the polynyas. Interestingly, the strength and regionality of the relationships are much stronger with a 1-month lag in RCP. While there are stronger connections in East Antarctica also, the polynya-RCP relationship is highly concentrated in the Amundsen Sea.

RCP has the opposite effects on surface wind as ACP. Anomalously strong RCP is associated with relatively weak (strong) southerly airflow in the northern Ross (Bellingshausen) Sea. However, the relationships are diminished along the coasts. Anomalously strong RCP is also associated with enhanced westerly airflow along the west Bellingshausen/east Amundsen coast. Thus, its influence on wind in both directions are counterintuitive when coupled with the polynya-RCP relationships found in the current study. A potential explanation is provided later in the chapter, after presentation of the polynya responses to ASL location.

Amundsen Sea Low: Longitude

Influence of ASL intensity (ACP and RCP) on surface conditions is complicated by its variable location. During the polynya season, ASL location (LON and LAT) controls the spatial variability of its influence [Coggins and McDonald, 2015]. Thus, understanding the relationship between ASL location and coastal polynya variability is important for proper understanding of polynya-ASL relationships. The influence of ASL location on coastal polynya variability has not been analyzed in previous studies.

Relationships between coastal polynyas and LON are particularly strong throughout West Antarctica, only excluding the western Ross Sea, with statistically significant relationships in 7 of the 9 polynyas (Figure 3e). LON has statistically significant positive (negative) relationships with polynyas in the Bellingshausen and Amundsen Seas (along the eastern Ross Ice Shelf). The strong relationships are driven by co-variability at the monthly level. LON has no influence on polynyas in the western Ross Sea and East Antarctica.

During the study period, LON spans approximately 180-290^{o}E with a mean location of approximately 224^{o}E. A westward (eastward) shift in LON promotes northerly (southerly) near surface wind anomalies in the Amundsen and Bellingshausen Seas [Raphael et al., 2018], significantly contributing to the closing (opening) of polynyas in that region. LON has an opposite effect east of the peninsula. When centered in the Bellingshausen-Amundsen Seas, the ASL reduces southerly airflow along the Ronne Ice Shelf. At this longitude, ASL influence on Ross Sea winds is relatively weak [Coggins and McDonald, 2015]. As the ASL migrates westward its influence on polynya growth in the western Ross Sea increases. During the polynya season, the ASL seldom

travels west of approximately 210°E into the Ross Sea embayment, maintaining the direct negative relationship between LON and the Okuma Bay Polynya (#25).

LON has weak influence on wind variability along most of the Ross Ice Shelf during the sea ice advance season. It only influences meridional wind at the eastern edge of the ice shelf [Raphael et al., 2018; Hosking et al., 2013], explaining its weak connection to polynyas in the western Ross Sea. LON has a statistically significant negative correlation with westerly surface wind along the Bellingshausen Sea coast [Raphael et al., 2018]. However, the relatively weak westerly wind associated with an eastward ASL position does not lead to increased polynya size, even though coastal polynya growth along the Bellingshausen coast is greatest with southeasterly wind [Nihashi and Ohshima, 2015].

The regionality of the strong relationships are much weaker with monthly lags in polynya variability (Figure 4e). With a 1-month lag, correlations become weaker (stronger) with West (East) Antarctica polynyas. Again, direct ASL connections to East Antarctica conditions are not supported by the exclusive West Antarctica ASL domain. With a 2-month lag, correlations become even weaker in all regions. Correlations are very weak with a 1-month lag in LON.

Amundsen Sea Low: Latitude

Monthly relationships between coastal polynyas and LAT are particularly strong in two regions – in the Amundsen and eastern Ross Seas of West Antarctica, and from Adelie Land to the Shackleton Ice Shelf in East Antarctica (Figure 3f). The relationships are primarily driven by co-variability at monthly and seasonal scales. The strength and regionality of the relationships become weaker with lags in polynya variability (Figure 4f). Significant relationships are only maintained in

the western Amundsen Sea and Prydz Bay. The correlations become very weak with a 1-month lag in LAT.

There are statistically significant positive correlations between LAT and near surface southerly wind anomalies in the Amundsen Sea [Raphael et al., 2018; Coggins and McDonald, 2015]. Northern ASL positions promote polynya growth in that region. The positive relationship between LAT and East Antarctica polynyas may be directly linked to the influence of SAM on LAT (r=-0.29; Figure 5). A northward shift in ASL is associated with a relatively weak SAM, which has a significant negative relationship with East Antarctica polynyas.

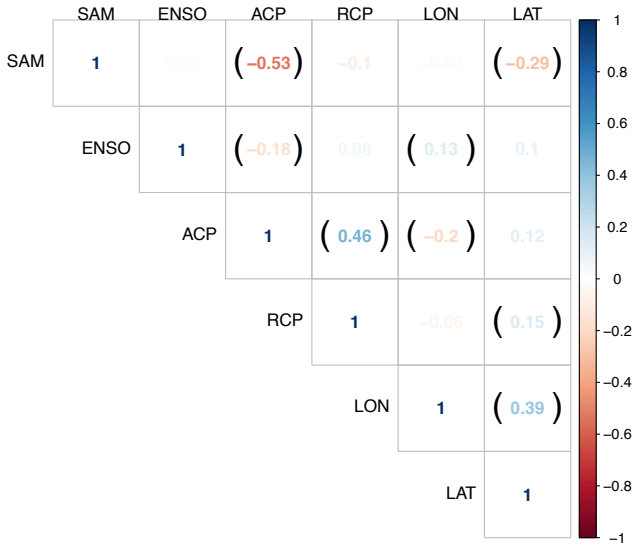

Figure 5: Cross correlation (r) matrix of large-scale atmospheric circulations – the Southern Annular Mode (SAM), El Niño-Southern Oscillation (ENSO) measured by the Southern Oscillation Index, and components of the Amundsen Sea Low: actual central pressure (ACP), relative central pressure (RCP), longitude (LON), and latitude (LAT). The scale bar to the right indicates the coefficient of correlation (r). Diamonds indicate statistically significant correlations at the 90% level.

Understanding the interaction and timing of the ASL intensity and position allows better interpretation of the polynya-RCP relationship. This relationship follows an intuitive pattern based on the mean meridional location of the ASL and the direction of flow around a low pressure center. However, in light of the RCP influence on near surface coastal winds, interpretation of the polynya-

wind-RCP relationship may not be that straightforward. The strong polynya-RCP relationship may be driven by a statistically significant RCP-LAT relationship (r=0.15; Figure 5), particularly at the annual and seasonal scales (r=0.5 and 0.74, respectively; not shown).

Minimum LAT (furthest south) is associated with westerly airflow to the north, in the ASL domain, and easterly airflow to the south, over land. Maximum LAT (furthest north) is associated with easterly airflow to the south, in the ASL domain, and westerly airflow north. Thus, the region south (north) of the ASL domain consistently experiences strong easterly (westerly) air flow anomalies associated with ASL, while the prevailing meridional wind direction influenced by LAT variability changes within the domain itself. Enhanced westerly wind from a southern LAT position may reduce easterly coastal sea ice flow from the Ross Gyre. With the RCP-LAT relationship, anomalously intense RCP is associated with a southern ASL position. Thus, more intense RCP may lead to the reduction in polynya size found in the Amundsen Sea.

The lack of RCP influence on meridional wind speed in the coastal Ross, Amundsen, and western Bellingshausen Seas does not support the connection between RCP intensity and polynya size. RCP also lacks major influence on zonal wind speed in the coastal Ross Sea. There does exist a region of relatively strong, but not statistically significant, positive RCP correlation with meridional wind near the Ross Ice Shelf Polynya. This is consistent with the positive (negative) polynya-RCP relationship in the Amundsen (western Ross) Sea where anomalously intense RCP is associated with anomalously small (large) polynyas. It is also consistent with the strong coastal West Antarctic westerly winds associated with a southern ASL position [Raphael et al., 2018] and small polynyas in the Amundsen and eastern Ross Seas.

Studies have revealed a late 20th/early 21st century tendency towards a more +SAM [Thompson et al., 2011; Gillett et al., 2008; Turner et al., 2009; Arblaster and Meehl, 2006; Marshall, 2003]. The negative relationship between the SAM and East Antarctica polynyas does not produce long term negative trends in polynya area as a response to the SAM trend. In fact, of the five polynyas around the continent with statistically significant trends (presented in chapter 2 of this study), the Vincennes and Barrier Bay Polynyas (#7 and 10, respectively) have positive trends, the Mertz Glacier Polynya (#3) has a negative trend due to the 2010 Mertz Ice Tongue calving event, and the Ronne Ice Shelf Polynya (#17) is not influenced by the SAM. The Cape Darnley Polynya (#13) has a statistically significant negative trend in size, as well as a strong negative trend in ice production [Tamura et al., 2016; Nihashi and Ohshima, 2015], and its variability is significantly influenced by the SAM. The long-term areal changes of this polynya may support a possible connection to the long-term linear trend of the SAM.

Park et al. [2018] found that the long term nonlinear trend in the large western Ross Ice Shelf Polynya's (#1) seasonal timing and area are driven by the nonlinear trends in the SAM and ENSO, respectively. The current study reports only weak polynya connections to the SAM and ENSO at that location, but the seasonal timing is not analyzed. All five long term polynya area trends are not supported by trends in ENSO or the ASL.

4. Conclusion

In all, 22 of the 25 coastal polynyas analyzed in the current study are significantly influenced by the SAM, ENSO, or the ASL. One polynya in Prydz Bay and two polynyas in the Haakon VII Sea are not significantly correlated with any of the three atmospheric patterns. Omitting the ASL influence on East Antarctica polynyas, 19 of the 25 coastal polynyas are significantly influenced by

at least one of the three atmospheric circulation features. Thus, three East Antarctica coastal polynyas are significantly influenced only by the ASL. This is important because the ASL has an exclusive West Antarctica domain that prohibits direct interaction with East Antarctica.

The regionality of the significant relationships is consistent with the regionality of sea ice response to the SAM, ENSO, and the ASL. The SAM is a circumpolar phenomenon, but its strongest influence on coastal sea ice is in East Antarctica, east of Prydz Bay [Raphael and Hobbs, 2014; Simpkins et al., 2012], which is reflected in the SAM influence on East Antarctica polynyas. ENSO is a tropical phenomenon with very strong global connections. Its strongest extratropical connection is in West Antarctica where polynyas in the Amundsen and western Ross Sea are greatly influenced by it. The ASL is an exclusively West Antarctica phenomenon that significantly influences all polynyas in West Antarctica.

Even though Haakon VII Sea ice extent and concentration are influenced by the SAM, LON, and RCP within the study period [Hobbs et al., 2016; Simpkins et al., 2012], none of the 3 atmospheric patterns are very influential on polynya size throughout that region. This highlights the different meridional responses felt by the sea ice edge, pack ice, and coastline. The particular coastal influence of the atmospheric patterns on wind and sea ice motion coupled with the effects from a ridged coastline determines the polynya response.

Variability within the atmospheric circulations primarily occurs at the monthly scale with strong variations also at the seasonal scale. Interannual variability and long term linear trends account for relatively small proportions of the variance. Only ENSO is driven by interannual variability. In most Antarctic coastal polynyas, variability is strongest at the monthly scale, as discussed in

Chapter 2. Generally, interannual polynya variability is weak, except in the Weddell, Bellingshausen, and east Amundsen Seas where more of the overall variability is interannual rather than seasonal. The strong connections between polynyas and the SAM, ACP and LAT are primarily driven by monthly and seasonal co-variability. Strong connections with ENSO and LON are primarily driven at the annual and monthly levels, respectively. Connections with RCP are primarily driven by seasonal level co-variability. Thus, large-scale polynya-atmosphere analyses done at the annual scale mask much of the interactions.

Future studies may also further improve general understanding of relationships between Antarctic coastal polynyas and large-scale atmospheric patterns by analyzing polynya relationships to other Southern Hemisphere climate patterns. While the SAM, ENSO, and ASL are considered great sources of Southern Ocean sea ice and wind variability, influences from other phenomena such as the Zonal Wave 3 pattern, Semi-Annual Oscillation, and Antarctic Circumpolar Wave may contribute to polynya variability. Additional climate patterns directly linked to ENSO, such as the Pacific-South American pattern, Atlantic Multi-decadal Oscillation, and Pacific Inter-decadal Oscillation, may also be explored.

Chapter 4

A regional analysis

1. Introduction

Antarctica is completely surrounded by coastal polynyas, from which a subset of the 25 largest and most frequently recurring is shown in Figure 1. Much of the current polynya literature focuses on individual polynyas that form in regions with extraordinary conditions. The Ross and Ronne Ice Shelf Polynyas were historically considered the largest and most productive of all Antarctic coastal polynyas, and they exist along the most expansive ice shelves in the Southern Ocean [Ross Ice Shelf Polynya: Park et al., 2018; Cheng et al., 2017; Nakata et al., 2015; Kwok et al., 2007; Kern et al., 2007; Nihashi et al., 2005; Arrigo and van Dijken, 2004, 2003a, 2003b; Bromwich et al., 1998, 1994, 1993; Carrasco and Bromwich, 1993; Ronne Ice Shelf Polynya: Hollands et al., 2013; Fiedler et al., 2010; Hunke and Ackley, 2001; Both: Drucker et al., 2011]. The Terra Nova Bay and Mertz Glacier Polynyas develop along the Victoria Land (in the western Ross Sea) and Adelie Land coasts, respectively. Both are regions of very high wind velocity flowing across the pronounced Drygalski and Mertz Glacier Ice Tongues, respectively [Terra Nova Bay Polynya: Knuth and Cassano, 2011; Fusco et al., 2009; Parmiggiani, 2005; Frezzotti and Mabin, 2004; Smith et al., 1990; Kurtz and Bromwich, 1985, 1983; Bromwich and Kurtz, 1984; Mertz Glacier Polynya: Snow et al., 2016; Campagne et al., 2015; Lacarra et al., 2014; Shadwick et al., 2013; Tamura et al., 2012; Kusahara et al., 2011; Marsland et al., 2007, 2004; Kern et al., 2007]. The development, production, and variability of these four polynyas constitute the majority of Antarctic coastal polynya studies.

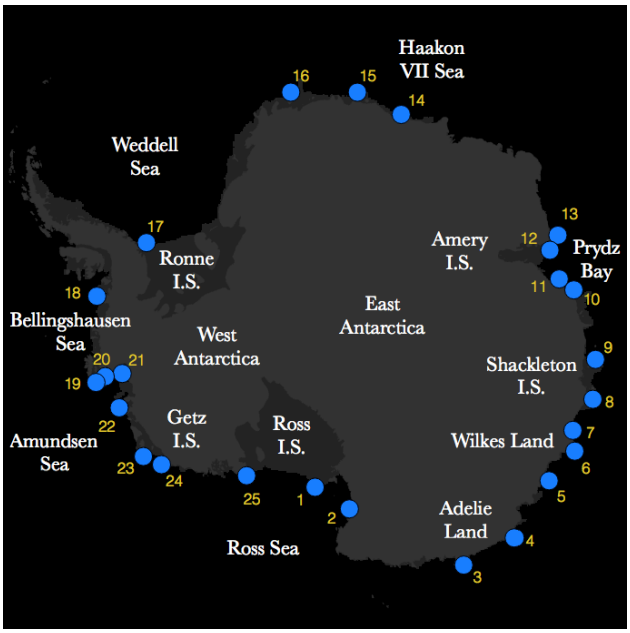

Figure 1: a) Locations of the largest 25 Antarctic coastal polynyas. Relevant oceanic and continental place names are labeled throughout. Light and dark grey areas represent the landmass and ice shelves, respectively. b) The table presents the number, name, and abbreviation of each polynya.

1.	Ross Ice Shelf	(RIS)	26.	Breid Bay	(BrB)
2.	Terra Nova Bay	(TNB)	27.	East Lazarev Ice Shelf	(ELIS)
3.	Mertz Glacier	(MG)	28.	Jelbart Ice Shelf	(JIS)
4.	Dibble Glacier	(DG)	29.	Ronne Ice shelf	(RON)
5.	Dalton	(Da)	30.	Bellingshausen Sea	(BS)
6.	Cape Poinsett	(CP)	31.	Ferrero Bay	(FB)
7.	Vincennes Bay	(VB)	32.	Cranton Bay	(CB)
8.	Shackleton Ice Shelf	(SIS)	33.	Pine Island Bay	(PIB)
9.	Davis Sea	(DS)	34.	Amundsen Sea	(AS)
10.	Barrier Bay	(BaB)	35.	Wrigley Gulf	(WG)
11.	Prydz Bay	(PB)	36.	Getz Ice Shelf	(GIS)
12.	Mackenzie Bay	(MB)	37.	Okuma Bay	(OB)
13.	Cape Darnley	(CD)			

Current polynya literature also includes Antarctic coastal polynya research on single and multi-polynya systems from other regions such as Vincennes Bay, Cape Darnley, Commonwealth Bay along Adelie Land, and eastern Queen Maud Land in the Haakon VII Sea [Kitade et al., 2014; Ohshima et al., 2013; Wendler et al., 1997; Ishikawa et al., 1996; Cotton and Michael 1994]. However, very little research has focused on regional scale analyses. Here, the regional scale generally refers to geographic extents larger than a single ice shelf, excluding the exceptionally large Ross and Ronne Ice Shelves, and smaller than the size of West Antarctica. The Ross and

Weddell embayments are the most popular locations for regional studies [Paul et al., 2015; Haid et al., 2015; Haid and Timmerman, 2013; Martin et al., 2007; Markus et al., 1998]. Some studies focus on polynyas in East Antarctica, from Adelie Land to the eastern Haakon VII Sea coast [Labrousse et al., 2018; Massom et al., 1998].

While some studies analyze the response of near neighbor polynyas to migrating storm systems [Bromwich et al., 1998; Parish and Bromwich, 1998; Bromwich et al., 1993], current literature still lacks research focused on synchronized polynya development and variability at the regional scale. This is important because contemporaneous polynya responses to environmental conditions are significantly associated with processes at the synoptic scale or larger. The literature also lacks delineations of entirely relevant geographies that are defined by the spatial extent of natural phenomena. Instead, regional delineations in previous polynya studies are determined a priori, based on continental geographies such as the Ross and Weddell Sea embayments.

Greater understanding of the geographic distances over which synchronized polynya dynamics occur may be attained through circumpolar analyses. Montes-Hugo and Yuan [2012] provide research on coastal polynyas around Antarctica. However, the spatial density of their polynya distribution does not lend the research to regional delineations and representative analyses within each region. Other studies have analyzed circumpolar polynya systems with greater spatial density [Nihashi et al., 2017; Li et al., 2016; Ohshima et al., 2016; Tamura et al., 2016, 2008, 2007; Nihashi and Ohshima, 2015; Kern, 2009; Zwally et al., 1985]. However, they do not investigate the specific geographic extents over which large scale forcing influence polynya systems.

Using continental geographies to spatially define the scale of a study potentially omits important contributors and processes important for the regional analysis. The geographic extent of the study may not align with the proper scale of governing processes. For instance, the Ross Sea sector contains the most significant rates of positive sea ice concentration trends in the Southern Ocean [Liu et al., 2004]. However, the region of strong positive trend actually extends to Adelie Land in East Antarctica. Thus, it may be useful for studies analyzing the positive sea ice trend to extend their region of interest beyond the western continental boundary of the Ross Sea embayment, into East Antarctica.

While previous studies have not identified groups of polynyas based on regimes of compatible characteristics, this type of regional classification has been performed on the sea ice field. Zwally et al. [1983] classified 5 sectors based on the effects of various regional oceanographic and meteorological features, such as cyclonic gyres, summer sea ice melt, and strong ocean stratification. Since their advent, these sectors have been employed in many other sea ice studies. For example, Zwally et al. [2002] provides an in-depth statistical analysis of the sea ice-surface temperature association in each sector around the Southern Ocean. Cavalieri and Parkinson [2008] provide a study of sea ice extent in each sector. Gloersen et. al. [1993] uses the 5 sectors in a global study of sea ice variability. Stroeve et al. [2016] use the sectors in their study on the distribution of various ice types. Parkinson and Cavalieri [2012] use the sectors in their analysis of Antarctic sea ice variability and trends. Later, Raphael and Hobbs [2014] used spatial autocorrelation to define 5 alternative sectors with distinct sea ice regimes. Schroeter et al. [2017] and Hobbs et al. [2016] use these sector delineations.

In sea ice studies relevant to the current work, researchers have investigated sea ice variability as a partial function of variability within atmospheric circulations such as the Southern Annular Mode (SAM) [Simpkins et al., 2012; Lefebvre et al., 2004; Hall and Visbeck, 2002; Venegas 2003], El Niño-Southern Oscillation (ENSO) [Schroeter et al., 2017; Yuan and Martinson 2001, 2000; Carleton, 2003; Kwok and Comiso, 2002a; Yuan, 2004; Stammerjohn et al., 2008], the Antarctic Circumpolar Wave (ACW) [White and Peterson, 1996], the Semi-Annual Oscillation (SAO) [van den Broeke, 2000], Zonal Wave 3 (ZW3) [Renwick et al., 2012; Raphael, 2007], and the Amundsen Sea Low (ASL) [Hosking et al., 2013; Turner et al., 2009, 2013, 2016; Fogt et al., 2012; Raphael et al., 2018]. Studies have attributed the strongest sea ice responses to variability in the SAM, ENSO, ASL, and ZW3. ENSO and ASL are particularly influential in West Antarctica where the trends and variability in sea ice concentration and extent are strongest.

The current chapter of this study analyzes regions of strong polynya variability and inter-polynya co-variability to delineate polynya groups. This chapter then determines the strength of influences from prominent large-scale atmospheric circulation patterns on polynya group delineations and variability. Last, it compares the spatial extents of the proposed polynya groups to independent regional delineations created by other studies using sea ice characteristics.

2. Data and Methods

2.1 Data

The polynya and atmospheric datasets used in this chapter are the monthly polynya area and atmospheric circulation pattern datasets discussed in Chapters 1 and 2, respectively. The polynya area dataset was created using thin ice and fastice detection algorithms [Tamura et al., 2007; Nihashi and Ohshima, 2015] with input from Special Sensor Microwave Imager satellite data

[Armstrong et al., 1994]. The Southern Annular Mode (SAM) and Amundsen Sea Low (ASL) indices were obtained from the British Antarctic Survey, and the Southern Oscillation Index used to analyze influence from the El Niño-Southern Oscillation (ENSO) was obtained from the National Oceanic and Atmospheric Administration. More detailed descriptions of the polynya and atmospheric circulation data and the steps for processing them are presented in chapters 2 and 3, respectively.

2.2 Methods of analysis

This study uses monthly mean polynya variability to identify polynya groups, determine the relative contribution of each polynya to the total circumpolar system variance, and determine the extent to which large-scale atmospheric influences contribute to regional polynya variability. The same analyses are also provided using the annual, seasonal, and monthly temporal components of each polynya to determine the temporal scales at which these relationships take place. All statistically significant relationships are determined using the 90% significance level.

First, the general circumpolar system of polynyas is analyzed using Pearson cross correlations (PCor) for each polynya pair throughout the entire 25-polynya circumpolar system. This offers important information about near neighbor polynya correlations, the regional continuity of significant polynya correlations, and the relative strength of inter-regional polynya pair relationships. Next, the variability of the entire system is analyzed using Principal Component Analysis (PCA). Each individual polynya's contribution to the major principal components of the 25-polynya system is analyzed and is used to also identify regionality within the system. This process identifies locations of very dynamic and synchronous polynyas and indicates whether their spatial distribution has an autocorrelative pattern. To delineate regions of strong inter-polynya co-variability, Gaussian Mixture Modelling (GMM) and Hierarchical Agglomerative Clustering (HAC) are employed.

HAC is a stepwise grouping technique that begins with each object as an individual group, then successively combines groups, aiming to minimize total intra-group variance at each step [Rokach and Maimon, 2005]. The process is continued until a single group remains in the end. In this study, HAC is applied using Ward's method, which minimizes intra-group variance measured through the sum of square error (SSE) [Ward, 1963]. The HAC method requires input of a predetermined number of polynya groups. In many cases, such as in the current study, the number of groups is unknown beforehand. To determine an appropriate and meaningful number of groups, the HAC process is performed to match the group total determined during application of the GGM process (discussed later in this section).

A disadvantage of the HAC method is its inability to separate objects previously assigned to the same group. This means polynyas in the same group are stuck together even when there may be more favorable changes to the intra-group SSE. Thus, delineations of higher order, or larger scale, groupings are largely limited by delineations at lower orders, or smaller scales. However, this type of grouping is suited for datasets with a hierarchical structure [Yim and Ramdeen, 2015], such as the polynya co-variability at different temporal and spatial scales. For instance, lower order groupings may be driven by daily dynamics along ice shelves, while a higher order grouping may be driven by decadal variability across an entire continent.

Also, the HAC method is unable to allocate partial group membership, which exacerbates the limitation introduced by permanent groupings. The desire of this study is to produce hard polynya group delineations. Acknowledgements are made for instances of partial group membership when it occurs at different temporal scales, which is information that can be gathered from the strict

grouping at different scales. Another limitation of the HAC method is its algorithmic process that does not account for stochastic variations in polynya variability and thus does not identify the polynya co-variability that is driven by the physical processes of interest. Polynyas have high daily and sub-daily size variations, but at the monthly, seasonal, and annual timescales used in this study, the temporal variations are thought to have relatively low randomness that would interfere with the grouping process. So, this drawback of the algorithmic process may be less effective at the temporal scale of interest in this study.

The GMM method actively models the dataset using series of Gaussian curves to distinguish high density centers (clusters) of data points, which indicate relatively close relationships among variables [Scrucca et al., 2016]. Also, the GMM method actively updates models to fit the presumed true co-variance while considering the stochastic variability. Thus, 1) it is not limited by decisions made earlier in the process; 2) it models the processes that govern the polynya size distributions and relationships and does not respond to noise that does not contribute to inter-polynya co-variability; and 3) it actively identifies density centers with successive addition and subtraction of Gaussian curves, automatically locating the clusters and eliminating the need for foreknowledge of the clusters, which is sometimes unattainable. So, the GMM process actively accounts for some of the general drawbacks of HAC and may be useful for polynya grouping at even finer scales.

The GMM process determines the optimal number of polynya groups using Bayesian Information Criterion (BIC), which attempts to maximize the GMM fit and minimize the number of polynya groups and the use of excessive data points [Konishi and Kitagawa, 2008]. Due to the minimization criterion, this method only identifies the polynya group with the strongest internal

co-variability, except at the seasonal scale where the number of data points for each polynya is minimal – only seven timesteps. Using BIC omits much of the regionality within circumpolar polynya variability. Thus, for this study, the GMM process is coerced to generate between 2 and 9 polynya groups. The model fit with the greatest number of contiguous regional scale groups is chosen. The series of GMM outputs is treated as a progressively dissociative (or divisive) process so the number of groups increase with each step – the opposite of agglomerative. Preference is generally given to the maximum number of groups that is identified without the newest group delineation interfering with a previous regional scale grouping.

After establishing regional polynya groups, the strength of inter-regional co-variations is analyzed by correlating the mean standard-normal polynya area of each regional group. Due to the strong relationships between surface wind speed, polynya area and large-scale atmospheric circulations [Tamura et al., 2016; Kwok et al., 2007; Bromwich et al., 1998], this study hypothesizes a strong influence from atmospheric circulation mechanisms on the regionality of polynya variability. To determine the strength of influence of the atmospheric circulations, each polynya is regressed to indices describing each atmospheric circulation mechanism (SAM, ENSO, and ASL), the GMM process is reapplied, and the changes in group delineations are analyzed. Also, using the original data series, the mean standard-normal polynya area within each group is correlated with each atmospheric pattern. All methods of analysis are also applied to each temporal component.

3. Results

3.1 Near Neighbor Inter-polynya Correlation

Correlation matrices (Figure 2) show the strength of correlations among the 25 Antarctic coastal polynyas analyzed in this study. Part a shows the correlations for monthly mean polynya variability.

Parts c, e, and g show correlations at the annual, seasonal, and monthly temporal scales, respectively. The matrices display negative relationships, which are not provided by some of the grouping techniques utilized later in the study. The diagonal line of dark blue cells represents perfect lag-0 autocorrelation. The numbers listed in the left and upper margins correspond to the polynya numbers in Figure 1. Parts b, d, f, and h respectively map polynya group outputs determined from the matrices. 2 major regions are consistently revealed through near neighbor correlations – Amundsen Sea (#19-24) and Haakon VII Sea (#14-16).

With monthly mean polynya variations (Figure 2a-b), polynyas nearer each other generally have stronger co-variability. However, the strength of the near neighbor correlations is not uniform. This creates regional clustering, albeit relatively weak clustering, with many overlapping regions of strong cross correlations. The most distinct regions of strong internal co-variability occur in the Bellingshausen-Amundsen-eastern Ross region (#18-24), Haakon VII Sea (#14-16), and the Wilkes Land-Prydz Bay region (#3-13). Clusters are much more defined at the annual (Figure 2c-d) and seasonal (Figure 2e-f) scales. Interannual variations create 4 polynya groups located in the western Ross Sea and Adelie Land (#1-3), the Shackleton Ice Shelf and eastern Prydz Bay (#9-13), Haakon VII Sea (#14-16), and the Bellingshausen-Amundsen-eastern Ross region (#18-24). Seasonal variations create 3 polynya groups with very strong clustering from Adelie Land to the Shackleton Ice Shelf/eastern Prydz Bay (#4-10), Haakon VII Sea (#14-16), and spanning across the Amundsen, Ross, and Adelie coasts (#19-25, 1-3). When each polynya is regressed to annual and seasonal variability, the resulting monthly co-variability more distinctly displays the 3 major regions of polynya co-variability produced with monthly means (Figure 2g-h).

Two polynyas are associated with virtually all negative polynya-pair correlations at the monthly and seasonal scales – the Ronne Ice Shelf (#17) and MacKenzie (#12) Polynyas. They are located

along the Ronne Ice Shelf and in western Prydz Bay, respectively. The Ronne Ice Shelf Polynya has the only negative nearest neighbor correlation, which occurs at the monthly and annual scales. It also has the only negative non-neighbor polynya-pair relationships at the seasonal scale. At the annual scale, there is a significant negative inter-regional relationship between polynyas of the Bellingshausen-Amundsen-eastern Ross region and the Haakon VII Sea.

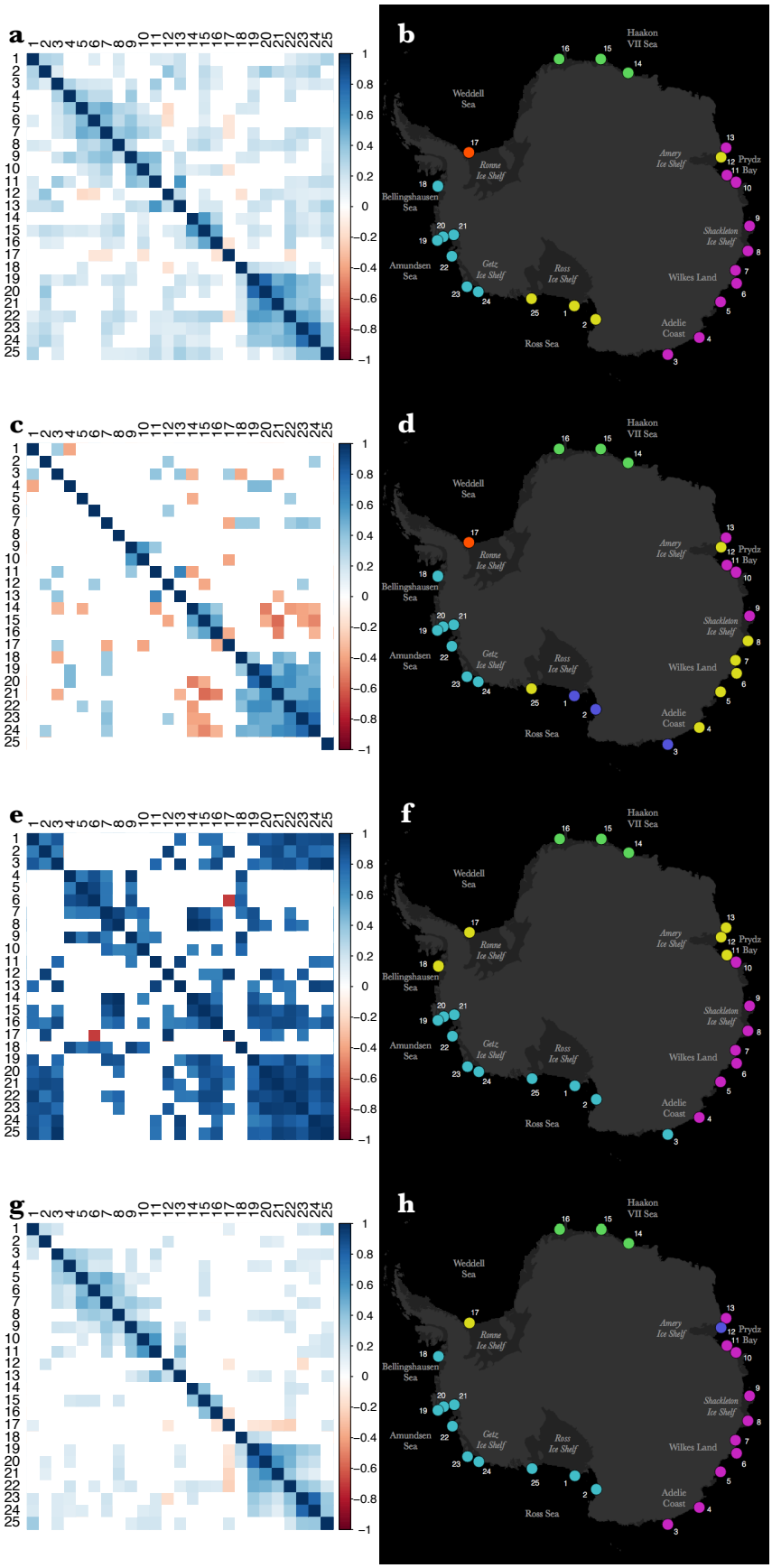

Figure 2: Correlation matrices indicating the strength of relationships (r) between each of the 25 largest and most frequent Antarctic coastal polynyas using a) monthly mean timeseries and their c) annual, e) seasonal, and g) monthly temporal components. Blue (red) color indicates statistically significant positive (negative) correlations at the 90% significance level. Color intensity represents strength of correlation. Numbers in the left and upper margins represent the 25 polynyas.

Parts b, d, f, and h display maps of the polynya groups presented in parts a, c, e, and g, respectively.

3.2 Contributions to circumpolar polynya system variance

PCA is utilized to discover the individual polynyas and regions that contribute most to the circumpolar variance of the primary principal components at each spatial scale. PCA on the monthly mean variability identifies 2 significant principal components (PCx) that account for approximately 20% and 12% of total Antarctic polynya variability (Figure 3a-c). Polynyas located in the Amundsen and eastern Ross Seas provide the greatest contributions to PC1 (~40%), while PC2 variance is primarily attributed to a group of polynyas in Wilkes Land (~23%), the western Shackleton Ice Shelf and eastern Prydz Bay (~14%), and the eastern Amundsen Sea (~14%). Polynyas in the Haakon VII, Weddell, and Bellingshausen Seas contribute very little to the primary principal components.

At the annual scale, PC1 is the only significant component as it accounts for ~22% of the total circumpolar variance (Figure 3d-f). Again, polynyas in the Amundsen and eastern Ross Seas account for the greatest amount of variance in PC1 (~48%). Polynyas in the Haakon VII Sea account for a significant proportion of the total system variance as well (~16%).

At the seasonal scale, the first two PC's are significant and account for ~55% and ~28% of the total variance, respectively (Figure 3g-i). The largest regional contributions to PC1 disproportionately occur within the Amundsen-Ross-Adelie Land regions (~49%), the Haakon VII Sea (~15%), and the western Wilkes Land-eastern Shackleton Ice Shelf region (~9%). Contributions to PC2 occur within the Adelie-Wilkes region (~25%), the Weddell-Bellingshausen Seas (~16%), and the Davis Sea Polynya along the Shackleton Ice Shelf (~8%).

At the monthly scale, with annual and seasonal influences removed, the first two PC's account for 16% and 11% of total variance, respectively (Figure 3j-l). Amundsen Sea polynyas and the East

Antarctica polynyas between Adelie Land and eastern Prydz Bay account for the greatest proportion of PC1 variance (~36% and ~40%, respectively). The same two regions also account for the greatest variance in PC2 (~30% and ~40%, respectively).

As the level of aggregation increases and the temporal scale becomes coarser, greater proportions of variance are concentrated in the top principal components, particularly PC1. This is due to the decrease in variability with increase in scale. Variability at larger temporal scales occur over larger geographic extents. Thus, polynya co-variability increases as temporal scales get larger.

Based on the results of the PCA application in this section, PCA is not a highly suitable method for relatively fine scale regional polynya group delineation. The delineations produced indicate polynyas with relatively large contributions to the primary modes of circumpolar variability. This masks the unique variability patterns that may distinguish regions from each other. However, the regional delineations that are provided by the primary PC's indicate coarse scale delineations.

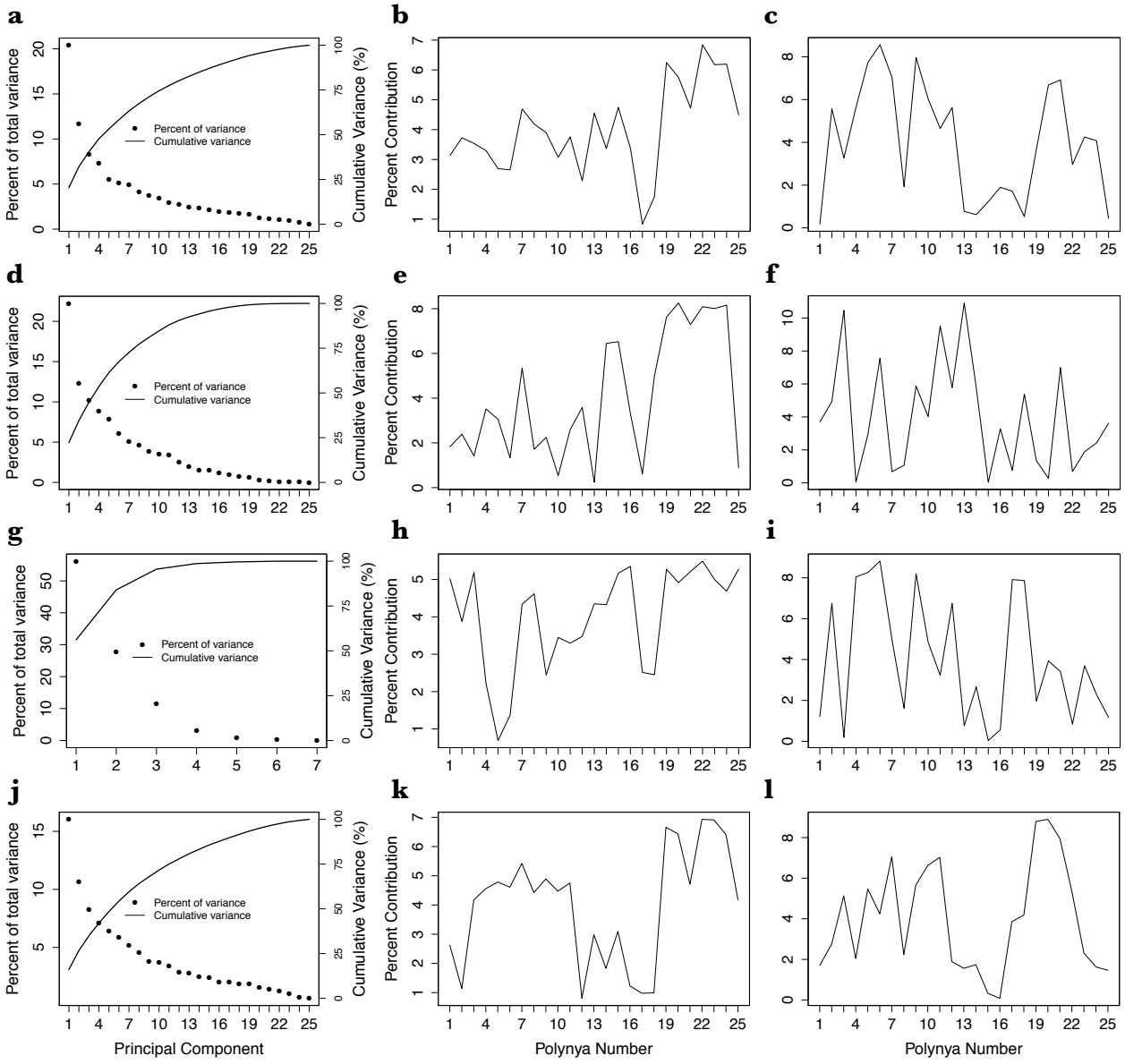

Figure 3: Scree plots (a, d, g, j) and individual polynya contributions to each of the first two principal components (b-c, e-f, h-i, k-l) from Principal Component Analysis on monthly mean data (a-c) and its temporal components at the annual (d-f), seasonal (g-i), and monthly (j-l) scales.

3.3 Model-based polynya groups

When GMM is used on monthly mean polynya variability, 4 groups of strong polynya co-variability are delineated. The first group spans the Bellingshausen, Amundsen, and eastern Ross Seas (Figure 4a). The second group is along the Wilkes Land coast and includes eastern Shackleton

Ice Shelf. The third group includes polynyas along western Shackleton Ice Shelf and in Prydz Bay. The fourth group consists of the Haakon VII Sea polynyas. An additional polynya group is constituted based on a lack of strong co-variability, compared to the established polynya groups, and contains the remaining polynyas.

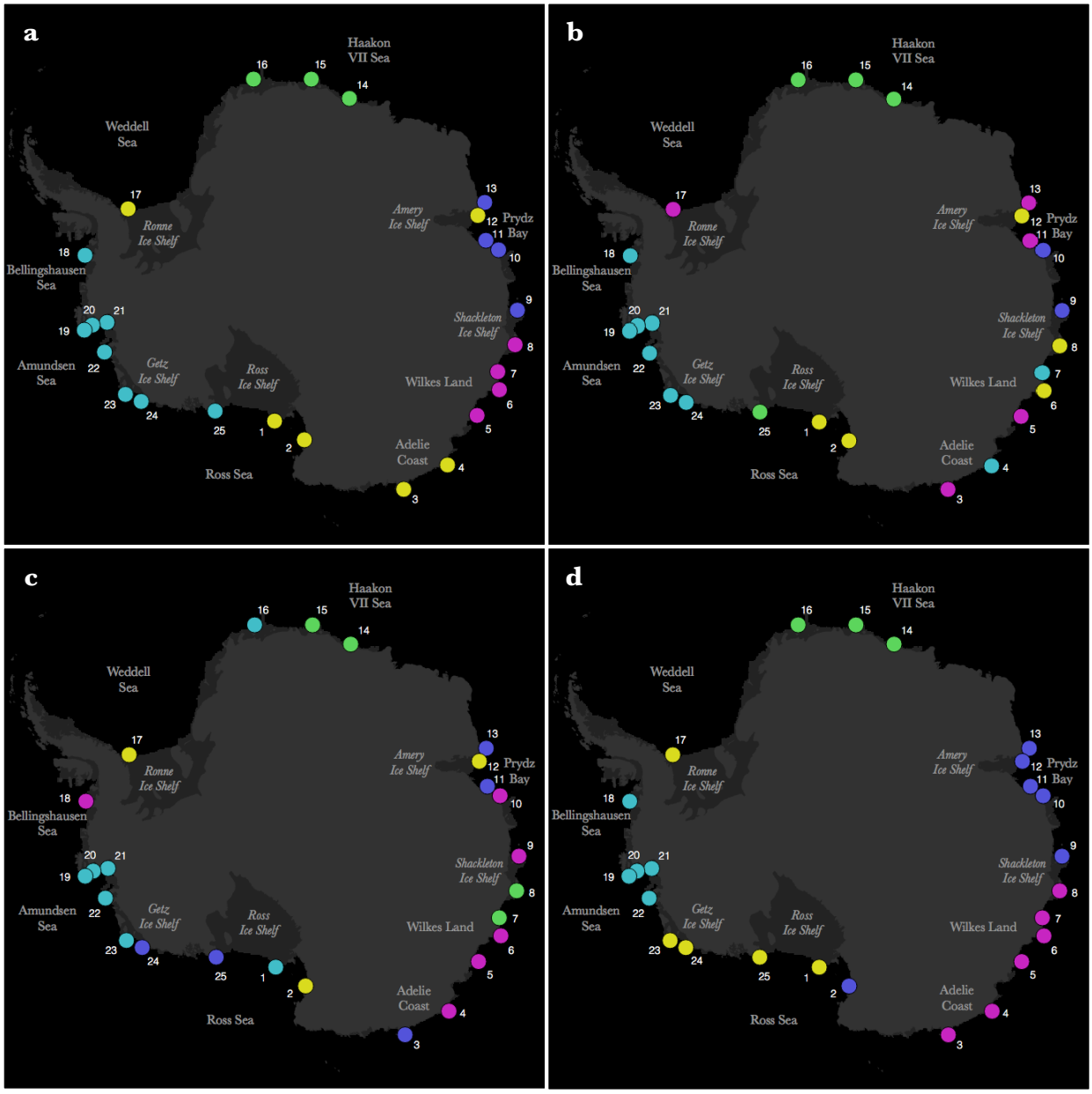

Figure 4: Polynya groups delineated using Gaussian mixture models on a) monthly mean polynya

co-variability. Polynya groups also delineated from b) annual, c) seasonal, and d) monthly temporal components. Each color represents a different group.

At the annual scale, 2 distinct groups are identified based on strong internal co-variability (Figure 4b). The first group forms along the West Antarctica coastline in the Bellingshausen, Amundsen, and eastern Ross Seas (#18-24). The second group consists of the Haakon VII Sea polynyas (#14-16). The remaining polynyas constitute several disjointed groups due to relatively weak co-variability. Polynya co-variability at the seasonal scale produces contiguous groups in the Amundsen Sea (#19-23) and along the Wilkes coast (#4-6) as well as many highly disjointed groups (Figure 4c).

At the monthly scale, 4 groups of highly co-variable polynyas are identified (Figure 4d). The first group, with the strongest internal synchronization, forms in the Bellingshausen and Amundsen Seas (#18-22). The other 3 distinct groups occur in East Antarctica. The first spans from Adelie Land to the eastern Shackleton Ice Shelf (#3-8). The second contains polynyas in Prydz Bay and Davis Sea (#9-13). The third consists of Haakon VII Sea polynyas (#14-16). The Ross and Weddell Sea polynyas each have unique monthly variability patterns, and their grouping here is based on weak co-variability, compared to the other groups. It is important to note that when the GMM process is coerced to identify only two polynya groups (section 2.2), it identifies relatively strong polynya co-variability that spans the entirety of the East Antarctica coastline. Thus, there is a continental scale influence that produces monthly scale co-variability that is not associated with interannual or seasonal variations.

Generally, the GMM results show that a significant portion of the very strong co-variability that contributes to the grouping within the Bellingshausen, Amundsen, and eastern Ross Seas is driven at the annual scale. A significant portion of the strong co-variability and grouping of the Bellingshausen and Amundsen Sea polynyas is also driven at the monthly scale. Thus, when annual variability is removed, the eastern Ross Sea polynyas are no longer closely associated with the Bellingshausen and Amundsen Sea polynyas. The results also show that continental geography plays an important role in polynya co-variability, particularly at the monthly scale. There is a significantly distinguishable difference in monthly coastal polynya variability between East and West Antarctica. Although seasonality significantly influences virtually all natural variability and inter-polynya relationships are very strong at the seasonal scale, seasonal polynya variability is a poor indicator for regional co-variability analyses. In fact, the strong similarity between virtually all seasonal polynya variability makes it more difficult to distinguish among regional groups.

3.4 Algorithm-based polynya groups

Using HAC produces similar results as the GMM method with strong group delineations in the Amundsen-Bellingshausen Seas, Haakon VII Sea, and the Wilkes Land coast, particularly at the monthly scale (Figure 5a-b). The delineation between the Prydz Bay and Wilkes coast polynya groups is relatively consistent with a dividing line through the Shackleton Ice Shelf for both the HAC and GMM methods. Polynyas in the Ross and Weddell Seas are the least co-variable around Antarctica. The delineation of the polynya groups in those two regions is based on the lack of strong, positive inter-polynya co-variability, compared to other group delineations, which is also identified with both methods. However, polynya group delineations using HAC at the annual and seasonal scales produce different results than the GMM process.

At the annual scale (Figure 5c-d), Haakon VII Sea polynyas create the only distinguishable polynya group found also within the GMM-derived regions. The distinct HAC-delineated West Antarctica group consists of polynyas spanning the Bellingshausen and eastern Ross Seas with the addition of the Vincennes Bay and Shackleton Ice Shelf Polynyas (#7-8, respectively). All other groups are spatially discontinuous.

At the seasonal scale, the Amundsen and Ross Sea polynyas (#20-25 and #1) and the Wilkes Land polynyas (#4-6) constitute two contiguous, regional scale polynya groups (Figure 5e-f). All other regions contain disjointed groups due to the weak distinction in regional seasonal polynya variability. This is consistent with other methods of analysis employed in this study.

At the monthly scale, when annual and seasonal variability is removed from each polynya, West Antarctica and Haakon VII Sea group delineations are consistent with those found before annual and seasonal variability were removed (Figure 5g-h). The biggest result of removing the larger scale variations occurs in East Antarctica between Adelie Land and Prydz Bay where one dominant polynya group is identified (#3-11).

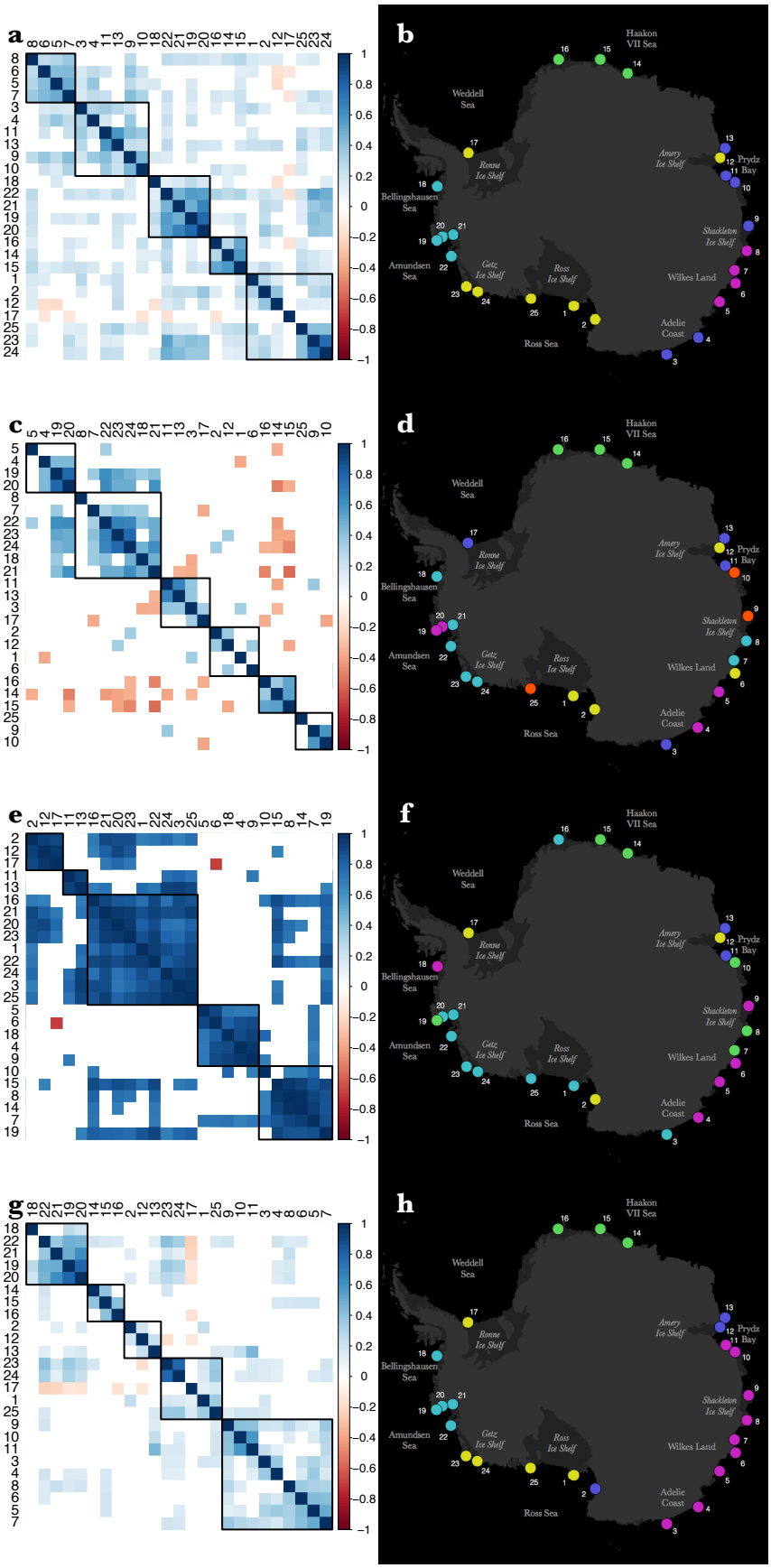

Figure 5: Correlation matrix for the 25 largest and most frequent Antarctic coastal polynyas using a) monthly mean polynya timeseries and their c) annual, e) seasonal, and g) monthly temporal components. Black boxes indicate polynya groups derived using hierarchical agglomerative clustering. Polynya numbers in top and left margins are reorder to display polynya groupings. Blue (red) color indicates statistically significant positive (negative) correlations at the 90% significance level. Color intensity corresponds to strength of correlation. Diagonal line of dark blue cells indicates perfect lag-0 autocorrelation.
Parts b, d, f, and h display maps of the polynya groups presented in parts a, c, e, and g, respectively.

In addition to the HAC-derived grouping, Figure 5 (a, c, e, g) shows negative relationships between polynya groups, particularly at the annual scale. Polynyas within the Haakon VII Sea group are negatively correlated with many other polynyas around Antarctica. They are most consistently positively correlated with polynyas from the group dominated by Bellingshausen and Amundsen Sea polynyas. ENSO is known to have a strong influence on climate conditions in these two regions. The role of ENSO and other large-scale atmospheric patterns are explored in subsection 3.6.

Using the near neighbor Pearson cross-correlation (PCor), principal component analysis (PCA), gaussian mixture model (GMM), and hierarchical agglomerative clustering (HAC) methods produces varying regional polynya group delineations. However, there are some areas of consistency among the methods. Monthly mean polynya co-variability consistently groups the Haakon VII Sea polynyas (polynyas #14-16). Strong polynya grouping also occurs in the Bellingshausen-Amundsen-eastern Ross region (#18-25). However, the PCA and HAC methods do not include the Bellingshausen Sea polynya (#18) and the eastern Ross Sea polynyas (#23-25), respectively, in the grouping. All 4 methods also group the Wilkes Land polynyas (#5-8). Results from PCor reveal that the Davis Sea polynya (#9) is significantly correlated with the Wilkes Land polynyas, but it is also more significantly correlated with Prydz Bay polynyas (#10, 11, 13). Thus, the Prydz Bay polynya group consistently consists of polynyas #9-11 and 13. Only the PCA method (in principal component 2) groups the MacKenzie Bay polynya (#12) with the Prydz Bay polynya group. Through PC2, PCA is also the only method that omits the Cape Darnley Polynya (#13) from the Prydz Bay polynya group.

Polynyas #1-4, 12, and 17 generally exhibit weak cross correlation with one another. Here, it is noted that multiple methods do indicate strong correlations between the western Ross Sea polynyas (#1-2) and between the Adelie Land polynyas (#3-4). The grouping of polynyas #1-4, 12, and 17, determined by the GMM method, determine a final polynya group that is not delineated based on their strong inter-polynya co-variability, but rather on the collection of the remaining polynyas with relatively weak correlations compared to the internal co-variability of the other 4 polynya groups.

At the annual scale, the four grouping methods again consistently group the Haakon VII Sea polynyas (#14-16). PCA yields a much weaker connection between the Jelbart Ice Shelf Polynya (#16) to the other 2 polynyas in the region, particularly in regards to PC1, which explains approximately 22% of the total circumpolar polynya variability. Three of the four grouping methods group polynyas within the Bellingshausen-Amundsen-eastern Ross region (#18-24). Only the HAC method assigns polynyas of this region to multiple groups. While PCor results indicate strong correlation between western Ross and eastern Adelie Land polynyas (#1-3), no other method does so. In fact, the other methods consistently limit group delineations to the Haakon VII, Bellingshausen, and Amundsen Seas.

At the seasonal scale, the four grouping methods consistently delineate a contiguous polynya group along the Wilkes coast (#4-6). 3 of the 4 methods also group polynyas spanning between the Amundsen Sea and eastern Adelie coast (#19-25 and 1-3). Only the GMM method separates polynyas in the Amundsen Sea (#19-23) from virtually all the polynyas in the Ross and Adelie regions.

At the monthly scale, the 4 grouping methods consistently group polynyas in the Amundsen Sea (#19-22). Three of the four methods group polynyas in the Ross Sea (#23-25 and 1). Only the PCA method omits polynyas along the Ross Ice Shelf (#25 and 1). Also, three of the four methods group Adelie Land and Wilkes Land polynyas (#3-11). Only the GMM method omits polynyas in the Davis Sea and eastern Prydz Bay (#9-11). All grouping methods, except PCA, group the Haakon VII Sea polynyas (#14-16).

Combining the results from the 4 methods applied across the 4 temporal scales, 6 distinct polynya groups are identified – Ross, Amundsen-Bellingshausen (A-B), Weddell, Haakon, Prydz, and Wilkes (Figure 6). These general delineations are the first sectors based on polynya variability. They differ from sectors delineated from sea ice characteristics. These differences are further described in subsection 3.7.

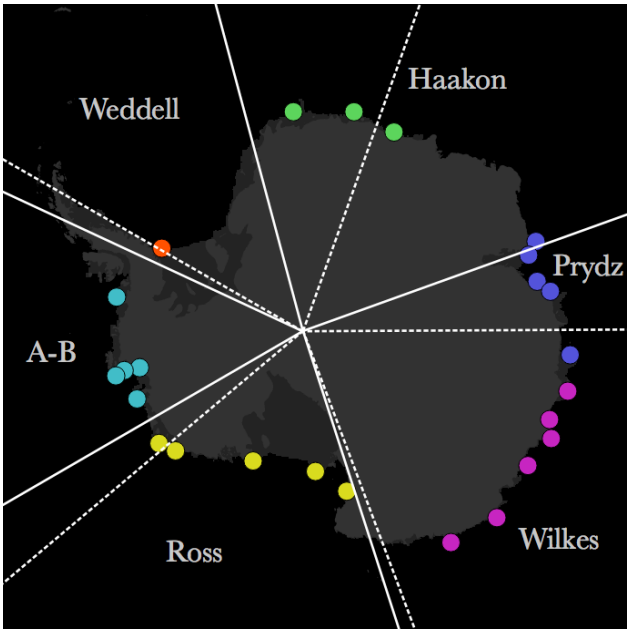

Figure 6: Circumpolar distribution of the 25 largest and most frequently occurring Antarctica coastal polynyas color-coded by groups, which are based on co-variability. White lines indicate regional delineations for sea ice sectors determined by Zwally et al. (1983, dashed lines) and Raphael and Hobbs (2014, solid lines).

3.5 Inter-regional relationships

Using the 6 polynya groups, inter-regional relationships are investigated. Using monthly mean polynya variations, there are statistically significant positive correlations between each region,

excluding the Weddell (Figure 7a). The Weddell region has only weak relationships that are positive with the Ross and negative with the others. At the annual scale (Figure 7b), the two adjacent West Antarctica regions, the Ross and A-B, and the two adjacent East Antarctica regions, Prydz Bay and Wilkes, have statistically significant positive relationships. The Weddell and Haakon regions have weak negative relationships with all other groups. While the Haakon has stronger relationships than the Weddell, its only statistically significant relationship is with the A-B region. At the seasonal scale (Figure 7c), all inter-regional relationships are positive, except between the Weddell and Wilkes. The Ross and A-B regions are significantly correlated with each other and the Prydz Bay. The A-B is significantly correlated with the Haakon as well. At the monthly scale (Figure 7d), when annual and seasonal variability is removed, the Ross, A-B, Prydz Bay, and Wilkes have statistically significant positive relationships with one another, omitting the weak positive relationship between the A-B and Prydz groups. The A-B and Weddell have the only statistically significant negative relationship.

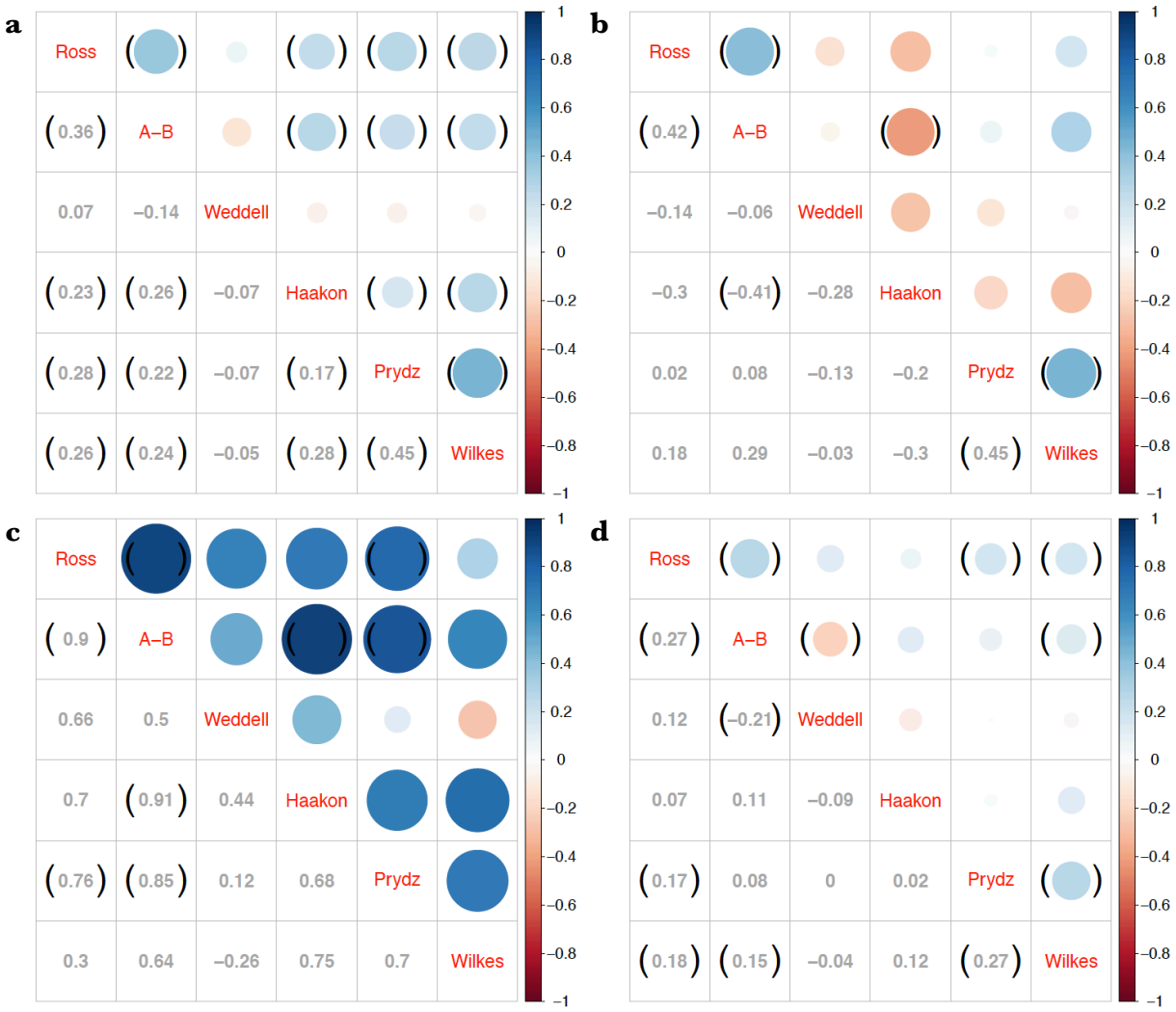

Figure 7: Matrices showing correlations (r) between the mean standard-normal variability of each regional polynya group for the a) original timeseries at monthly timesteps and the extracted b) annual, c) seasonal, and d) monthly temporal components. Blue (red) color indicates positive (negative) correlations. Color intensity represents strength of correlation. Round brackets indicate significant correlations at the 90% significance level.

Thus, the most consistent inter-regional relationships occur between the Ross and A-B, which has positive correlations at every scale; the A-B and Haakon, whose negative relationship at the annual

scale and positive relationship at the seasonal scale mask the significance in its monthly mean correlation; and Prydz Bay and Wilkes, which is driven by co-variability at the annual scale.

3.6 The role of large-scale atmospheric circulations

The relatively expansive spatial contiguities of the polynya groups suggest that large-scale factors are important contributors to polynya co-variability. Coastal polynya variability is primarily driven by surface wind velocity and direction [Kwok et al., 2007; Bromwich and Kurtz, 1984], particularly at daily and sub-daily timescales. Monthly, seasonal, and interannual variations are strongly linked to sea ice motion and atmospheric flow. Sea ice motion anomalies themselves are also influenced by atmospheric circulations [Kwok et al., 2017; Kwok, 2010]. Thus, polynya co-variability at these temporal scales may be influenced by atmospheric circulations that operate at the synoptic scale or larger. To test the level of influence that atmospheric circulation patterns have on polynya co-variability, the grouping process is repeated on polynya variability that is regressed to the Southern Annular Mode (SAM), El Niño-Southern Oscillation (ENSO), and the Amundsen Sea Low's (ASL) actual central pressure (ACP), relative central pressure (RCP), longitude (LON), and latitude (LAT). Ocean circulations may also influence large-scale variations in sea ice motion and polynya variability. Contributions from ocean circulation is outside the scope of this study. Future studies on Southern Ocean currents may enhance general understanding of large-scale polynya variability.

Delineation of polynya groups using the GMM process with monthly mean polynya variability is not influenced by the SAM, ACP, or RCP. Thus, their results are similar to the grouping provided in Figure 8a, which indicates GMM groupings without any atmospheric factors removed (the same as Figure 4a). When the effects of LON are removed from each polynya, the Bellingshausen Sea polynya (#18) is no longer grouped with polynyas in the Amundsen and eastern Ross Seas, which

shows the influence that LON has on their co-variability (Figure 8b). The polynyas in the Bellingshausen and Weddell Seas (#18 and 17) are both regrouped with polynyas along the Wilkes coast. With an ASL central location at approximately 224°E, just west of the Getz Ice Shelf, removing the longitudinal migration of the ASL makes its influence on polynya variability out of reach of the Bellingshausen and Weddell Sea polynyas. It also leaves the other atmospheric patterns to govern West Antarctica polynya co-variability, which maintains the grouping of polynyas in the Amundsen and eastern Ross Seas. Removing the effect of ENSO from all polynyas causes a similar response when grouping the polynya in the Weddell Sea with the polynyas along Wilkes coast (Figure 8c).

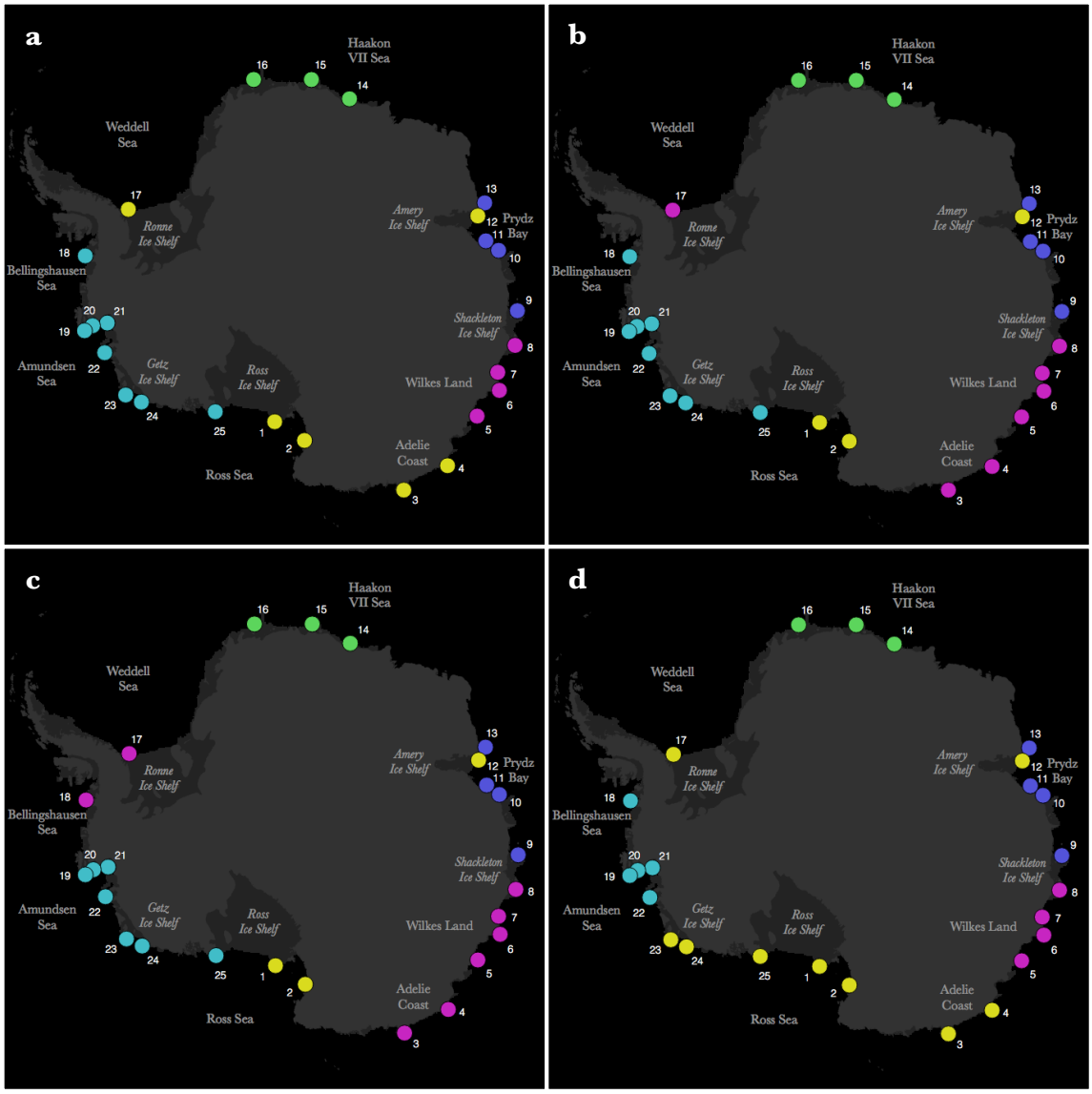

Figure 8: a) Polynya groups delineated using Gaussian mixture models on monthly mean polynya co-variability. Parts b-d display groups derived from a similar process after removing the effects of the Amundsen Sea Low's b) longitude, c) the El Niño-Southern Oscillation, and the Amundsen Sea Low's d) latitude from each polynya. Each color represents a different group.

Removing the effect of LON also causes the GMM process to group both Adelie Land polynyas with the polynyas along the Wilkes coasts. Again, accounting for ENSO produces a similar assignment of both Adelie Land polynyas. Even though neither Adelie Land polynyas are

significantly influenced by LON or ENSO, as presented in chapter 3 of this study, the two phenomena (ASL location and ENSO) have enough of an influence to weaken the co-variability between Adelie Land and Wilkes Land polynyas. Since the ASL is an exclusively West Antarctica system, its influence on the Adelie Land polynyas may be due to its significant relationship with ENSO (r=0.41 at the annual scale). When the effects of LAT are removed, the polynyas in the eastern Ross Sea (#23-25) are no longer grouped with the Bellingshausen and Amundsen Sea polynyas (Figure 8d). LAT has statistically significant positive relationships with the eastern Ross Sea polynyas, as well as each polynya in the Amundsen Sea. A northern ASL position is associated with larger polynyas in the Amundsen and eastern Ross Seas, which greatly contributes to the polynyas' strong co-variability and grouping. Thus, removing the influence of LAT leads to weaker inter-polynya co-variability in that region. However, additional large-scale drivers beyond LAT are able to maintain the co-variability between polynyas in the Bellingshausen and Amundsen Seas. The combined effects of the atmospheric circulation patterns are influential in the Bellingshausen Sea, eastern Ross Sea, and Adelie region.

At the annual scale, polynya group delineations are not influenced much by ENSO and the ASL (ACP, RCP, LON, LAT). Their results remain similar to Figures 9a and 4b. Removing the effects of the SAM on all polynyas strengthens regional polynya co-variability in polynyas across Adelie Land (#3-5) and the Shackleton Ice Shelf (#8-10), revealing the ability of the SAM to desynchronize polynyas in East Antarctica (Figure 9b). It also reveals that polynyas in close proximity may respond differently to the same large-scale forcing acting on their region. For instance, once the effects of the SAM are removed, Shackleton Ice Shelf Polynya (#8) variability becomes more synchronized with the two polynyas immediately to the west. Chapter 3 of this study shows that +SAM is associated with stronger westerly winds that influence weaker easterly ice flow

and smaller polynyas in East Antarctica. This relationship is not significant with the Shackleton Ice Shelf Polynya (#8) because, unlike its neighbors that expand westward, it expands northward due to static ice features blocking growth to the east and west. Thus, the significant influence that the SAM has on zonal wind and ice flow is less effective on the variability of the Shackleton Ice Shelf Polynya, and removing the effects of SAM increases its synchronization with nearby polynyas.

Removing the combined effects of all six atmospheric factors at once reduces general polynya synchronization around Antarctica (Figure 9c), indicating strong influence that the atmospheric patterns have on annual circumpolar polynya co-variability. Removing the effects of ENSO, ACP, RCP, LON, and LAT individually did not have much influence on polynya group delineations potentially because the influences of the other atmospheric patterns were able to maintain the strong co-variability within the polynyas of the Haakon VII Sea and the Amundsen and Ross region.

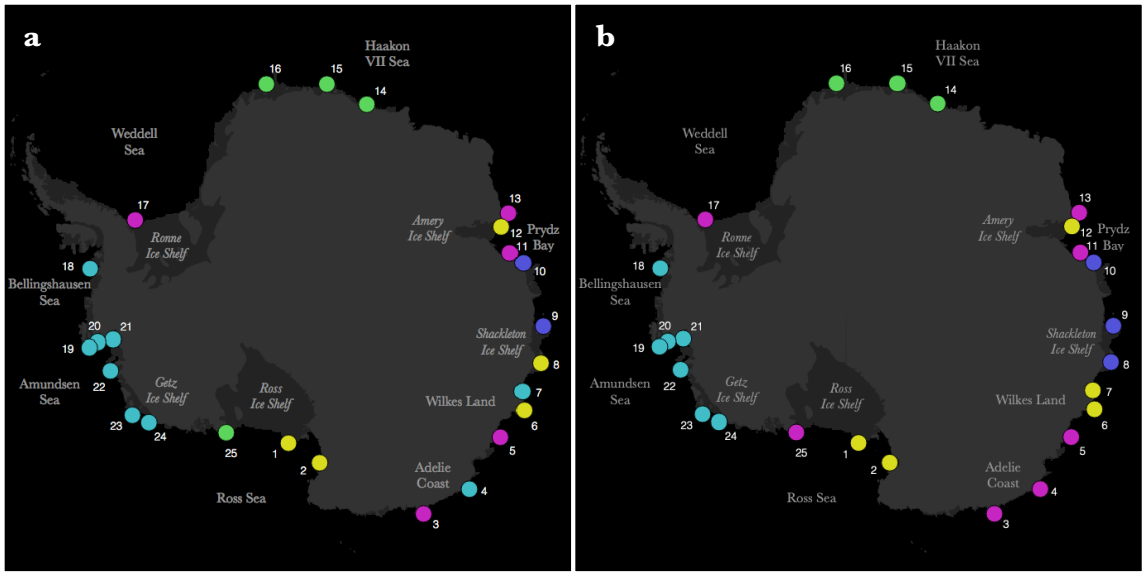

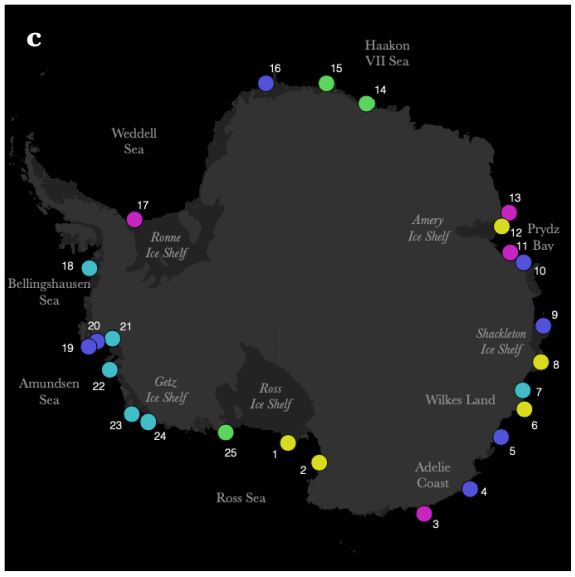

Figure 9: a) Polynya groups delineated using Gaussian mixture models on annual polynya co-variability. Parts b-c display groups derived from a similar process after removing the effects of b) the Southern Annular Mode and c) the combined effects of the Southern Annular Mode, El Niño-Southern Oscillation, and Amundsen Sea Low from each polynya. Each color represents a different group.

At the seasonal scale, most atmospheric factors analyzed have at least a small influence on polynya group boundaries. Polynyas along Wilkes Land (#4-6) and in the Amundsen Sea (#19-23) constitute the only two regional polynya groups (Figures 10a and 4c). The latter is characterized by its relatively weak inter-polynya co-variability, compared to the Wilkes Land and disjointed groups. When the effects of each atmospheric pattern are removed, only LAT contributes to changes in the Wilkes Land polynya group delineation (Figure 10e). The Wilkes Land group expands to the Barrier Polynya in the eastern Prydz Bay (#4-10), which suggests that the influence of LAT decreased the strength of polynya co-variability along the Wilkes coast. Again, associations between the ASL and East Antarctica polynyas are most likely driven by their relationships to other large-scale patterns. Even though the Shackleton Ice Shelf Polynya (#8) is located within the new range of the Wilkes Land polynya group, it is not grouped with its neighbors due to its topological relationship with the nearby static ice boundaries. This effect is similar in the annual scale grouping. Individually removing the effects of the SAM, ACP, RCP, and LAT each result in a very slight shrinking of the Amundsen Sea polynya group (#20-23; Figure 10b-e, respectively). The Ferrero Bay Polynya (#19) is small and has the most northern position of all polynyas in the

Amundsen Sea so it is the least insulated by the Amundsen Sea embayment. Thus, it is the most susceptible to wind and ice motion forces moving across the region.

When removing the seasonal effects of the SAM and RCP from each polynya (Figure 10b-c, respectively), co-variability within the Haakon VII Sea strengthens to delineate a new significant polynya group. This means the Haakon VII polynyas have varying responses to both the SAM and RCP, which decreases synchronization in polynya variability throughout the region. Given the exclusive West Antarctica influence of the ASL, the RCP influence in the Haakon VII Sea may actually be due to its strong seasonal relationship with the SAM ($r=0.77$). The Haakon VII Sea polynyas and RCP are all responding to the SAM.

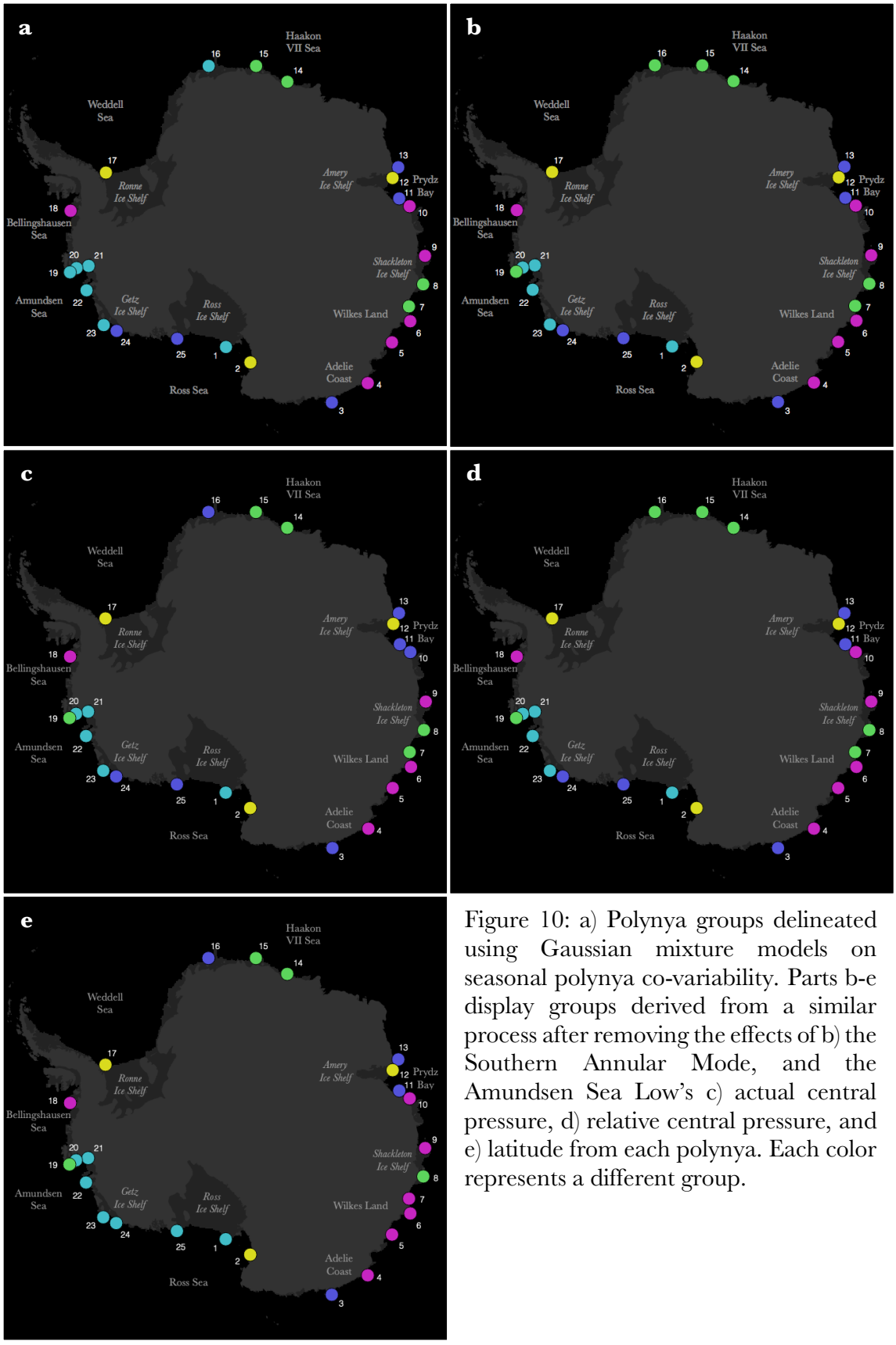

Figure 10: a) Polynya groups delineated using Gaussian mixture models on seasonal polynya co-variability. Parts b-e display groups derived from a similar process after removing the effects of b) the Southern Annular Mode, and the Amundsen Sea Low's c) actual central pressure, d) relative central pressure, and e) latitude from each polynya. Each color represents a different group.

Due to the strong seasonality in each polynya and atmospheric pattern, the combination of all six atmospheric circulation variables is able to statistically explain virtually all circumpolar seasonal polynya variability. Thus, after accounting for the influence of the atmospheric factors, the GMM process is unable to delineate polynya groups.

There are 5 very distinct polynya groups derived from monthly polynya variations, with annual and seasonal variability removed (Figures 11a and 4d). The group delineations are not influenced by the SAM, ENSO, RCP, and LAT. The greatest contribution comes from ACP and LON as they influence co-variability between polynyas within the Wilkes Land (#3-8) and Prydz Bay (#9-13) regions. Removing the effects of ACP weakens the co-variability within both regions (Figure 11b). Removing the effects of LON strengthens the co-variability between the two regions and groups them together (#3-11) (Figure 11c). This suggests that the influence of ACP and LON strengthens the inter-polynya relationships and weakens inter-regional relationships in this region. The influence of LON also reduces the co-variability between the Bellingshausen Sea Polynya (#18) and polynyas in the Amundsen Sea (#19-22). Thus, when accounting for annual and seasonal variability, the combined effects from all six atmospheric circulation factors is concentrated in East Antarctica and primarily driven by the influence of ACP and LON. Again, these results represent a connection between aspects of the ASL and East Antarctica, which may be caused by the association between ACP and the SAM.

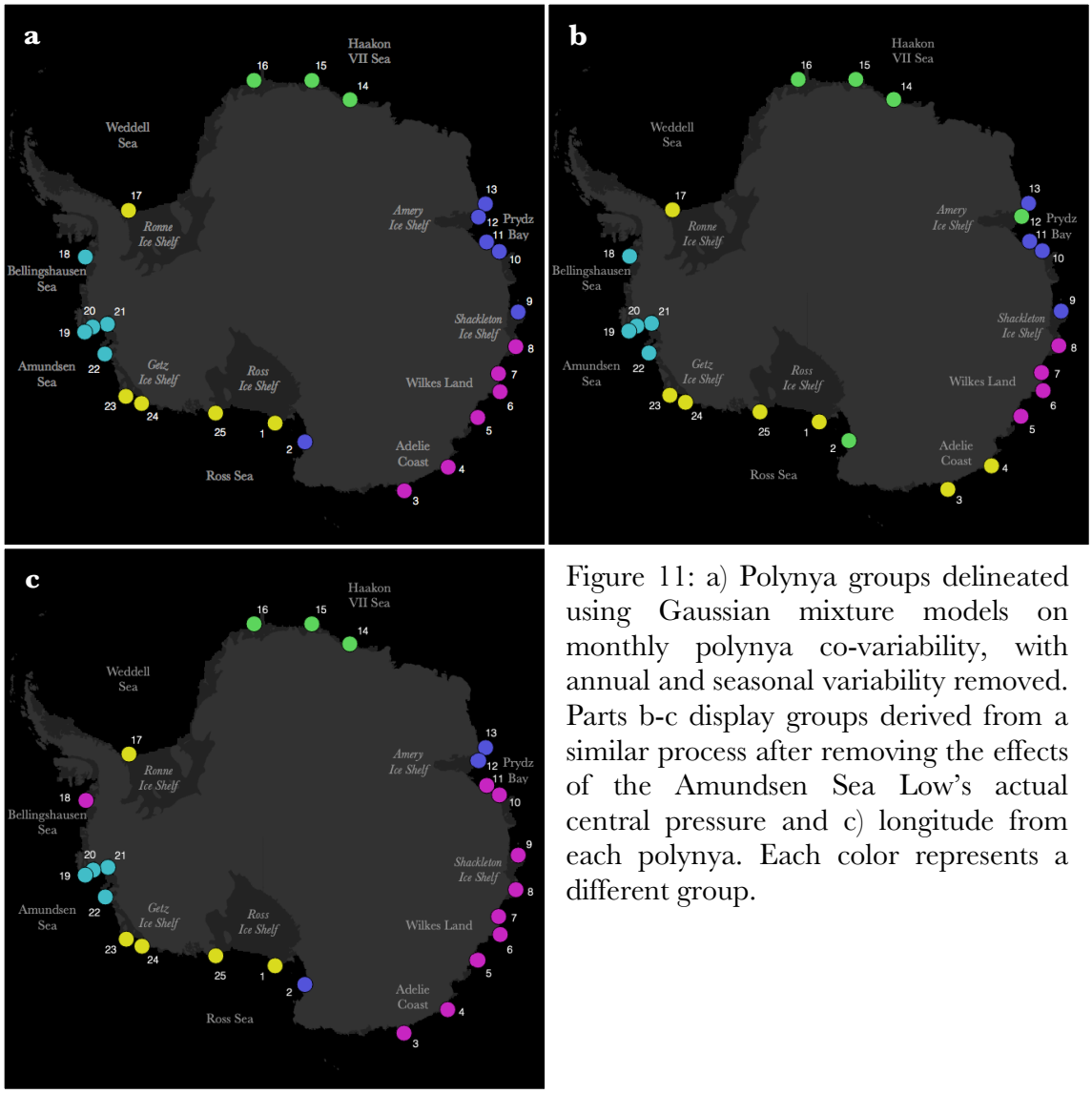

Figure 11: a) Polynya groups delineated using Gaussian mixture models on monthly polynya co-variability, with annual and seasonal variability removed. Parts b-c display groups derived from a similar process after removing the effects of the Amundsen Sea Low's actual central pressure and c) longitude from each polynya. Each color represents a different group.

To quantify the level of influence that each atmospheric circulation pattern has on the polynya groups, the mean standard-normal polynya area within each group is correlated with each atmospheric circulation pattern. The ACP has a statistically significant correlation with the mean variability of the Ross polynya group (Figure 12a). All atmospheric patterns, excluding the SAM, are significantly correlated with the A-B group. Only LON is significantly correlated with the Weddell, and no atmospheric pattern is significantly correlated with the Haakon. The SAM and LAT have significant correlations with the Prydz and Wilkes groups.

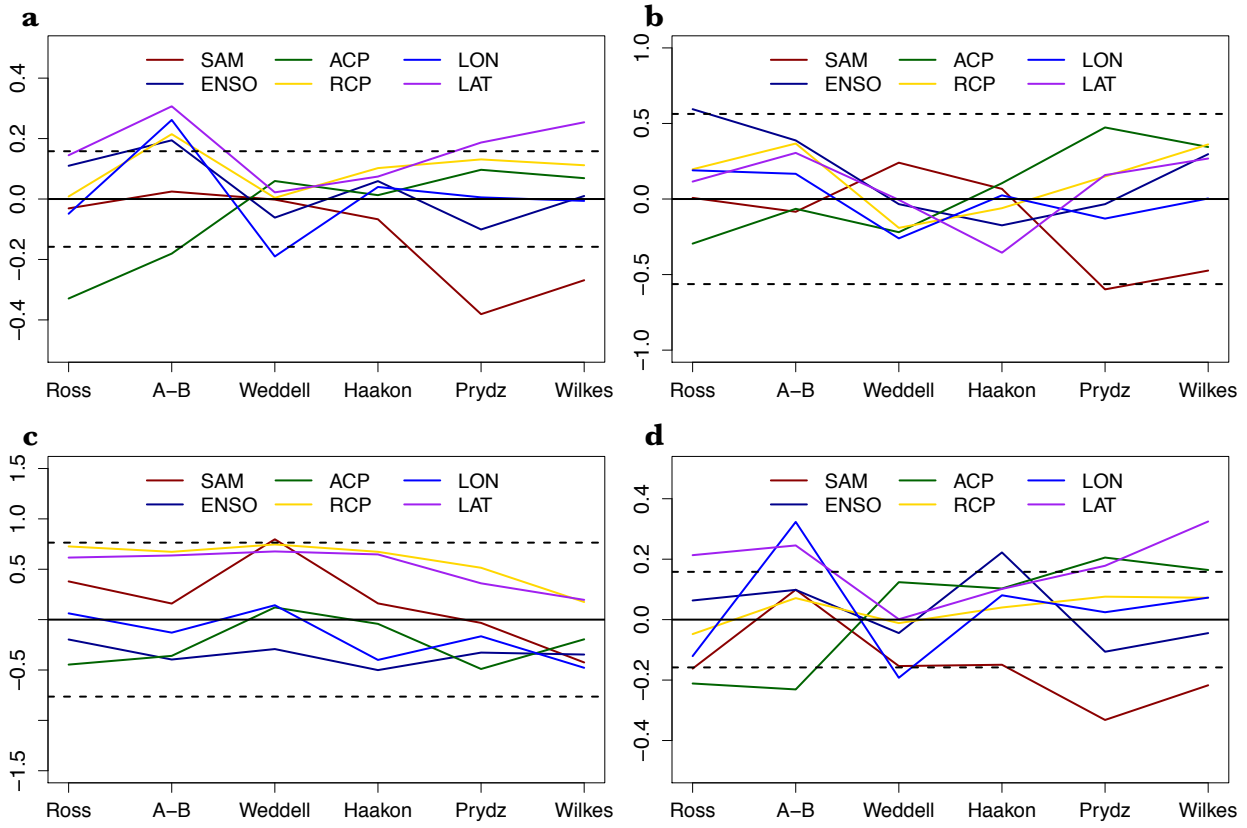

Figure 12: Correlations (r) between each of the atmospheric circulations – the Southern Annular Mode (SAM), El Niño-Southern Oscillation (ENSO), and the Amundsen Sea Low's actual central pressure (ACP), relative central pressure (RCP), longitude (LON), and latitude (LAT) – and mean variability of a) monthly mean polynya variability for polynyas within each region. Similar correlations are presented for the b) annual, c) seasonal, and d) monthly temporal components of the polynya variability. The solid black line indicates no correlation. Dashed black lines indicate statistical significance at the 90% significance level.

At the annual scale, only ENSO is significantly correlated with the Ross group, while the A-B, Weddell, Haakon, and Wilkes have no significant correlations (Figure 12b). The Prydz group is only significantly correlated with SAM. At the seasonal scale, the only significant correlation is

between the SAM and the Weddell group, which entirely consists of the Ronne Ice Shelf Polynya (Figure 12c). When annual and seasonal variability are removed, correlations at the monthly scale are stronger overall (Figure 12d). The ACP, LAT, and the SAM are significantly correlated with the Ross group, and ACP, LAT, and LON are significantly correlated with the A-B group. LON and ENSO have the sole significant correlations with the Weddell and Haakon, respectively. The ACP, LAT, and the SAM are significantly correlated with both the Prydz and Wilkes groups.

The strongest influences from the atmospheric patterns occur at the monthly scale where the ASL and the SAM are most influential. The weakest relationships occur at the seasonal scale when virtually none of the atmospheric patterns are influential on a regional basis. This is true despite the importance of seasonal scale relationships between individual polynyas and atmospheric patterns (chapter 3). The ASL also has very weak influence on mean regional polynya variability at the annual scale. ENSO and the SAM are only significantly influential in the Ross and the Prydz-Wilkes regions, respectively. The Weddell and Haakon regions are the least influenced by any of the three major modes of climate variability analyzed in this study.

3.7 Sea ice sectors

The regional polynya group delineations identified in the current study align generally well with Antarctic sea ice regimes. Polynya groups are displayed in Figure 6. The two regions of significant change in sea ice concentration and timing occur in the Ross Sea and the Amundsen-Bellingshausen Sea. The A-B polynya group spatially coincides with the sector of significantly decreasing sea ice concentration and annual duration. The Ross polynya group generally aligns with the region of significantly positive trends in sea ice concentration and duration. However, the sector of positive sea ice trends extends to Adelie Land of East Antarctica, which is inconsistent with the eastern boundary of the corresponding polynya group that is entirely confined to the Ross

Sea. The Wilkes and Prydz groups are located in regions of intermittently significant negative trends in sea ice concentration near the coast and generally weak sea ice duration trends with various directions. The Haakon polynya group is located within a region of very weak decline in sea ice concentration and duration, and the Weddell group is located within a region of generally weak sea ice concentration and duration trends near the coast. Sea ice concentration and duration are increasing in the Eastern Weddell, but decreasing in the Western Weddell, where the prominent Ronne Ice Shelf polynya is located [Simpkins et al., 2012; Stammerjohn et al., 2012; Liu et al., 2004].

The general alignment between polynya regions and sea ice regimes suggests a direct connection between them. Current literature lacks understanding of the interaction between polynya and sea ice variability. The polynya-sea ice relationship is complicated by the bidirectional influence as well as the mutual contribution to both mediums from large-scale atmospheric and oceanic factors. On one hand, polynya ice production greatly contributes to total regional sea ice content [Drucker et al., 2011]. On the other hand, steep increases in sea ice concentration and sea ice velocity may reduce polynya size through increasing sea ice compaction and backfill downwind of the polynya [Nihashi and Ohshima, 2015]. The direct connection and rate of influence between polynyas and sea ice have not been studied in this way. Also, atmospheric perturbations greatly influence temporal variability in both polynya activity, as most notably shown in chapter 2 of this study as well as in Bromwich and Kurtz [1984] and Tamura et al. [2016], and sea ice content [Raphael et al., 2018; Hobbs et al., 2016; Stammerjohn et al., 2008; and many more].

The polynya group delineations also align generally well with the sea ice sectors determined by previous studies, which represents the regional connection between polynyas and sea ice or their

mutual responses to regionally specific large-scale factors. Figure 6 demarcates the sea ice sector boundaries presented by Zwally et al. [1983] as dashed white lines and the boundaries presented by Raphael and Hobbs [2014] as solid white lines. Zwally et al. [1983] and Raphael and Hobbs [2014] both present five sectors of distinct sea ice regimes that will be compared to the six polynya groups identified in the current study. The Antarctic peninsula is a very common geographic boundary line that has a significant influence on surface conditions.

The strong association of the Bellingshausen and Amundsen Seas (the A-B region), as well as their dissociation from the Ross Sea, are also consistent boundary lines for sector delineation. The transition between the A-B and Ross regions and the eastern boundary of the Weddell region differ between studies. Zwally et al. [1983] includes much of the Haakon region within the Weddell sector, while Raphael and Hobbs [2014] agrees with the current study in limiting the Weddell sector boundaries to the Weddell embayment. Transitions between the Ross sector and East Antarctica sectors is consistent among the three studies [Zwally et al., 1983; Raphael and Hobbs, 2014; and the current study], but the three studies differ in the classification of the Prydz Bay region. Raphael and Hobbs separate East Antarctica into two sectors by grouping the Prydz and Wilkes regions. Zwally et al. [1983] groups the Prydz and the eastern Haakon region. In the current study, the Haakon, Prydz, and Wilkes define three distinct regions.

4. Conclusion

Building upon previous regional Antarctic coastal polynya studies, the current study identifies the contribution of each coastal polynya to the total variability within the circumpolar 25-polynya system. This is calculated for monthly mean polynya area and its annual, seasonal, and monthly scale variations. This study also delineates contiguous regions of significant polynya co-variability,

analyzes the influence of three prominent large-scale atmospheric circulation phenomena, and compares the polynya regions to sea ice regimes. The polynya regions identified highlight important scales at which polynya dynamics occur. The largest spatial scale at which significant Antarctic coastal polynya co-variability occurs is delineated by the continental landmasses and this is strongest at the monthly scale. Thus, there appears to be a continental scale influence that produces monthly co-variability among the polynyas that is not associated with interannual or seasonal variations.

Results from near neighbor Pearson correlations, principal component analyses, gaussian mixture modeling (GMM), and hierarchical agglomerative clustering (HAC) consistently highlight 6 groups of polynyas based on inter-polynya co-variability – Ross, Amundsen-Bellingshausen, Weddell, Haakon, Prydz, and Wilkes. While these groups are based solely on temporal co-variability, without any introduction of spatial ordering, strong spatial contiguities are prominent in the results. At the monthly scale, polynyas in closer proximity to one another generally have stronger co-variability, but the strength of near neighbor correlations varies spatially, producing regional clustering. The regionality appears to be driven by co-variability at the annual and monthly scales. While there is strong circumpolar seasonal synchronization in polynya variability, there is relatively low regionality at the seasonal scale. This is due to the virtually equal seasonal variability.

The Amundsen-Bellingshausen and Haakon polynya groups are the two most consistent polynya groups and have the strongest intra-group co-variability across spatial scales. This may be due to the remote location of the Haakon polynyas, which causes them to respond to factors that other polynyas are not spatially connected to in the same way, and the location of the Amundsen-

Bellingshausen region west of the Antarctic Peninsula where very strong climatic factors exist. The Ross and Weddell groups are characterized by their relatively weak inter-polynya co-variability.

There are statistically significant positive relationships among the mean variability of all regional groups, except the Weddell group, which consists solely of the Ronne Ice Shelf polynya. The significant positive inter-regional correlations are primarily driven by positive seasonal scale co-variability. At the annual level, there are statistically significant positive relationships between the Ross and Amundsen-Bellingshausen groups and between the Prydz and Wilkes groups. The Amundsen-Bellingshausen and Haakon groups have a statistically significant negative relationship. At the monthly scale, when accounting for annual and seasonal variability, the Ross, Amundsen-Bellingshausen, Prydz, and Wilkes groups generally have statistically significant positive inter-regional relationships. The relationship between the Ross and Amundsen-Bellingshausen groups are the strongest and are consistently significant at all scales. The relationship between the Prydz and Wilkes groups is also consistent, only lacking statistical significance at the seasonal scale. Similar to relationships at the individual polynya level, the Weddell group has negative correlations with the other groups at all temporal scales. This may be due to the Ronne Ice Shelf Polynya's location east of the Antarctic Peninsula where the influences on polynya size is opposite of those experienced to the west of the Peninsula.

The Southern Annular Mode, El Niño-Southern Oscillation, and the Amundsen Sea Low all significantly contribute to the mean variability of various regional polynya groups around Antarctica. Influence from the SAM is strongest in East Antarctica where the continent reaches far north, the sea ice field is limited, and other large-scale climatic drivers are less prominent. Influences from ENSO and the ASL are primarily concentrated in West Antarctica. West

Antarctica's position near the South Pacific and directly west of the Antarctic Peninsula allows ENSO and the ASL to have great influence in the region.

ENSO and all four characteristics of the ASL are statistically significant contributors to variability in the Amundsen-Bellingshausen region. This is driven largely by interactions at the monthly scale where the majority of significant large-scale atmospheric influence takes place. Only the SAM has significant seasonal scale influence and this is limited to the Weddell region. The SAM and ENSO have significant annual scale influences in the Prydz and Ross regions, respectively. The Weddell and Haakon regions are the least influenced by any of the three major modes of climate variability analyzed in this study. Contributions from the SAM may drive the continental scale delineation between East and West Antarctica polynya variability. The connection between polynyas and large-scale atmospheric phenomena is supported by the atmosphere's influence on coastal and offshore sea ice drift [Kwok et al., 2017; Kwok et al., 2007]. -SAM, La Niña, and a deep ASL contribute to increased wind speed around the Southern Ocean and increased polynya area in many regions.

While the atmospheric circulation patterns are influential to mean regional polynya variability, their influence does not significantly affect the regional polynya group delineations at all scales. The combined effect of the atmospheric circulation patterns only results in slight adjustments of the polynya groups in the Bellingshausen Sea, eastern Ross Sea, and Adelie Land. However, the atmospheric circulations are very influential on annual scale delineations, particularly in the Amundsen-Bellingshausen and Haakon regions. Seasonality within the atmospheric circulation patterns have very little influence on regional delineations. Thus, drivers for regional polynya

group delineations may occur in the ocean and ice currents, which are strongly linked to continental geometry.

The regional polynya group delineations align generally well with Antarctic sea ice regimes. The A-B and Ross polynya groups spatially coincide with sectors of significantly decreasing and increasing sea ice concentration and annual duration, respectively. The Wilkes and Prydz groups generally align with regions of intermittently significant negative trends in sea ice concentration near the coast and generally weak sea ice duration trends. The Haakon and Weddell polynya groups align with regions of very weak decline in sea ice concentration and duration near the coast. The general alignment between the spatial extent of the polynya groups and sea ice regimes suggest that the polynyas and ice receive significant contributions from similar large-scale influences or significant interaction between the polynyas and the sea ice field. To determine this, future studies should analyze correlations between polynya activity, such as areal dynamics and ice production, and sea ice characteristics, such as variability in ice concentration. To determine confounding influences from the wind, future studies must account for wind variability. This type of analysis may also be beneficial at daily and sub-daily scales.

Chapter 5

Conclusion

Every year, during the ice advance season, coastal polynyas provide important spaces for gas, heat, and moisture to transfer between the ocean and atmosphere. Within that context, coastal polynyas have the highest rates of sea ice production and Antarctic bottom water formation, as well as other important ecological and atmospheric influences, in the Southern Ocean. Thus, variability within the polynyas is vitally important to understanding the changes in these mediums. Even though many studies have analyzed polynya variability, most previous studies focus on daily and interannual scales, leaving gaps in our knowledge of polynya influences and relationships at other scales. The goal of this study was to identify the most important scales of polynya variability, analyze individual and regional polynya variability at those various scales, and understand polynya responses to large-scale atmospheric circulation patterns. To perform this study, a 26-year circum-Antarctic coastal polynya dataset was created with sufficiently high temporal resolution and spatial density.

The results of this study show that the cumulative area within the circumpolar 25-polynya system has a statistically significant positive trend. However, only five individual polynyas have statistically significant long-term trends, which are all non-linear. The three significant negative trends are due to abrupt changes in the icescape. Both significant positive trends are due to significant increases in polynya size from 1992 to 2002, with virtually no trend after that. The direction of all polynya trends exhibit spatial clustering in 4 major regions. Two of which have exclusively positive trends, and the others have predominantly negative trends. The 5 statistically significant trends in individual polynyas exist within the regions of corresponding dominant long-term change.

The 4 greatest contributors to sea ice production, deep water formation, and biological activity decreased in areal extent throughout the study period. The next largest producers of coastal sea ice increased in areal extent during the same period. Thus, the greatest contributors to polynya area and ice production change over time. These changes influence the overall productivity of the Southern Ocean. Significant polynya trends are seldom found when analyzing annual means. They are much more frequently found with sub-annual variability. Thus, trends produced from annual variability mask most of the long-term changes in polynya area.

This study also found that while polynya trends are important for long-term influences on the environment, they actually account for a very small proportion of mean polynya variability. Most polynya variability occurs at the daily scale, followed by monthly and seasonal variations. Very little variability occurs interannually. The large proportion of monthly and seasonal variability promote the need for studies of drivers at those two particular scales. Interannual variability masks sub-annual activity, such as variability within the polynyas themselves and their interaction with large-scale atmospheric phenomena.

The Southern Annular Mode (SAM), El Nino-Southern Oscillation (ENSO), and the Amundsen Sea Low (ASL) significantly contribute to individual and regional coastal polynya variability. 22 of the 25 polynyas analyzed in the current study are significantly influenced by the SAM, ENSO, or the ASL. The regionality of the significant relationships is consistent with the regionality of sea ice response to the three atmospheric factors. The SAM is a circumpolar phenomenon, but its strongest influence on coastal sea ice is in East Antarctica [Raphael and Hobbs, 2014; Simpkins et al., 2012], which is also reflected in the polynya-SAM relationship. ENSO is a tropical

phenomenon with very strong global effects. Its strongest extratropical connection is in West Antarctica where the polynya-ENSO relationship is significant. The ASL is an exclusively West Antarctica phenomenon that significantly influences all polynyas in West Antarctica. The coastal influence of the atmospheric patterns on coastal wind and ice motion, coupled with the effects from a ridged coastline, greatly influences polynya size. The significant influences that the SAM and the ASL have on polynyas are primarily driven by monthly and seasonal co-variability. Strong influences from ENSO are primarily driven at the annual level. Future studies may further improve general understanding of large-scale polynya-atmosphere interaction by analyzing polynya relationships to other important Southern Hemisphere climate patterns such as Zonal Wave 3 and the Semi-Annual Oscillation.

Next, this study found that variability in the large-scale atmospheric patterns exhibit regional influence. Using Pearson correlations (PCor), principal component analyses (PCA), gaussian mixture modeling (GMM), and hierarchical agglomerative clustering (HAC), six regional polynya groups are delineated – Ross, Amundsen-Bellingshausen, Weddell, Haakon, Prydz, and Wilkes. While these groups are based solely on temporal co-variability, without any introduction of spatial ordering, strong spatial contiguities are prominent. The regionality appears to be driven by co-variability at the annual and monthly scales. While there is strong circumpolar seasonal synchronization in polynya variability, there is relatively low regionality at the seasonal scale. This is due to the virtually equal seasonal variability around the entire continent.

The Amundsen-Bellingshausen and Haakon polynya groups are the two most consistent groups and have the strongest intra-group co-variability across spatial scales. The Ross and Weddell groups are characterized by their relatively weak inter-polynya co-variability. There are statistically

significant positive relationships between the mean variability of all regional groups, except the Weddell group, which has negative relationships at all scales. The significant inter-regional correlations are primarily driven at the seasonal scale. The relationship between the Ross and Amundsen-Bellingshausen groups are the strongest and are consistently significant at all scales. The relationship between the Prydz and Wilkes groups is also consistent, only lacking statistical significance at the seasonal scale. The largest spatial scale at which significant inter-polynya co-variability occurs is delineated by the differences in monthly variability between East and West Antarctica. Contributions from the SAM may drive these continental scale delineations.

Lastly, this study found that while atmospheric circulation patterns significantly influence mean regional polynya variability, they do not significantly affect regional delineations. Instead, drivers for group delineations occur in the ocean currents, which are strongly linked to continental geometry and location. This gives a greater amount of specific accountability to general ocean currents than that offered in past studies. This is the first study to delineate regional polynya groups based on size characteristics. The regional polynya group delineations produced here align generally well with Antarctic sea ice regimes. The general alignment between the spatial extent of the polynya groups and sea ice regimes suggest that the polynyas and ice receive significant contributions from similar large-scale influences or there is significant interaction between the polynyas and the sea ice field. Currently, the influence of polynya variability on the sea ice field downstream is not well understood. This is a point of potentially fruitful future research.

References

Ackley, S. F., C. A. Geiger, J. C. King, E. C. Hunke, and J. Comiso (2001), The Ronne polynya of 1997/98: observations of air-ice-ocean interaction, in Annals of Glaciology, Vol 33, edited by M. O. Jeffries and H. Eicken, doi:10.3189/172756401781818725.

Adolphs, U., and G. Wendler (1995), A Pilot-Study On The Interactions Between Katabatic Winds And Polynyas At The Adelie Coast, Eastern Antarctica, Antarctic Science, 7(3), 307-314.

Anderson, P. S. (1993), Evidence For An Antarctic Winter Coastal Polynya, Antarctic Science, 5(2), 221-226.

Andreas, E. L., P. S. Guest, P. O. G. Persson, C. W. Fairall, T. W. Horst, R. E. Moritz, and S. R. Semmer (2002), Near-surface water vapor over polar sea ice is always near ice saturation, Journal of Geophysical Research-Oceans, 107(C10), doi:10.1029/2000jc000411.

Andreas, E. L., C. A. Paulson, R. M. Williams, R. W. Lindsay, and J. A. Businger (1979), Turbulent Heat-Flux From Arctic Leads, Boundary-Layer Meteorology, 17(1), 57-91, doi:10.1007/bf00121937.

Arblaster, J. M., and G. A. Meehl (2006), Contributions of external forcings to southern annular mode trends, Journal of Climate, 19(12), 2896-2905, doi:10.1175/jcli3774.1.

Armstrong, R., K. Knowles, M. J. Brodzik, and M. A. Hardman (1994), DMSP SSM/I-SSMIS Pathfinder Daily EASE-Grid Brightness Temperatures, Version 2. Used subset with years 1992-2017. Boulder, Colorado USA. NASA National Snow and Ice Data Center Distributed Active Archive Center. doi: https://doi.org/10.5067/3EX2U1DV3434. Accessed October 1, 2017.

Arrigo, K. R., D. H. Robinson, R. B. Dunbar, A. R. Leventer, and M. P. Lizotte (2003a), Physical control of chlorophyll a, POC, and TPN distributions in the pack ice of the Ross Sea, Antarctica, Journal of Geophysical Research-Oceans, 108(C10), doi:10.1029/2001jc001138.

Arrigo, K. R., and G. L. van Dijken (2003a), Impact of iceberg C-19 on Ross Sea primary production, Geophysical Research Letters, 30(16), doi:10.1029/2003gl017721.

Arrigo, K. R., and G. L. van Dijken (2003b), Phytoplankton dynamics within 37 Antarctic coastal polynya systems, Journal of Geophysical Research-Oceans, 108(C8), doi:10.1029/2002jc001739.

Arrigo, K. R., and G. L. van Dijken (2004), Annual changes in sea-ice, chlorophyll a, and primary production in the Ross Sea, Antarctica, Deep-Sea Research Part Ii-Topical Studies in Oceanography, 51(1-3), 117-138, doi:10.1016/j.dsr2.2003.04.003.

Arrigo, K. R., D. L. Worthen, and D. H. Robinson (2003b), A coupled ocean-ecosystem model of the Ross Sea: 2. Iron regulation of phytoplankton taxonomic variability and primary production, Journal of Geophysical Research-Oceans, 108(C7), doi:10.1029/2001jc000856.

Beckmann, A., H. H. Hellmer, and R. Timmermann (1999), A numerical model of the Weddell Sea: Large-scale circulation and water mass distribution, Journal of Geophysical Research-Oceans, 104(C10), 23375-23391, doi:10.1029/1999jc900194.

Bromwich, D. H., J. F. Carrasco, Z. Liu, and R. Y. Tzeng (1993a), Hemispheric Atmospheric Variations And Oceanographic Impacts Associated With Katabatic Surges Across The Ross Ice Shelf, Antarctica, Journal of Geophysical Research-Atmospheres, 98(D7), 13045-13062, doi:10.1029/93jd00562.

Bromwich, D. H., Y. Du, and T. R. Parish (1994), Numerical-Simulation Of Winter Katabatic Winds From West Antarctica Crossing Siple Coast And The Ross Ice Shelf, Monthly Weather Review, 122(7), 1417-1435, doi:10.1175/1520-0493(1994)122<1417:nsowkw>2.0.co;2.

Bromwich, D. H., and D. D. Kurtz (1984), Katabatic Wind Forcing Of The Terra-Nova Bay Polynya, Journal of Geophysical Research-Oceans, 89(NC3), 3561-3572, doi:10.1029/JC089iC03p03561.

Bromwich D.H., A.J. Monaghan, A.N. Rogers, M.L. Van Woert, K.R. Arrigo (1998), Winter Atmospheric Forcing of the Ross Sea Polynya, American Geophysical Union – Ocean, Ice, And Atmosphere: Interactions At The Antarctic Continental Margin, Antarctic Research Series, 75, 101-133, http://citeseerx.ist.psu.edu/viewdoc/download?doi=10.1.1.515.5490&rep=rep1&type=pdf

Bromwich, D. H., F. M. Robasky, R. A. Keen, and J. F. Bolzan (1993b), Modeled Variations Of Precipitation Over The Greenland Ice-Sheet, Journal of Climate, 6(7), 1253-1268, doi:10.1175/1520-0442(1993)006<1253:mvopot>2.0.co;2.

Cai, W. J., and P. G. Baines (1996), Interactions between thermohaline- and wind-driven circulations and their relevance to the dynamics of the Antarctic Circumpolar Current, in a coarse-resolution global ocean general circulation model, Journal of Geophysical Research-Oceans, 101(C6), 14073-14093, doi:10.1029/96jc00669.

Campagne, P., et al. (2015), Glacial ice and atmospheric forcing on the Mertz Glacier Polynya over the past 250 years, Nature Communications, 6, 9, doi:10.1038/ncomms7642.

Carleton, A. M. (2003), Atmospheric teleconnections involving the Southern Ocean, Journal of Geophysical Research-Oceans, 108(C4), doi:10.1029/2000jc000379.

J.F. Carrasco and D.H. Bromwich (1993), Satellite and Automatic Weather Station Analyses of Katabatic Surges Across the Ross Ice Shelf, Antarctic Meteorology and Climatology: Studies Based On Automatic Weather Stations – Antarctic Research Series, 61, 93-108. doi:10.1029/AR061p0093.

Cavalieri, D. J., and C. L. Parkinson (2008), Antarctic sea ice variability and trends, 1979-2006, Journal of Geophysical Research-Oceans, 113(C7), doi:10.1029/2007jc004564.

Cheng, Z., X. P. Pang, X. Zhao, and C. Tan (2017), Spatio-Temporal Variability and Model Parameter Sensitivity Analysis of Ice Production in Ross Ice Shelf Polynya from 2003 to 2015, Remote Sensing, 9(9), doi:10.3390/rs9090934.

Cheon, W. G., C. B. Cho, A. L. Gordon, Y. H. Kim, and Y. G. Park (2018), The Role of Oscillating Southern Hemisphere Westerly Winds: Southern Ocean Coastal and Open-Ocean Polynyas, Journal of Climate, 31(3), 1053-1073, doi:10.1175/jcli-d-17-0237.1.

Coggins, J. H. J., and A. J. McDonald (2015), The influence of the Amundsen Sea Low on the winds in the Ross Sea and surroundings: Insights from a synoptic climatology, Journal of Geophysical Research-Atmospheres, 120(6), 2167-2189, doi:10.1002/2014jd022830.

Comiso, J. (2010), Polar Oceans From Space, Polar Oceans from Space, 41, 1-507, doi:10.1007/978-0-387-68300-3.

Comiso, J. C., R. Kwok, S. Martin, and A. L. Gordon (2011), Variability and trends in sea ice extent and ice production in the Ross Sea, Journal of Geophysical Research-Oceans, 116, doi:10.1029/2010jc006391.

Cotton, J. H., and K. J. Michael (1994), The Monitoring Of Katabatic Wind-Coastal Polynya Interaction Using AVHRR Imagery, Antarctic Science, 6(4), 537-540.

Drucker, R., S. Martin, and R. Kwok (2011), Sea ice production and export from coastal polynyas in the Weddell and Ross Seas, Geophysical Research Letters, 38, 4, doi:10.1029/2011gl048668.

Fiedler, E. K., T. A. Lachlan-Cope, I. A. Renfrew, and J. C. King (2010), Convective heat transfer over thin ice covered coastal polynyas, Journal of Geophysical Research-Oceans, 115, doi:10.1029/2009jc005797.

Fogt, R. L., A. J. Wovrosh, R. A. Langen, and I. Simmonds (2012), The characteristic variability and connection to the underlying synoptic activity of the Amundsen-Bellingshausen Seas Low, Journal of Geophysical Research-Atmospheres, 117, doi:10.1029/2011jd017337.

Frezzotti, M. and M.C.G. Mabin (1994) 20th Century Behaviour of Drygalski Ice Tongue, Ross Sea, Antarctica, Annals of Glaciology, 20, 397–400, doi:10.3189/172756494794587492.

Fusco, G., G. Budillon, and G. Spezie (2009), Surface heat fluxes and thermohaline variability in the Ross Sea and in Terra Nova Bay polynya, Continental Shelf Research, 29(15), 1887-1895, doi:10.1016/j.csr.2009.07.006.

Gillett, N. P., D. A. Stone, P. A. Stott, T. Nozawa, A. Y. Karpechko, G. C. Hegerl, M. F. Wehner, and P. D. Jones (2008), Attribution of polar warming to human influence, Nature Geoscience, 1(11), 750-754, doi:10.1038/ngeo338.

Gloersen, P., W. J. Campbell, D. J. Cavalieri, J. C. Comiso, C. L. Parkinson, and H. J. Zwally (1993), Satellite Passive Microwave Observations And Analysis Of Arctic And Antarctic Sea-Ice, 1978-1987, Annals of Glaciology, Vol 17, 149-154.

Goosse, H., and T. Fichefet (2001), Open-ocean convection and polynya formation in a large-scale ice-ocean model, Tellus Series a-Dynamic Meteorology and Oceanography, 53(1), 94-111, doi:10.1034/j.1600-0870.2001.01061.x.

Gordon, A. L., M. Visbeck, and J. C. Comiso (2007), A possible link between the Weddell Polynya and the Southern Annular Mode, Journal of Climate, 20(11), 2558-2571, doi:10.1175/jcli4046.1.

Haid, V., and R. Timmermann (2013), Simulated heat flux and sea ice production at coastal polynyas in the southwestern Weddell Sea, Journal of Geophysical Research-Oceans, 118(5), 2640-2652, doi:10.1002/jgrc.20133.

Haid, V., R. Timmermann, L. Ebner, and G. Heinemann (2015), Atmospheric forcing of coastal polynyas in the south-western Weddell Sea, Antarctic Science, 27(4), 388-402, doi:10.1017/s0954102014000893.

Hall, A., and M. Visbeck (2002), Synchronous variability in the southern hemisphere atmosphere, sea ice, and ocean resulting from the annular mode, Journal of Climate, 15(21), 3043-3057, doi:10.1175/1520-0442(2002)015<3043:svitsh>2.0.co;2.

Hall, R. T., and D. A. Rothrock (1987), Photogrammetric Observations Of The Lateral Melt Of Sea Ice Floes, Journal of Geophysical Research-Oceans, 92(C7), 7045-7048, doi:10.1029/JC092iC07p07045.

Hobbs, W. R., R. Massom, S. Stammerjohn, P. Reid, G. Williams, and W. Meier (2016), A review of recent changes in Southern Ocean sea ice, their drivers and forcings, Global and Planetary Change, 143, 228-250, doi:10.1016/j.gloplacha.2016.06.008.

Holland, P. R., and R. Kwok (2012), Wind-driven trends in Antarctic sea-ice drift, Nature Geoscience, 5(12), 872-875, doi:10.1038/ngeo1627.

Hollands, T., V. Haid, W. Dierking, R. Timmermann, and L. Ebner (2013), Sea ice motion and open water area at the Ronne Polynia, Antarctica: Synthetic aperture radar observations versus model results, Journal of Geophysical Research-Oceans, 118(4), 1940-1954, doi:10.1002/jgrc.20158.

Hosking, J. S., A. Orr, G. J. Marshall, J. Turner, and T. Phillips (2013), The Influence of the Amundsen-Bellingshausen Seas Low on the Climate of West Antarctica and Its Representation in Coupled Climate Model Simulations, Journal of Climate, 26(17), 6633-6648, doi:10.1175/jcli-d-12-00813.1.

Hunke, E. C., and S. F. Ackley (2001), A numerical investigation of the 1997-1998 Ronne Polynya, Journal of Geophysical Research-Oceans, 106(C10), 22373-22382, doi:10.1029/2000jc000640.

Ishikawa, T., J. Ukita, K. I. Ohshima, M. Wakatsuchi, T. Yamanouchi, and N. Ono (1996), Coastal polynyas off East Queen Maud Land observed from NOAA AVHRR data, Journal of Oceanography, 52(3), 389-398, doi:10.1007/bf02235932.

Jacobs, S. S. (2004), Bottom water production and its links with the thermohaline circulation, Antarctic Science, 16(4), 427-437, doi:10.1017/s095410200400224x.

Kern, S. (2009), Wintertime Antarctic coastal polynya area: 1992-2008, Geophysical Research Letters, 36, doi:10.1029/2009gl038062.

Kern, S., G. Spreen, L. Kaleschke, S. De La Rosa, and G. Heygster (2007), Polynya signature simulation method polynya area in comparison to AMSR-E 89 GHz sea-ice concentrations in the Ross Sea and off the Adelie Coast, Antarctica, for 2002-05: first results, Annals of Glaciology, 46(1), doi:10.3189/172756407782871585.

Kimura, N., and M. Wakatsuchi (2011), Large-scale processes governing the seasonal variability of the Antarctic sea ice, Tellus Series a-Dynamic Meteorology and Oceanography, 63(4), 828-840, doi:10.1111/j.1600-0870.2011.00526.x.

Kitade, Y., K. Shimada, T. Tamura, G. D. Williams, S. Aoki, Y. Fukamachi, F. Roquet, M. Hindell, S. Ushio, and K. I. Ohshima (2014), Antarctic Bottom Water production from

the Vincennes Bay Polynya, East Antarctica, Geophysical Research Letters, 41(10), 3528-3534, doi:10.1002/2014gl059971.

Knuth, S. L., and J. J. Cassano (2011), An Analysis of Near-Surface Winds, Air Temperature, and Cyclone Activity in Terra Nova Bay, Antarctica, from 1993 to 2009, Journal of Applied Meteorology and Climatology, 50(3), 662-680, doi:10.1175/2010jamc2507.1.

Konishi, S. and G. Kitagawa (2008), Information Criteria and Statistical Modeling, Springer Series in Statistics, 211-237, Book.

Kottmeier, C., and D. Engelbart (1992), Generation And Atmospheric Heat-Exchange Of Coastal Polynyas In The Weddell Sea, Boundary-Layer Meteorology, 60(3), 207-234, doi:10.1007/bf00119376.

Kurtz, D. and D.H. Bromwich (1983), Satellite Observed Behavior Of The Terra-Nova Bay Polynya, Journal of Geophysical Research-Oceans and Atmospheres, 88(NC14), 9717-9722, doi:10.1029/JC088iC14p09717.

Kurtz, D. and D.H. Bromwich (1985), A Recurring, Atmospherically Forced Polynya in Terra Nova Bay, American Geophysical Union, Oceanology of the Antarctic Continental Shelf – Antarctic Research Series 43. https://doi.org/10.1029/AR043p0177.

Kusahara, K., H. Hasumi, and G. D. Williams (2011), Impact of the Mertz Glacier Tongue calving on dense water formation and export, Nature Communications, 2, doi:10.1038/ncomms1156.

Kwok, R. (2010), Satellite remote sensing of sea-ice thickness and kinematics: a review, Journal of Glaciology, 56(200), 1129-1140.

Kwok, R., and J. C. Comiso (2002a), Southern Ocean climate and sea ice anomalies associated with the Southern Oscillation, Journal of Climate, 15(5), 487-501, doi:10.1175/1520-0442(2002)015<0487:socasi>2.0.co;2.

Kwok, R., and J. C. Comiso (2002b), Spatial patterns of variability in Antarctic surface temperature: Connections to the Southern Hemisphere Annular Mode and the Southern Oscillation, Geophysical Research Letters, 29(14), doi:10.1029/2002gl015415.

Kwok, R., J. C. Comiso, S. Martin, and R. Drucker (2007), Ross Sea polynyas: Response of ice concentration retrievals to large areas of thin ice, Journal of Geophysical Research-Oceans, 112(C12), doi:10.1029/2006jc003967.

Kwok, R., S.S. Pang, and S. Kacimi (2017), Sea ice drift in the Southern Ocean: Regional patterns, variability, and trends. Elem Sci Anth, 5, 32. DOI:http://doi.org/10.1525/elementa.226

Labrousse, S., et al. (2018), Coastal polynyas: Winter oases for subadult southern elephant seals in East Antarctica, Scientific Reports, 8, 15, doi:10.1038/s41598-018-21388-9.

Lacarra, M., M.-N. Houssais, C. Herbaut, E. Sultan, and M. Beauverger (2014), Dense shelf water production in the Adelie Depression, East Antarctica, 2004-2012: Impact of the Mertz Glacier calving, Journal of Geophysical Research-Oceans, 119(8), 5203-5220, doi:10.1002/2013jc009124.

Lefebvre, W., H. Goosse, R. Timmermann, and T. Fichefet (2004), Influence of the Southern Annular Mode on the sea ice-ocean system, Journal of Geophysical Research-Oceans, 109(C9), 12, doi:10.1029/2004jc002403.

Li, X. C., E. P. Gerber, D. M. Holland, and C. Yoo (2015a), A Rossby Wave Bridge from the Tropical Atlantic to West Antarctica, Journal of Climate, 28(6), 2256-2273, doi:10.1175/jcli-d-14-00450.1.

Li, X. C., D. M. Holland, E. P. Gerber, and C. Yoo (2014), Impacts of the north and tropical Atlantic Ocean on the Antarctic Peninsula and sea ice, Nature, 505(7484), 538-+, doi:10.1038/nature12945.

Li, X. C., D. M. Holland, E. P. Gerber, and C. Yoo (2015b), Rossby Waves Mediate Impacts of Tropical Oceans on West Antarctic Atmospheric Circulation in Austral Winter, Journal of Climate, 28(20), 8151-8164, doi:10.1175/jcli-d-15-0113.1.

Li, Y., R. B. Ji, S. Jenouvrier, M. B. Jin, and J. Stroeve (2016), Synchronicity between ice retreat and phytoplankton bloom in circum-Antarctic polynyas, Geophysical Research Letters, 43(5), 2086-2093, doi:10.1002/2016gl067937.

Liu, J. P., J. A. Curry, and D. G. Martinson (2004), Interpretation of recent Antarctic sea ice variability, Geophysical Research Letters, 31(2), doi:10.1029/2003gl018732.

Liu, J. P., D. G. Martinson, X. J. Yuan, and D. Rind (2002), Evaluating Antarctic sea ice variability and its teleconnections in global climate models, International Journal of Climatology, 22(8), 885-900, doi:10.1002/joc.770.

Maksym, T., S. E. Stammerjohn, S. Ackley, and R. Massom (2012), Antarctic Sea Ice-A Polar Opposite?, Oceanography, 25(3), 140-151.

Markus, T., and B. A. Burns (1995), A Method To Estimate Subpixel-Scale Coastal Polynyas With Satellite Passive Microwave Data, Journal of Geophysical Research-Oceans, 100(C3), 4473-4487, doi:10.1029/94jc02278.

Markus, T., C. Kottmeier, and E. Fahrbach (1998), Ice Formation in Coastal Polynyas In the Weddell Sea and Their Impact on Oceanic Salinity, Antarctic Sea Ice: Physical Processes, Interactions And Variability – Antarctic Research Series, 74, 273-292. https://doi.org/10.1029/AR074p0273.

Marshall, G. J. (2003), Trends in the southern annular mode from observations and reanalyses, Journal of Climate, 16(24), 4134-4143, doi:10.1175/1520-0442(2003)016<4134:titsam>2.0.co;2.

Marsland, S. J., N. L. Bindoff, G. D. Williams, and W. F. Budd (2004), Modeling water mass formation in the Mertz Glacier Polynya and Adelie Depression, East Antarctica, Journal of Geophysical Research-Oceans, 109(C11), doi:10.1029/2004jc002441.

Marsland, S. J., J. A. Church, N. L. Bindoff, and G. D. Williams (2007), Antarctic coastal polynya response to climate change, Journal of Geophysical Research-Oceans, 112(C7), doi:10.1029/2005jc003291.

Martin, A. J., A. Hines, and M. J. Bell (2007), Data assimilation in the FOAM operational short-range ocean forecasting system: A description of the scheme and its impact, Quarterly Journal of the Royal Meteorological Society, 133(625), 981-995, doi:10.1002/qj.74.

Massom, R. A., P. T. Harris, K. J. Michael, and M. J. Potter (1998), The distribution and formative processes of latent-heat polynyas in East Antarctica, in Annals of Glaciology, Vol 27, 1998, edited by W. F. Budd, pp. 420-426, International Glaciological Society, Cambridge.

Montes-Hugo, M. A., and X. J. Yuan (2012), Climate patterns and phytoplankton dynamics in Antarctic latent heat polynyas, Journal of Geophysical Research-Oceans, 117, doi:10.1029/2010jc006597.

Nakata, K., K. I. Ohshima, S. Nihashi, N. Kimura, and T. Tamura (2015), Variability and ice production budget in the Ross Ice Shelf Polynya based on a simplified polynya model and satellite observations, Journal of Geophysical Research-Oceans, 120(9), 6234-6252, doi:10.1002/2015jc010894.

National Snow and Ice Data Center (2018), State of the Cryosphere: Sea Ice, https://nsidc.org/cryosphere/sotc/sea_ice.html. Accessed November 1, 2018.

Nicholls, K.W. (2001), Sub Ice-Shelf Circulation and Processes, Ocean Currents, Elsevier Ltd. – 1st edition of Encyclopedia of Ocean Sciences, 5, 2892–2901, Book.

Nicholls, N. (2008), Recent trends in the seasonal and temporal behaviour of the El Nino-Southern Oscillation, Geophysical Research Letters, 35(19), 4, doi:10.1029/2008gl034499.

Nihashi, S., and K. I. Ohshima (2015), Circumpolar Mapping of Antarctic Coastal Polynyas and Landfast Sea Ice: Relationship and Variability, Journal of Climate, 28(9), 3650-3670, doi:10.1175/jcli-d-14-00369.1.

Nihashi, S., K. I. Ohshima, M. O. Jeffries, and T. Kawamura (2005), Sea-ice melting processes inferred from ice-upper ocean relationships in the Ross Sea, Antarctica, Journal of Geophysical Research-Oceans, 110(C2), doi:10.1029/2003jc002235.

Nihashi, S., K. I. Ohshima, and T. Tamura (2017), Sea-Ice Production in Antarctic Coastal Polynyas Estimated From AMSR2 Data and Its Validation Using AMSR-E and SSM/I-SSMIS Data, IEEE Journal of Selected Topics in Applied Earth Observations and Remote Sensing, 10(9), 3912-3922, doi:10.1109/jstars.2017.2731995.

Ohshima, K. I., Y. Fukamachi, G.D. Williams, et al. (2013), Antarctic Bottom Water production by intense sea-ice formation in the Cape Darnley polynya, Nature Geoscience, 6(3), 235-240, doi:10.1038/ngeo1738.

Ohshima, K.I., S. Nihashi, and K. Iwamoto (2016), Global view of sea-ice production in polynyas and its linkage to dense bottom water formation, Geoscience Letters, 3, DOI 10.1186/s40562-016-0045-4.

Parish, T. R., and D. H. Bromwich (1998), A case study of Antarctic katabatic wind interaction with large-scale forcing, Monthly Weather Review, 126(1), 199-209, doi:10.1175/1520-0493(1998)126<0199:acsoak>2.0.co;2.

Parish, T. R., P. Pettre, and G. Wendler (1993), The Influence Of Large-Scale Forcing On The Katabatic Wind Regime At Adelie Land, Antarctica, Meteorology and Atmospheric Physics, 51(3-4), 165-176, doi:10.1007/bf01030492.

Park, J., H. C. Kim, Y. H. Jo, A. Kidwell, and J. Hwang (2018), Multi-temporal variation of the Ross Sea Polynya in response to climate forcings, Polar Research, 37, 13, doi:10.1080/17518369.2018.1444891.

Parkinson, C. L., and D. J. Cavalieri (2012), Antarctic sea ice variability and trends, 1979-2010, Cryosphere, 6(4), 871-880, doi:10.5194/tc-6-871-2012.

Parmiggiani, F. (2005), Analysis of polynya size fluctuations by means of active and passive microwave radiometers, Proceedings of the SPIE - The International Society for Optical Engineering, 5977(1), doi:10.1117/12.629601.

Paul, S., S. Willmes, and G. Heinemann (2015), Long-term coastal-polynya dynamics in the southern Weddell Sea from MODIS thermal-infrared imagery, Cryosphere, 9(6), 2027-2041, doi:10.5194/tc-9-2027-2015.

Raddatz, R. L., R. J. Galley, and D. G. Barber (2012), Linking the Atmospheric Boundary Layer to the Amundsen Gulf Sea-Ice Cover: A Mesoscale to Synoptic-Scale Perspective from Winter to Summer 2008, Boundary-Layer Meteorology, 142(1), 123-148, doi:10.1007/s10546-011-9669-2.

Raphael, M. N. (2007), The influence of atmospheric zonal wave three on Antarctic sea ice variability, Journal of Geophysical Research-Atmospheres, 112(D12), doi:10.1029/2006jd007852.

Raphael, M. N. and W. Hobbs (2014), The influence of the large-scale atmospheric circulation on Antarctic sea ice during ice advance and retreat seasons, Geophysical Research Letters, 41, 5037–5045, doi:10.1002/2014GL060365.

Raphael, M.N., M.M. Holland, L. Landrum, and W.R. Hobbs (2018), Links between the Amundsen Sea Low and sea ice in the Ross Sea: seasonal and interannual relationships, Climate Dynamics, https://doi.org/10.1007/s00382-018-4258-4.

Raphael, M. N., G. J. Marshall, J. Turner, R. L. Fogt, D. Schneider, D. A. Dixon, J. S. Hosking, J. M. Jones, and W. R. Hobbs (2016), The Amundsen Sea Low: Variability, Change, and Impact on Antarctic Climate, Bulletin of the American Meteorological Society, 97(1), 111-121, doi:10.1175/bams-d-14-00018.1.

Renfrew, I. A., J. C. King, and T. Markus (2002), Coastal polynyas in the southern Weddell Sea: Variability of the surface energy budget, Journal of Geophysical Research-Oceans, 107(C6), doi:10.1029/2000jc000720.

Renwick, J. A., A. Kohout, and S. Dean (2012), Atmospheric Forcing of Antarctic Sea Ice on Intraseasonal Time Scales, Journal of Climate, 25(17), 5962-5975, doi:10.1175/jcli-d-11-00423.1.

Rokach, L. and O. Maimon (2005), Data Mining and Knowledge Discovery Handbook, Chapter 15: Clustering Methods, Springer, Boston, MA, 321-352, https://doi.org/10.1007/b107408. Book.

Schroeter, S., W. Hobbs, and N.L. Bindoff (2017), Interactions between Antarctic sea ice and large-scale atmospheric modes in CMIP5 models, The Cryosphere, 11, 789-803, https://doi.org/10.5194/tc-11-789-2017.

Scrucca, L., M. Fop, T.B. Murphy, and A.E. Raftery (2016), mclust 5: Clustering, Classification and Density Estimation Using Gaussian Finite Mixture Models, The R Journal, 8(1). 289-317, https://www.ncbi.nlm.nih.gov/pmc/articles/PMC5096736/#idm140245753498960title

Shadwick, E. H., S. R. Rintoul, B. Tilbrook, G. D. Williams, N. Young, A. D. Fraser, H. Marchant, J. Smith, and T. Tamura (2013), Glacier tongue calving reduced dense water formation and enhanced carbon uptake, Geophysical Research Letters, 40(5), 904-909, doi:10.1002/grl.50178.

Simpkins, G. R., L. M. Ciasto, D. W. J. Thompson, and M. H. England (2012), Seasonal Relationships between Large-Scale Climate Variability and Antarctic Sea Ice Concentration, Journal of Climate, 25(16), 5451-5469, doi:10.1175/jcli-d-11-00367.1.

Smith, S. D., R. D. Muench, and C. H. Pease (1990), Polynyas And Leads - An Overview Of Physical Processes And Environment, Journal of Geophysical Research-Oceans, 95(C6), 9461-9479, doi:10.1029/JC095iC06p09461.

Snow, K., B. M. Sloyan, S. R. Rintoul, A. M. Hogg, and S. M. Downes (2016), Controls on circulation, cross-shelf exchange, and dense water formation in an Antarctic polynya, Geophysical Research Letters, 43(13), 7089-7096, doi:10.1002/2016gl069479.

Stammerjohn, S., R. Massom, D. Rind, and D. Martinson (2012), Regions of rapid sea ice change: An inter-hemispheric seasonal comparison, Geophysical Research Letters, 39, doi:10.1029/2012gl050874.

Stammerjohn, S. E., D. G. Martinson, R. C. Smith, X. Yuan, and D. Rind (2008), Trends in Antarctic annual sea ice retreat and advance and their relation to El Nino-Southern Oscillation and Southern Annular Mode variability, Journal of Geophysical Research-Oceans, 113(C3), doi:10.1029/2007jc004269.

Stroeve, J. C., S. Jenouvrier, G. G. Campbell, C. Barbraud, and K. Delord (2016), Mapping and assessing variability in the Antarctic marginal ice zone, pack ice and coastal polynyas in two sea ice algorithms with implications on breeding success of snow petrels, Cryosphere, 10(4), 1823-1843, doi:10.5194/tc-10-1823-2016.

Tamura, T., K. I. Ohshima, A. D. Fraser, and G. D. Williams (2016), Sea ice production variability in Antarctic coastal polynyas, Journal of Geophysical Research-Oceans, 121(5), 2967-2979, doi:10.1002/2015jc011537.

Tamura, T., K. I. Ohshima, T. Markus, D. J. Cavalieri, S. Nihashi, and N. Hirasawa (2007), Estimation of thin ice thickness and detection of fast ice from SSM/I data in the Antarctic Ocean, Journal of Atmospheric and Oceanic Technology, 24(10), 1757-1772, doi:10.1175/jtech2113.1.

Tamura, T., K. I. Ohshima, and S. Nihashi (2008), Mapping of sea ice production for Antarctic coastal polynyas, Geophysical Research Letters, 35(7), doi:10.1029/2007gl032903.

Tamura, T., G. D. Williams, A. D. Fraser, and K. I. Ohshima (2012), Potential regime shift in decreased sea ice production after the Mertz Glacier calving, Nature Communications, 3, doi:10.1038/ncomms1820.

Thompson, D. W. J., and S. Solomon (2002), Interpretation of recent Southern Hemisphere climate change, Science, 296(5569), 895-899, doi:10.1126/science.1069270.

Thompson, D. W. J., S. Solomon, P. J. Kushner, M. H. England, K. M. Grise, and D. J. Karoly (2011), Signatures of the Antarctic ozone hole in Southern Hemisphere surface climate change, Nature Geoscience, 4(11), 741-749, doi:10.1038/ngeo1296.

Thompson, D. W. J., and J. M. Wallace (2000), Annular modes in the extratropical circulation. Part I: Month-to-month variability, Journal of Climate, 13(5), 1000-1016, doi:10.1175/1520-0442(2000)013<1000:amitec>2.0.co;2.

Thompson, D. W. J., J. M. Wallace, and G. C. Hegerl (2000), Annular modes in the extratropical circulation. Part II: Trends, Journal of Climate, 13(5), 1018-1036, doi:10.1175/1520-0442(2000)013<1018:amitec>2.0.co;2.

Trenberth, K. E., and P. D. Jones (2007), Observations: Surface and Atmospheric Climate Change, 235-336 pp., Cambridge University Press, New York.

Turner, J., J. C. Comiso, G. J. Marshall, T. A. Lachlan-Cope, T. Bracegirdle, T. Maksym, M. P. Meredith, Z. M. Wang, and A. Orr (2009), Non-annular atmospheric circulation change induced by stratospheric ozone depletion and its role in the recent increase of Antarctic sea ice extent, Geophysical Research Letters, 36, doi:10.1029/2009gl037524.

Turner, J., J. S. Hosking, G. J. Marshall, T. Phillips, and T. J. Bracegirdle (2016), Antarctic sea ice increase consistent with intrinsic variability of the Amundsen Sea Low, Climate Dynamics, 46(7-8), 2391-2402, doi:10.1007/s00382-015-2708-9.

Turner, J., T. Phillips, J. S. Hosking, G. J. Marshall, and A. Orr (2013), The Amundsen Sea low, International Journal of Climatology, 33(7), 1818-1829, doi:10.1002/joc.3558.

Ushio, S., T. Takizawa, K. I. Ohshima, and T. Kawamura (1999), Ice production and deep-water entrainment in shelf break polynya off Enderby Land, Antarctica, Journal of Geophysical Research-Oceans, 104(C12), 29771-29780, doi:10.1029/1999jc900249.

Van den Broeke, M. (2000), The semi-annual oscillation and Antarctic climate. Part 4: A note on sea ice cover in the Amundsen and Bellingshausen Seas, International Journal of Climatology, 20(4), 455-462, doi:10.1002/(sici)1097-0088(20000330)20:4<455::aid-joc482>3.0.co;2-m.

Venegas, S. A. (2003), The Antarctic Circumpolar Wave: A combination of two signals?, Journal of Climate, 16(15), 2509-2525, doi:10.1175/1520-0442(2003)016<2509:tacwac>2.0.co;2.

Ward, J. H. (1963), HIERARCHICAL GROUPING TO OPTIMIZE AN OBJECTIVE FUNCTION, Journal of the American Statistical Association, 58(301), 236-&, doi:10.2307/2282967.

Wendler, G., D. Gilmore, and J. Curtis (1997), On the formation of coastal polynyas in the area of Commonwealth Bay, Eastern Antarctica, Atmospheric Research, 45(1), 55-75, doi:10.1016/s0169-8095(97)00024-0.

White, W. B., and R. G. Peterson (1996), An Antarctic circumpolar wave in surface pressure, wind, temperature and sea-ice extent, Nature, 380(6576), 699-702, doi:10.1038/380699a0.

Worby, A. P., and I. Allison (1991), Ocean Atmosphere Energy Exchange Over Thin, Variable Concentration Antarctic Pack Ice, 184-190 pp.

Yim, O. and K.T. Ramdeen (2015), Hierarchical Cluster Analysis: Comparison of Three Linkage Measures and Application to Psychological Data, The Quantitative Methods for Psychology, 11(1), 8-21, http://dx.doi.org/10.20982/tqmp.11.1.p008.

Yuan, X. J. (2004), ENSO-related impacts on Antarctic sea ice: a synthesis of phenomenon and mechanisms, Antarctic Science, 16(4), 415-425, doi:10.1017/s0954102004002238.

Yuan, X. J., and C. H. Li (2008), Climate modes in southern high latitudes and their impacts on Antarctic sea ice, Journal of Geophysical Research-Oceans, 113(C6), doi:10.1029/2006jc004067.

Yuan, X. J., and D. G. Martinson (2000), Antarctic sea ice extent variability and its global connectivity, Journal of Climate, 13(10), 1697-1717, doi:10.1175/1520-0442(2000)013<1697:asieva>2.0.co;2.

Yuan, X. J., and D. G. Martinson (2001), The Antarctic Dipole and its predictability, Geophysical Research Letters, 28(18), 3609-3612, doi:10.1029/2001gl012969.

Zwally, H.J., J.C. Comiso, and A.L. Gordon (1985), Antarctic Offshore Leads and Polynyas and Oceanographic Effects, Antarctic Research Series, Oceanology of the Antarctic

Continental Shelf, 43, https://agupubs.onlinelibrary.wiley.com/doi/10.1029/AR043p0203.

Zwally, H. J., J. C. Comiso, C. L. Parkinson, D. J. Cavalieri, and P. Gloersen (2002), Variability of Antarctic sea ice 1979-1998, Journal of Geophysical Research-Oceans, 107(C5), doi:10.1029/2000jc000733.

Zwally, H. J., C. L. Parkinson, and J. C. Comiso (1983), Variability Of Antarctic Sea Ice And Changes In Carbon-Dioxide, Science, 220(4601), 1005-1012, doi:10.1126/science.220.4601.1005.